

Control of Innate Immunity by RNA Metabolism

by

Chun Kew

Control of Innate Immunity by RNA Metabolism

Inaugural–Dissertation

zur

Erlangung des Doktorgrades

der Mathematisch-Naturwissenschaftlichen Fakultät

der Universität zu Köln

vorgelegt von

Chun Kew

aus Hongkong

Köln, 2019

Berichterstatter: Prof. Dr. Adam Antebi

Prof. Dr. Thorsten Hoppe

Tag der mündlichen Prüfung: 05.09.2018

Acknowledgements

First, I would like to thank my supervisor Prof. Dr. Adam Antebi for giving me the opportunity to perform my doctoral research in his laboratory. Special thanks to Prof. Dr. Thorsten Hoppe and Prof. Dr. Mats Paulsson as well for their participation in my thesis committee.

Second, I would also like to acknowledge Dr. Raja Ganesan, Dr. Wenming Huang, Dr. Parul Methrotra, Dr. Nirmal Robinson and Dr. Varnesh Tiku for their intellectual inputs and other contributions to this work.

Last but not least, I thank all my friends in both Cologne and Hong Kong, my family and all the members of the Antebi department for their continuous support.

Abstract

Innate immunity is key to defense against infections. Its high complexity and interactions with other systems make it relatively difficult to study in mammals. The nematode *C. elegans* is particularly useful for studying innate immunity due to its conserved biology and genetic manipulability. However, our knowledge of *C. elegans* immunity is still limited, especially on what is the upstream stimulus that controls innate immune responses in the worms.

In this study, we used *C. elegans* as the model to investigate how immune responses are triggered. First, we found that the nucleolar protein fibrillarin, a rRNA 2'-O-methyltransferase indispensable for rRNA maturation, plays an important role. Fibrillarin reduction is able to confer resistance in wild-type animals and also infection sensitive mutants. Upon infection, it was observed that fibrillarin levels decrease. Since fibrillarin is a major nucleolar protein, nucleolar size was also examined. Infection leads to a shrinkage of nucleoli, suggesting reduction of fibrillarin and nucleolar size is a beneficial host response promoting resistance. Fibrillarin reduction inhibits rRNA maturation, and therefore leads to reduced levels of mature rRNA and reduced translation. Using *ifg-1* and *ife-1* loss of function mutants, we found that reduction of translation is sufficient to prolong survival upon infection. Further, knocking down fibrillarin does not significantly enhance the *ifg-1* mutant survival, suggesting they may function in overlapping pathways, probably translation. Similar to the observations in worms, infection also reduces fibrillarin protein levels in human epithelial cells and also murine macrophages. Reduction of fibrillarin is also able to promote survival in mammalian cells after infection. Interestingly, fibrillarin RNAi suppresses pro-inflammatory cytokine secretion but promotes production of anti-inflammatory cytokines and clearance of intracellular bacteria. These data suggest that reduction of fibrillarin is an evolutionarily conserved host response to initiate protective mechanisms.

Second, we identified that the essential splicing factor *rnp-6* also controls innate immunity. Infection alters splicing of the *ret-1* splicing reporter and *tos-1* transcript, suggesting an interesting connection between splicing and infection. It was found that a novel gain of function mutation of *rnp-6* results in immunodeficiency in *C. elegans*. Both resistance and induction of anti-microbial genes are compromised in the mutant.

Activity of RNP-6 negatively correlates with resistance. Overexpression of RNP-6 compromises survival upon infection while reducing its expression by RNAi is sufficient to activate immune responses and drive resistance. Further investigations revealed that the effect is mediated by *pmk-1*, the worm's homolog of p38 MAPK. RNAi mediated reduction of RNP-6 activates PMK-1. On the other hand, gain of function of *rnp-6* suppresses *P. aeruginosa* induced PMK-1 activation. Intriguingly, the mutation of *rnp-6* is able to suppress the splicing remodeling induced by infection. Further, RNAi against other splicing factors also induces infection resistance and activation of PMK-1, indicating that the splicing machinery may be a general control factor for innate immune responses, and perturbing splicing is an inducer of immunity.

The data present in this study highlight the critical roles of rRNA biogenesis and mRNA splicing in innate immunity. We suggest that reduction of fibrillarin and perturbation of splicing are two of the upstream stimuli for innate immunity in *C. elegans*. A tight connection exists between initiation of immune responses and RNA metabolism, which is previously underappreciated.

Zusammenfassung

Angeborene Immunität ist der Schlüssel zur Abwehr von Infektionen. Die hohe Komplexität und die Interaktion mit anderen Systemen macht es jedoch relativ schwierig diese in Säugetieren zu studieren. Der Nematode *C. elegans* ist daher wegen seiner konservierten Biologie und genetischen Manipulierbarkeit besonders gut geeignet um angeborene Immunität zu untersuchen. Unser Verständnis von Immunität in *C. elegans* ist jedoch nach wie vor limitiert – besonders die Stimuli, welche die Immunantwort in Würmern regulieren sind nur rudimentär beschrieben.

In dieser Arbeit haben wir *C. elegans* als Modell genutzt, um zu untersuchen wie Immunantworten ausgelöst werden. Unsere erste Entdeckung war, dass das nucleoläre Protein Fibrillarin, eine rRNA 2'-O-methyl Transferase, welche unabdingbar für die rRNA-Produktion ist, eine wichtige Rolle spielt. Gesenkte Fibrillarin Level führen zu einer höheren Infektionsresistenz in Wild Typ Würmern und auch in Würmern, welche normalerweise eine höhere Infektionssensitivität aufweisen. In infizierten Würmern konnten wir gesenkte Fibrillarin Level messen. Da es sich bei Fibrillarin um ein großes nucleoläres Protein handelt, untersuchten wir ebenfalls die nucleoläre Größe. Eine Infektion führte zu einer Verkleinerung von Nukleoli, was zu der Annahme führt, dass reduzierte Fibrillarin Level und eine Verkleinerung der Nucleoli sich positiv auf die Immunantwort des Wirtes auswirken und Infektionsresistenz fördern. Die Verringerung von Fibrillarin inhibiert die rRNA-Reifung und führt deshalb zur Reduktion von fertiger rRNA und einer herabgesetzten Translationsrate. Indem wir *ifg-1* und *ife-1* Würmer, beides loss-of-function-Mutationen, nutzten fanden wir heraus, dass eine verringerte Translationsrate ausreichend ist, um das Überleben bei einer Infektion zu verlängern. Außerdem fanden wir heraus, dass eine zusätzliche Verringerung von Fibrillarin das Überleben von *ifg-1* Mutanten nicht signifikant verlängerte. Dies legt Nahe, dass beide in überlappenden Signalwegen eingeordnet werden können, wobei es sich hierbei wahrscheinlich um die Translationsregulation handelt.

Ähnlich zu unseren Beobachtungen im Wurm, konnten wir ebenfalls beobachten, dass eine Infektion die Fibrillarin Level auch in menschlichen Epithel Zellen und aus Mäusen isolierten Makrophagen verringerte. Die Senkung von Fibrillarin führte außerdem zu

einer höheren Überlebensrate von Säugetierzellen bei einer Infektion. Interessanterweise unterdrückte eine Senkung von Fibrillarin durch RNAi die Sekretion von pro-inflammatorischen Zytokinen, und führte zu einer erhöhten Produktion von anti-inflammatorischen Zytokinen und einer Reduktion intrazellulärer Bakterien. Diese Daten implizieren, dass eine Reduzierung von Fibrillarin ein evolutionär konservierter Mechanismus der Immunantwort des Wirtes ist, um protektive Mechanismen zu initiieren.

Als zweiten Punkt identifizierten wir, dass der essenzielle Spleiß-Faktor *rnp-6* ebenfalls ein Regulator von angeborener Immunität ist. Bei einer Infektion beobachteten wir ein verändertes Spleißen des *ret-1* Spleiß-Reporters und des *tos-1* Transkripts. Beides legt nahe, dass es eine interessante Verbindung zwischen Spleißen und einer Infektion geben könnte. Wir beobachteten, dass eine neue Gain-of-function Mutation von *rnp-6* in einer Immunschwäche in *C. elegans* resultiert. Sowohl Resistenz, als auch die Induktion von anti-mikrobiellen Genen sind in diesen Mutanten gestört. Die Aktivität von RNP-6 korreliert negativ mit Infektionsresistenz. Eine Überexpression von RNP-6 kompromittiert nicht nur das Überleben bei einer Infektion sondern auch eine Reduktion des Proteins durch RNAi reicht aus, um eine Immunantwort zu aktivieren und Infektionsresistenz zu fördern. Weitere Untersuchungen zeigten, dass der Effekt durch *pmk-1*, das Wurm Homolog von p38 MAPK, reguliert wird. Die Reduktion von RNP-6 durch RNAi aktiviert PMK-1. Auf der anderen Seite unterdrückt die gain-of-function Mutation in *rnp-6* die *P. aeruginosa* induzierte Aktivierung von PMK-1. Interessanterweise führt die Mutation von *rnp-6* nicht zu einer Um-Modellierung des Spleißens, welche normalerweise durch eine Infektion herbeigeführt wird. Weiterhin führt die Verringerung weiterer Spleiß-Faktoren durch RNAi ebenfalls zu einer Infektionsresistenz und der Aktivierung von PMK-1. Dies signalisiert dass die Spleiß-Maschinerie möglicherweise ein genereller Kontrollmechanismus der angeborenen Immunantwort ist und dass ein gestörtes Spleißen ein Induktor von Immunität ist.

Die in dieser Arbeit präsentierten Daten heben die kritische Rolle der Biogenese von rRNA und des Spleißens von mRNA für die angeborene Immunität hervor. Wir proponieren, dass eine Verringerung von Fibrillarin und eine Störung des Spleißens zwei wichtige Regulatoren von angeborener Immunität in *C. elegans* sind. Es existiert

eine enge Verbindung zwischen der Initiation einer Immunantwort und RNA-Metabolismus, welche bisher nicht genug Beachtung gefunden hat.

Abbreviations

12-O-Tetradecanoylphorbol-13-acetate	PMA
4-hydroxyphenyllactic acid	HPLA
β-D-1-thiogalactopyranoside	IPTG
American Type Culture Collection	ATCC
Analysis of variance	ANOVA
Bone marrow derived macrophage	BMDM
Brain heart infusion	BHI
Branch-point binding protein	BBP
Clustered Regularly Interspaced Short Palindromic Repeats	CRISPR
Colony-forming unit	CFU
Damage associated molecular pattern	DAMP
Database for Annotation, Visualization and Integrated Discovery	DAVID
Deoxyribonucleic acid	DNA
Differential interference contrast	DIC
Differentially expressed gene	DEG
Dulbecco's modified Eagle's medium	DMEM
Enzyme-linked immunosorbent assay	ELISA
Endoplasmic reticulum	ER
Ethyl methanesulfonate	EMS
Far-upstream element	FUSE
Fetal calf serum	FCS
Gene Ontology	GO
Fibrillar center	FC
FUSE binding protein	FBP
Dense fibrillar component	DFC
G-protein coupled receptor	GPCR
Glyceraldehyde 3-phosphate dehydrogenase	GAPDH
Green fluorescent protein	GFP
Herpes simplex virus-1	HSV-1

Horseradish peroxidase	HRP
Human immunodeficiency virus	HIV
Hutchinson-Gilford progeria syndrome	HGPS
Insulin-like signaling	IIS
Lactate dehydrogenase	LDH
Lipopolysaccharide	LPS
Lysogeny broth	LB
Mechanistic target of rapamycin	mTOR
Messenger RNA	mRNA
Mitogen-activated protein kinase	MAPK
Multiplicity of infection	MOI
Nematode growth media	NGM
Non-significant	ns
Nuclear factor-kB	NF-kB
Open reading frame	ORF
Pathogen associated molecular pattern	PAMP
Pattern recognition receptors	PRR
Phosphate-buffered saline	PBS
Poly(U) Binding Splicing Factor 60	PUF60
Polymerase chain reaction	PCR
Precursor ribosomal RNA	pre-rRNA
Quantitative PCR	qPCR
Radioimmunoprecipitation assay	RIPA
Ribonucleic acid	RNA
Ribosomal DNA	rDNA
Ribosomal RNA	rRNA
RNA interference	RNAi
RNA recognition motif	RRM
Roswell Park Memorial Institute	RPMI
S-adenosylmethionine	SAM
Small interfering RNA	siRNA
Small nuclear RNA	snRNA
Small nuclear ribonucleoprotein	snRNP
Small nucleolar RNA	snoRNA

Small nucleolar ribonucleoprotein	snoRNP
Splicing factor 3b	SF3b
Splicing factor one	SF1
Standard deviation	s.d.
Standard error of the mean	s.e.m.
Sterile-alpha and Armadillo motif containing protein	SARM
Signal recognition particle	SRP
Toll-like receptor	TLR
Transcription factor EB	TFEB
Transfer RNA	tRNA
Transforming growth factor beta	TGF- β
Tris-buffered Saline and Tween20	TBST
Tryptic soy broth	TSB
Tryptic soy agar	TSA
U2 auxiliary factor	U2AF
Ubiquitin-proteasome system	UPS
Unfolded protein response	UPR

Table of Contents

Acknowledgements	I
Abstract	II
Zusammenfassung	IV
Abbreviations	VII
Table of Contents	X

CHAPTER 1 INTRODUCTION 1-28

1.1 An overview on the metazoan immune system	2
1.2 Characteristics of innate immunity	2
1.3 <i>C. elegans</i> as a genetic model for biological studies	4
1.4 <i>C. elegans</i> as a model host for infection	5
1.5 Pathogens of <i>C. elegans</i>	5
1.6 Signaling pathways of innate immunity in <i>C. elegans</i>	7
1.7 Detection of infection	11
1.8 Immune response effectors in <i>C. elegans</i>	16
1.9 Commensal bacteria in <i>C. elegans</i>	17
1.10 Functions of the nucleolus	18
1.11 Functions of fibrillarin	21
1.12 Introduction to mRNA splicing	23
1.13 Functions of PUF60/RNP-6	23
1.14 Aims of the study	27

CHAPTER 2 MATERIALS AND METHODS 29-39

2.1 Maintenance of <i>C. elegans</i> cultures	30
2.2 <i>C. elegans</i> killing assay	30
2.3 RNAi in <i>C. elegans</i>	31
2.4 Immunoblotting	31
2.5 <i>C. elegans</i> sample preparation for RNA analysis	33
2.6 RNA extraction and cDNA synthesis	33
2.7 Quantitative PCR	33

2.8 RNA sequencing and bioinformatic analysis	35
2.9 rRNA analysis	35
2.10 Puromycin incorporation assay	36
2.11 Mammalian cell cultures	36
2.12 Fibrillarin knockdown and overexpression in mammalian cell cultures	37
2.13 Infection of mammalian cells	37
2.14 Cell viability assays	37
2.15 Bacterial burden assay	38
2.16 Immunocytochemistry	38
2.17 Enzyme-linked immunosorbent assay (ELISA)	38
2.18 <i>tos-1</i> alternative splicing PCR assay	39
 CHAPTER 3 ROLES OF FIBRILLARIN IN HOST RESPONSES DURING INFECTION	 40-66
3.1 Introduction	41
3.2 Results	41
3.2.1 FIB-1/fibrillarin reduction enhances resistance against bacterial infection in <i>C. elegans</i>	41
3.2.2 Bacterial infection induces FIB-1/fibrillarin reduction and nucleolar shrinkage	45
3.2.3 FIB-1/fibrillarin reduction also confers resistance to infection sensitive mutants	48
3.2.4 FIB-1/fibrillarin reduction leads to reduced translation	52
3.2.5 Fibrillarin reduction protects against bacterial infection in mammalian cells	56
3.3 Discussion	61
3.4 Work contribution	66

CHAPTER 4 ROLES OF RNP-6 IN INNATE IMMUNITY	67-104
4.1 Introduction	68
4.2 Results	68
4.2.1 Infection alters splicing pattern	68
4.2.2 A mutation in the splicing factor <i>rnp-6</i> causes immunodeficiency	70
4.2.3 Transcriptomic profiling reveals substantial effects of the <i>rnp-6</i> mutation on infection induced transcriptional and splicing changes	75
4.2.4 RNP-6 inhibits immunity	92
4.2.5 RNP-6 mediates immunity through PMK-1	94
4.2.6 Mutual regulation of splicing and host responses to infection	97
4.3 Discussion	99
4.4 Work contribution	104
CHAPTER 5 FUTURE PERSPECTIVES	105-109
5.1 Investigating the mechanism of nucleolar functions in innate immunity	106
5.2 Investigating the mechanism of fibrillarin reduction	106
5.3 Probing nucleolar regulation of immunity in animal models	107
5.4 Elucidating splicing control of innate immunity	107
5.5 Studying control of innate immunity by splicing under other circumstances	107
5.6 Extending the findings of <i>rnp-6</i> to higher organisms	108
5.7 Exploring possible links between the nucleolus, splicing and immunity	109
CHAPTER 6 REFERENCES	110-125

SUPPLEMENTARY INFORMATION

126-129

Erklärung zur Dissertation

127

Curriculum Vitae

128

CHAPTER 1

INTRODUCTION

Introduction

1.1 An overview on the metazoan immune system

The immune system defends against microbial infections and is critical for the survival and fitness of the organisms. The two main immunity strategies are innate immunity and adaptive immunity. While the innate immune system can be found in all animals, the adaptive immune system is only found in vertebrates (Hirano, Das et al., 2011).

The innate immune system utilizes nonspecific defense mechanisms. These mechanisms include physical barriers, bacteria-digesting enzymes, and phagocytic cells (Tomlin & Piccinini, 2018). Some distinct characteristics of innate immunity will be discussed in the later section.

The adaptive immune system refers to the mechanism that operates antigen-specific immune responses. Pathogen specific antigens first must be processed by antigen-presenting cells. Processed antigens are then present to a class of specialized immune cells called lymphocytes (Osorio, Lambrecht et al., 2018). Activation of the antigen-specific lymphocytes leads to clonal expansion of T- and B-lymphocytes. A subset of T-cells called cytotoxic T-cells induces death of the cells that are infected by pathogens or are otherwise damaged or dysfunctional. The other set of T-cells called helper T-cells establishes and maximizes the capabilities of the immune system by producing immunomodulatory cytokines. Activated B-cells produce antibodies, which can bind specifically to the antigen and neutralize the antigen bearing pathogens. A minority of the activated lymphocytes are differentiated into memory cells, which can be swiftly activated when the same antigen is encountered again (Hirano et al., 2011).

1.2 Characteristics of innate immunity

Innate immunity is an evolutionarily ancient form of defense mechanism. In higher organisms, such as mammals, innate immunity cooperates with adaptive immunity to achieve the optimal protection. On the other hand, lower organisms, such as nematodes, depend solely on innate immunity. When compared to adaptive immunity,

which is regarded as more sophisticated and more recent in evolution (Mogensen, 2009), innate immunity has several distinct characteristics.

First, innate immunity exerts its effects extremely rapidly. Innate immunity does not require a previous exposure to the pathogen. The host can initiate a response immediately after detecting pathogen associated molecular patterns (PAMPs). PAMPs refer to molecules associated with pathogens but are missing in the hosts. Examples are long double strand RNA derived from viral replication (Liu, Olganier et al., 2016a), bacterial cells' components, such as lipopolysaccharide (LPS), flagellin and peptidoglycan (Mogensen, 2009). Molecules which are normally present in the host but detected in a wrong cellular compartment are also recognized as PAMPs. For instance, cytosolic DNA is a potent stimulus of innate immunity. Presence of DNA in cellular compartments other than the nucleus or mitochondria indicates an infection by a DNA virus (Dhanwani, Takahashi et al., 2017).

Second, innate immunity is a relative simple mechanism and is not restricted to specialized immune cells. Most cells in a human body can mount an innate immune response. For example, epithelial cells produce interferons upon viral infection without assistance from the adaptive immune system (Liu et al., 2016a). The simplicity of innate immunity makes it the ideal evolutionary choice for lower organisms, such as plants, nematodes and insects, whose relatively simple body structures do not allow the accommodation and specialization of immune cells (Rajamuthiah & Mylonakis, 2014).

Third, Innate immunity is not a highly specific process. Unlike adaptive immunity, which involves activation of antigen specific immune cells, effectors of innate immunity are not specific for a particular antigen but are effective against a wide range of pathogens. Interferons are well-known to inhibit replication of virtually all viruses (Liu et al., 2016a). Another example would be lysozyme, which can be found in secretions, such as tear and saliva. Lysozyme kills bacteria non-specifically by digesting bacterial cell wall (Ragland & Criss, 2017).

Fourth, innate immunity does not provide long-lasting immunity to the host. Adaptive immunity is known to provide long-term, sometimes even perpetual, protection. The

most famous example would be the smallpox vaccine. After immunization, the adaptive immune system gains unlimited full immunity to the smallpox virus (Fulginiti, Papier et al., 2003). Such protection is not seen in innate immunity presumably because the innate immune system does not have immunological memory

1.3 *C. elegans* as a genetic model for biological studies

Caenorhabditis elegans is used extensively as a genetic model for various biological investigations. It belongs to a large animal phylum called Nematodes. In nature, *C. elegans* feeds on bacteria and can be found in different ecological niches, including soil and rotting vegetative material (Felix & Duveau, 2012). The animal was originally introduced by Sydney Brenner decades ago as a model for development and neural science (Brenner, 1974). Nowadays, *C. elegans* is widely used in the scientific community for every aspect of biology. Some of the most important biological advancements in the last century were first discovered using *C. elegans*, such as the first complete cell lineage of an animal (Deppe, Schierenberg et al., 1978, Sulston & Horvitz, 1977), discovery of programmed cell death (Sulston & Horvitz, 1977), microRNAs (Lee, Feinbaum et al., 1993, Wightman, Ha et al., 1993), RNA interference (RNAi) (Fire, Xu et al., 1998) and genetics of ageing (Friedman & Johnson, 1988, Kenyon, Chang et al., 1993, Klass, 1983). More recently, *C. elegans* has also been used to investigate innate immunity and pathogenesis of microbial infections (Tan, Mahajan-Miklos et al., 1999a, Tan, Rahme et al., 1999b).

The success of *C. elegans* as a model organism comes from its various advantages. First, the worm normally exists as hermaphrodites, reproducing by self-fertilizing, thus allowing a colony of isogenic animals to be generated from one individual. Males can however be induced by heat shock, and this enables the generation of new strains by mating, making genetics incredibly easy in the worms. Second, the nematode has a very short generation time, about 3 days at 20°C (Brenner, 1974), as well as a short life-span of about 4 weeks (Kenyon et al., 1993). This enables rapid expansion of the population for screening and experiments. Third, methods for genetic manipulation are well-established, including transgene injection, RNAi by feeding and genome editing (Friedland, Tzur et al., 2013). Lastly, the transparent body of the worms enables real time in vivo imaging of internal structures and fluorescent reporters.

1.4 *C. elegans* as a model host for infection

C. elegans, as a bacterivore, encounters numerous different microorganisms in the wild. Many of these microorganisms can actually infect and cause diseases in the worms (Jiang & Wang, 2018). The worms can also be infected with pathogens from other animals, such as pathogenic bacteria from human (Kim & Ewbank, 2015). Due to its simple body structure and limited cell number, adaptive immunity is lacking in *C. elegans*. Therefore, to protect against infection, innate immunity is crucial for the worms. Importantly, the molecular mechanism, especially the signal transduction pathways, is well-conserved from human to *C. elegans*. Examples are *pmk-1*, which encodes the ortholog of mammalian mitogen-activated protein kinase (MAPK), and *hlh-30*, which encodes the ortholog of transcription factor EB (TFEB). All these genes play indispensable roles in mediating innate immunity in both worms and human (Kim, Feinbaum et al., 2002, Visvikis, Ihuegbu et al., 2014). The immune system of *C. elegans* can be viewed as a simplified and minimalistic version of that of higher organisms. Therefore, *C. elegans* could be a highly useful and relevant model for elucidating the molecular mechanism of innate immunity and the complex interaction between hosts and pathogens, which is extremely difficult to study in higher organisms.

1.5 Pathogens of *C. elegans*

Diverse pathogens are capable of infecting *C. elegans*. Some of them are natural nematode pathogens, while others do not naturally infect the worms but are used as an experimental tool for scientific investigations. These include diverse species of bacteria, fungi, viruses and unicellular eukaryotic parasites.

In 1999, a creative and pioneering study demonstrated that *C. elegans* can be used as a model host for *Pseudomonas aeruginosa* (Tan et al., 1999a), which is a human bacterial pathogen. Since then, other human pathogenic bacteria were shown by different laboratories to be able to infect *C. elegans*. These bacteria include *Salmonella enterica* (Aballay, Yorgey et al., 2000), *Yersinia pestis* (Joshua, Karlyshev et al., 2003), pathogenic *Escherichia coli* strains (Diard, Baeriswyl et al., 2007), *Enterococcus faecalis* (Garsin, Sifri et al., 2001) and *Staphylococcus aureus* (Sifri, Begun et al.,

2003). Non-human pathogens were also used to infect the worms. One noticeable example is *Bacillus thuringiensis*, which produces pore-forming crystal proteins with nematocidal and insecticidal activities (Wei, Hale et al., 2003). Generally, pathogenic bacteria and their associated toxins are ingested by the worms, which leads to colonization by the bacteria and destruction of the gut epithelium. Therefore the bacterial infection models of *C. elegans* are thought to be an excellent system for studying intestinal immunity (Cohen & Troemel, 2015).

Other than bacteria, fungus is also commonly employed as a *C. elegans* pathogen. *Drechmeria coniospora* is an endoparasitic nematophagous fungus and a non-human pathogen (Jansson, 1994). In contrast to bacteria, which the worms usually ingest, *D. coniospora* attaches to the surface of the worms. The hyphae penetrate the cuticle and the epidermis, spreading into the entire body of the worms. Studies have successfully utilized it to model innate immunity of the epidermis (Zugasti, Bose et al., 2014, Zugasti, Thakur et al., 2016).

A *C. elegans* model for antiviral innate immunity is a relatively new idea in the field. This could be partially explained by the lack of natural viruses capable of infecting the worm. Early experiments utilized viruses from other animal hosts to infect *C. elegans*. Flock House Virus and Vesicular Stomatitis Virus, which naturally cannot infect *C. elegans*, can be injected into the worms and establish an infection (Martin, Rex et al., 2017). Recently, the first natural *C. elegans* virus, Orsay virus, was identified (Felix, Ashe et al., 2011). The virus can transmit horizontally in the population without the need of injecting. It is supposed that Orsay virus would be a useful tool for future studies.

Microsporidia and oomycete, both are spore-forming unicellular eukaryotic parasites highly similar to fungi, can also infect *C. elegans*. Microsporidia were classified as protozoans or protists, but now are considered as fungi (Hibbett, Binder et al., 2007). The first microsporidia infection model of *C. elegans* was established in 2008. In the study, a novel species of microsporidia, *Nematocida parisii*, was isolated from a wild-caught worm. The parasite invades intestinal cells, where it replicates and undergoes sporogenesis (Troemel, Felix et al., 2008). Recently, an oomycete parasite was also found in a wild isolate of *C. elegans*. This novel oomycete pathogen, *Myzocytiopsis*

humicola, infects the worms through the body surface. Attachment of the oomycete initiates penetration of the nematode cuticle by the hypha, leading to spreading of the pathogen throughout the entire body of the worm (Osman, Fasseas et al., 2018).

1.6 Signaling pathways of innate immunity in *C. elegans*

Since *C. elegans* lacks the adaptive immune system, it solely relies on innate immunity. Other animals, including evolutionarily diverse species, such as insects and mammals, heavily rely on Toll-like receptors (TLRs) and nuclear factor- κ B (NF- κ B) for activation of immune responses (Buchon, Silverman et al., 2014). TLRs are a class of membrane-spanning proteins that recognize PAMPs derived from microbes. In mammals, the TLRs include TLR1, TLR2, TLR3, TLR4, TLR5, TLR6, TLR7, TLR8, TLR9, TLR10, TLR11, TLR12, and TLR13, though the latter three are missing in humans (Vijay, 2018). Interestingly, the fruit fly *Drosophila melanogaster* also relies on the homolog of TLR, Toll (also known as Toll-1), to initiate antimicrobial immune responses. *D. melanogaster* have nine Toll proteins. They recognize a secreted cytokine called Spätzle or PAMPs, such as viral glycoproteins (Buchon et al., 2014). It is worth mentioning that antimicrobial peptides and Toll/TLRs, which both have very conserved sequences from insects to mammals, were first discovered in *D. melanogaster* (Boman, Nilsson et al., 1972, Lemaitre, Nicolas et al., 1996), highlighting the usefulness of genetically trackable invertebrate animal models in immunological research. Further, transcription of antimicrobial genes in *D. melanogaster* is mediated by the NF- κ B transcription factors Dif and Relish. NF- κ B transcription factors also mediate expression of immune genes downstream of TLRs in mammals (Buchon et al., 2014).

In the *C. elegans* system, both TLRs and NF- κ B are missing (Kim & Ewbank, 2015). Unlike mammals and *D. melanogaster*, which possess multiple TLRs, the involvement of *tol-1*, the only TLR homolog in *C. elegans*, is not well-understood. Contradictory results can be seen in the literature. It was initially suggested that it does not have a function in the immune response (Pujol, Link et al., 2001) but later another study indicates that *tol-1* is required for *C. elegans* innate immunity (Tenor & Aballay, 2008). Nevertheless, *tol-1* is also required for pathogen avoidance and early embryonic development (Brandt & Ringstad, 2015, Chuang & Bargmann, 2005). Also, sequence

homolog fails to identify a homolog of NF- κ B in the worm's genome, suggesting that NF- κ B may not be conserved in *C. elegans* (Kim & Ewbank, 2015).

While the functions of TLR and NF- κ B are not conserved in *C. elegans*, immune response signaling is transduced by other evolutionarily conserved cascades. The first identified pathway in *C. elegans* is the MAPK pathway (Kim et al., 2002), which is an ancient cascade involved in stress resistance and immunity. In *C. elegans*, this pathway functions similarly as in other organisms, such as mammals and *D. melanogaster*. It is a linear phosphorylation cascade, where NSY-1 (MAP3K) phosphorylates SEK-1 (MAP2K), which in turn phosphorylates PMK-1 (MAPK). Phosphorylation of PMK-1 activates its activity. Activated PMK-1 further phosphorylates multiple transcription factors to modulate their activities. These transcription factors include ATF-7 and SKN-1 (Kim & Ewbank, 2015). The activation of the cascade depends on another gene called *tir-1*, an homolog of mammalian sterile-alpha and Armadillo motif containing protein (SARM) (Kim & Ewbank, 2015). It is suggested that the MAPK pathway mainly functions cell autonomously in the intestine against bacterial infection (Kim & Ewbank, 2015) and in the epidermis against fungal infection (Zugasti et al., 2014).

HLH-30, also known as TFEB in mammals, is another evolutionarily conserved mediator of innate immunity in *C. elegans*. HLH-30 is required for autophagy induction, lysosome biogenesis, lipid metabolism and lifespan extension in multiple longevity models, including dietary restriction, reduced insulin signaling, gonadal longevity and mitochondrial function impairment (Lapierre, De Magalhaes Filho et al., 2013). Intriguingly, this transcription factor is also involved in host defense responses. Upon infection, HLH-30 is activated and translocated into the nucleus. Loss of *hlh-30* results in severely hampered immune responses and compromised survival upon infection in *C. elegans* (Visvikis et al., 2014). HLH-30 binding elements are commonly found in antimicrobial and cytoprotective genes, whose expression is dependent on HLH-30. Importantly, TFEB is also required for expression of antimicrobial genes and cytokines in mammalian macrophages (Visvikis et al., 2014), highlighting the fundamental roles of HLH-30/TFEB in innate immunity across evolution. The upstream signaling is also conserved evolutionarily. In both mammals and *C. elegans*, pathogens induced HLH-

30/TFEB activation requires protein kinase D (*dkf-1* in worms), phospholipase C (*plc-1*) and G protein (*egl-30*) (Najibi, Labed et al., 2016).

The insulin like signaling (IIS) pathway also plays a crucial role in innate immunity in nematodes. DAF-2 is the receptor for insulin like peptides. Mutations in *daf-2* are well-known for inducing longevity and stress resistance in *C. elegans*. Its inactivation leads to the activation of its downstream transcription factor DAF-16 (Kenyon, 2011). Mutations of *daf-2* lead to constitutive activation of DAF-16, which is responsible for promoting expression of genes involved in innate immunity, stress resistance and longevity (Evans, Chen et al., 2008). Accordingly, *daf-2* mutants have enhanced resistance against multiple pathogens, in a manner completely dependent on *daf-16* (Garsin, Villanueva et al., 2003). Infection also induces expression changes in different insulin like peptides, which can affect DAF-2/DAF-16 activity (Evans, Kawli et al., 2008).

GATA factors are also required for host defense in *C. elegans*. GATA motif is frequently found in the promoter regions of genes that are induced by *P. aeruginosa* infection. The GATA factors ELT-2 and ELT-3 are required for normal resistance to bacterial intestinal infection and *D. coniospora* epidermal infection respectively (Head & Aballay, 2014, Pujol, Zugasti et al., 2008, Shapira, Hamlin et al., 2006). Loss of function of *elt-2* significantly reduces basal and infection-induced expression of immune genes. Other than infection resistance, the GATA factors also mediate resistance to osmotic stress. Interestingly, there is a substantial overlap between the up-regulated genes by infection and osmotic stress responsive genes (Rohlfing, Miteva et al., 2010). The roles of GATA factors in immune responses are conserved in mammals and *D. melanogaster* (Senger, Harris et al., 2006, Shapira et al., 2006).

Further, ATFS-1, which is activated upon mitochondrial stress, also mediates host responses to infection. During mitochondrial function impairment, import of ATFS-1 into the mitochondria is inhibited, which allows it to be transported into the nucleus and function as a transcription factor (Nargund, Pellegrino et al., 2012). Interestingly, infection by *P. aeruginosa* also triggers activation of ATFS-1. Worms lacking *atfs-1* are hyper-sensitive to *P. aeruginosa* infection and have hampered transcriptional responses, whereas hyper-activation of ATFS-1 improves survival, suggesting

mitochondria stress and ATFS-1 control innate immune responses in *C. elegans* (Pellegrino, Nargund et al., 2014).

Transforming growth factor beta (TGF- β) signaling has also been shown to control defense gene expression. Deletion of *dbl-1*, the ligand for DAF-4, which is one of the TGF- β receptors in worms, severely diminishes induction of antimicrobial genes upon fungal infection (Zugasti & Ewbank, 2009). Interestingly, TGF- β signaling controls immune responses in a non-cell autonomous manner, since expression of *dbl-1* under a neuronal promoter is sufficient to rescue the phenotype in the epidermis (Zugasti & Ewbank, 2009). Similarly, *dbl-1* mutants have reduced resistance to bacterial infection (Mallo, Kurz et al., 2002). The expression of some of the downstream targets is controlled by the canonical TGF- β pathway, which involves SMA proteins (Mochii, Yoshida et al., 1999). TGF- β signaling also plays an important role in immunity in mammals (Travis & Sheppard, 2014) and *D. melanogaster* (Clark, Woodcock et al., 2011).

β -catenin signaling is also required for immunity in *C. elegans* (Irazoqui, Ng et al., 2008). The pathway is controlled by the availability of Wnt, which is detected by cell surface receptors. The system is best known as the master controller of development in various animals. Mutation of the *bar-1*, the *C. elegans* homolog of β -catenin, or its downstream effectors, the homeobox gene *egl-5*, leads to a compromised immune response and reduced survival upon bacterial infection (Irazoqui et al., 2008). Importantly, the role of β -catenin signaling and homeobox transcription factors in anti-bacterial immunity is also conserved in mammals (Irazoqui et al., 2008) and fruit flies (Ryu, Nam et al., 2004).

Other than β -catenin signaling, another family of developmental genes, the apoptotic genes are also implicated in innate immunity in *C. elegans*. Upon infection, a network of a noncanonical unfolded protein response (UPR) are activated and required for resistance to pathogenic infections. This induction requires the apoptotic receptor CED-1 (Haskins, Russell et al., 2008). However, this result should be interpreted with cautions, since it may be an experimental artifact (see the following sections for more discussion) (Kim & Ewbank, 2015). Further, *cep-1*, the homology of the tumor suppressor p53, which plays multiple roles in apoptosis, ageing and cell cycle

progression (Chira, Gulei et al., 2018), also functions as a positive regulator of innate immunity (Fuhrman, Goel et al., 2009).

RNAi is a highly conserved biological phenomenon in different species. It is proposed that the natural function of RNAi is antiviral defense (Wilkins, Dishongh et al., 2005). In *C. elegans*, double-stranded RNAs derived from viral replication are recognized and cleaved by a complex consisting of DRH-1, DCR-1, and RDE-4 into 23 nt long primary small interfering RNAs (siRNAs). One strand of the duplex siRNA is then loaded into the Argonaute protein RDE-1 (Grishok, 2013). The RDE-1-siRNA complexes then bind to viral RNA targets based on sequence complementarity. This binding recruits RNA-dependent RNA polymerase to generate secondary siRNAs, which have the length of 22 nt instead of 23 nt. These secondary siRNAs complex with, and guide Argonaute proteins to viral RNA species, which are complementary to the siRNAs. The Argonaute proteins then initiate target RNA cleavage and inhibit virus replication (Grishok, 2013).

1.7 Detection of infection

To initiate an immune response, a potential threat must be first detected by the host. In mammals, it is usually achieved by pattern recognition receptors (PRRs), which recognized PAMPs, special molecules from the pathogens (Mogensen, 2009). Recently, the idea of damage-associated molecular patterns (DAMPs) has also raised. DAMPs refer to normal host molecules, whose mislocalization represents damages of host cells. Examples include extracellular DNA and ATP, which are normally restricted intracellularly. DAMPs can also be recognized by PRPs and trigger immune responses (Schaefer, 2014).

How *C. elegans* can detect infection is poorly understood. It is very intriguing that *C. elegans*, which normally feed on bacteria, is able differentiate different bacteria and induces immune responses only when feed on pathogenic bacteria (Kim & Ewbank, 2015). Both benign and pathogenic bacteria contain similar molecular patterns, such as LPS and peptidoglycan, suggesting the worms may not be reliant on classical PAMPs detection. However, in one study, it was found that wild-type *Salmonella* LPS is required for the elicitation of host responses (Aballay, Drenkard et al., 2003). How *C. elegans* worms specifically detect LPS from *Salmonella* bacteria remains to be seen.

Detection of pathogens by *C. elegans* likely involves G-protein coupled receptors (GPCRs). GPCRs are cell surface receptors with seven transmembrane domains coupled with G proteins (Hanlon & Andrew, 2015). Studies have shown that factors downstream to GPCRs affect immune responses. These factors include G proteins and arrestin. Loss of G proteins in *C. elegans* compromises immunity (Kawli, Wu et al., 2010, Najibi et al., 2016), while loss of arrestin, the negative regulator of GPCR signaling, provokes immune responses (Singh & Aballay, 2012). However, only three GPCRs have been shown to be involved in activation of innate immune responses. NPR-1, a G protein-coupled neuropeptide receptor, was found to contribute to host responses (Styer, Singh et al., 2008), although it is also suggested that the effect maybe due to differences in behavioral avoidance to the bacteria (Kim & Ewbank, 2015, Reddy, Andersen et al., 2009). Mutations in *octr-1*, which encodes an octopamine receptor, confer increased resistance to bacterial infection. OCTR-1 negatively regulates the non-canonical unfolded protein response involving the *abu* class of genes (the *abu* genes will be discussed in the later section) (Liu, Sellegounder et al., 2016b, Sun, Singh et al., 2011). However, latter studies indicate that these genes appear to be involved in pharyngeal grinder structural integrity but not immunity (George-Raizen, Shockley et al., 2014). Also, the reported reduced expression of *abu* genes in the *octr-1* mutants can be explained by the differences in developmental rate. Therefore the role of OCTR-1 in immunity has been disputed (Kim & Ewbank, 2015). GPCR DCAR-1 acts locally in the epidermis to regulate antimicrobial gene expression through the PMK-1 pathway upon fungal infection. Interestingly, the ligand for this GPCR is a tyrosine derivative 4-hydroxyphenyllactic acid (HPLA), which is not from the fungal pathogen but rather derived from the worm itself as an endogenous ligand (Zugasti et al., 2014). Other GPCRs responsible for activation of innate immunity remain to be seen. The inability of further identification could be explained by the unusual expansion of the GPCR family in *C. elegans*. There are more than one thousand of GPCRs in the worms' genome (Gupta & Singh, 2017). Presumably, they work in a co-operative and redundant manner, making the classical one-gene-one-phenotype genetics impossible to reveal the causative GPCRs.

A relatively new concept is the “effector-triggered immunity”, whereby the host is alerted to the associated damage caused by the pathogen instead of the molecular

patterns associated with the pathogen (Rajamuthiah & Mylonakis, 2014). Toxins produced by pathogens often interrupt essential cellular processes to inhibit anti-microbial mechanisms and, in some cases, to hijack cellular machineries to assist replication and transmission of the pathogens. Examples are *Pseudomonas* exotoxin (or exotoxin A) (Iglewski, Liu et al., 1977) and Shiga toxin from pathogenic *E. coli* strains (Pacheco & Sperandio, 2012). Both toxins inhibit protein translation of the host. Because these toxins have extremely diverse structures, it would be inefficient to have PRRs to recognize each individual toxin. Therefore, instead of having different PRRs for individual toxin, detecting the downstream damages caused by the pathogens and the associated toxins is more efficient and evolutionarily advantageous. The notion of effector-triggered immunity has been long appreciated in plants (Jones & Dangl, 2006, Rajamuthiah & Mylonakis, 2014) and more recently in animal models, such as *C. elegans* (Dunbar, Yan et al., 2012, Melo & Ruvkun, 2012), as well. In the absence of pathogens, RNAi or toxin-mediated disruption of core cellular processes, including proteostasis, mitochondrial respiration, and protein translation, induces expression of innate immune effectors and detoxification genes. RNAi of these essential processes also triggers behavioral avoidance to non-pathogenic bacteria (Melo & Ruvkun, 2012). These data suggest core cellular pathways are closely surveilled, and perturbations are interpreted as a sign of infection. A recent study shows that the bZIP transcription factor ZIP-2 is activated during pathogen induced translation blockage by *P. aeruginosa*. The regulation is mediated by the alternative upstream open reading frame (ORF). A reduction in translation promotes skipping of the upstream ORF and enhances translation of the downstream functional ORF. Expression of *irg-1* is then activated by the elevated level of ZIP-2 and CEBP-2 (Dunbar et al., 2012).

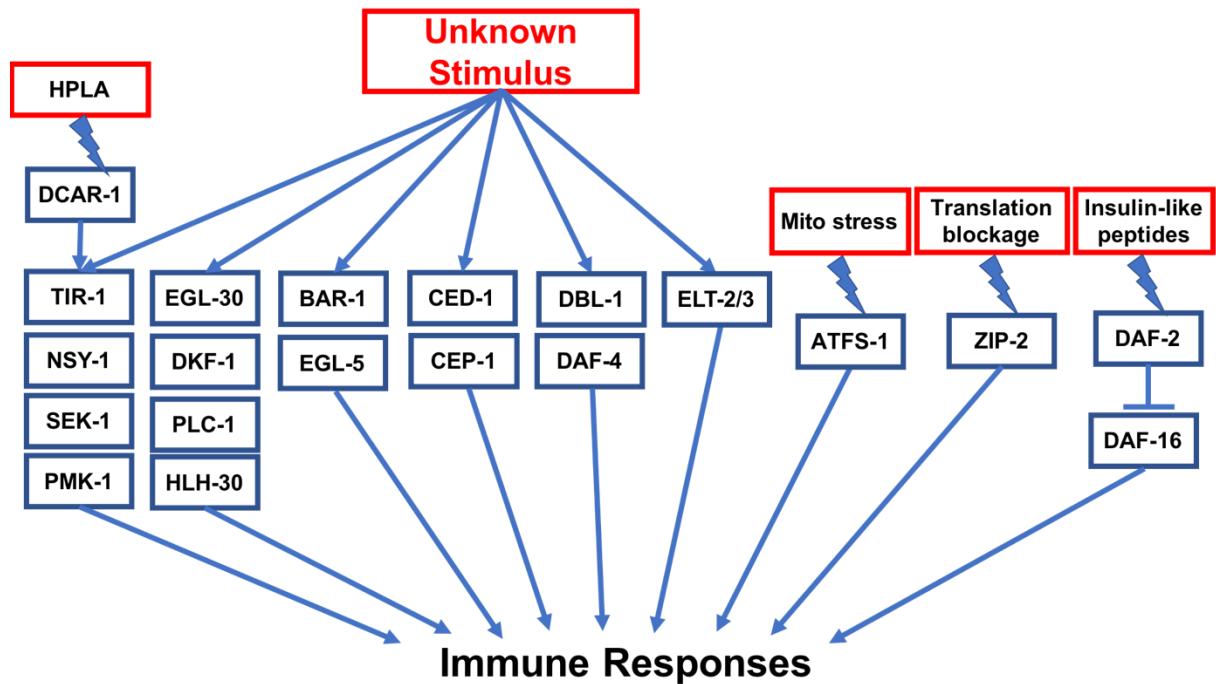



Figure 1. A simplified summary of the molecular signaling pathways of innate immunity in *C. elegans*. Major players are shown, namely the MAP kinase cascade, HLH-30/TFEB, β -catenin, TGF- β , GATA factors, CED-1/CEP-1, ATFS-1, ZIP-2 and insulin-like signaling pathway. Interestingly, in many cases, the exact stimulus which activates the pathways is unknown.



Toll/TLR	?	✓	✓
NF-κB	×	✓	✓
MAPKs	✓	✓	✓
TFEB	✓	?	✓
IIS signaling	✓	✓	?
GATA factors	✓	✓	✓
ATFS-1	✓	×	×
TGF-β signaling	✓	✓	✓
Wnt signaling	✓	✓	✓
ZIP-2	✓	×	×

Figure 2. A brief summary of the evolutionary conservation of the molecular components of innate immunity discussed in the previous sections. Tick marks indicate evolutionary conservation. Crosses indicate the factors are not conserved. ? means inconclusive due to contradictory literature or insufficiency study.

1.8 Immune response effectors in *C. elegans*

Detection of infection and its downstream signaling eventually lead to activation of immune effectors, which help to alleviate the stress. In *C. elegans*, the secretion of antimicrobial proteins represents a major evolutionarily conserved mechanism of innate immunity. Many of these small proteins, such as lysozymes or amoebapores, are highly bactericidal. The nematode possesses a large arsenal of antimicrobial proteins, including saposin-like amoebapores (23 SPP proteins), antibacterial factor-related proteins (6 ABF proteins), lysozymes (10 LYS and 6 ILYS proteins), thaumatins (8 THN proteins), C-type lectin (265 CLEC proteins), neuropeptide-like proteins (75 NLP proteins), nematode specific peptide (12 NSPB and 20 NSPC proteins) and caenacin (11 CNC proteins) (Kim & Ewbank, 2015).

The UPR also functions as a major immune response effector in *C. elegans*. UPR maintains endoplasmic reticulum (ER) homeostasis. ER stress is induced by accumulation of unfolded proteins in the ER, which can be caused by agents inhibiting protein folding, such as tunicamycin, or a sudden surge of ER dependent protein synthesis. Interestingly, infection with *P. aeruginosa* activates ER stress and XBP-1, which is a conserved transcriptional regulator of UPR. Genetic analysis revealed an indispensable role of XBP-1 in survival of *C. elegans* on *P. aeruginosa* specifically during larval development (Richardson, Kooistra et al., 2010). Infection induces massive production of secretory antimicrobial proteins, whose production causes ER stress, which can arrest development of the animals. In response, XBP-1 and UPR are activated to cope with the stress and facilitate normal development. Loss of *xbp-1* arrests development due to the unalleviated ER stress. Intriguingly, abolishing immune responses by deleting *pmk-1* reverses the phenotype of the *xbp-1* mutants. This suggests that a decrease in immune effector synthesis in the *pmk-1* mutant lessens ER stress in the absence of XBP-1, so promoting survival (Ewbank & Pujol, 2010, Richardson et al., 2010).

In addition to the above mentioned *xbp-1* mediated UPR, there is a non-canonical UPR comprised of the *abu* (Activated in Blocked Unfolded protein response) family of genes.

The *abu* family was first identified to be specifically upregulated in *xbp-1* mutants upon ER stress (Urano, Calton et al., 2002) and was suggested to play a role in immunity (Haskins et al., 2008). However, as discussed in the previous section, this idea has been seriously disputed (Kim & Ewbank, 2015). The *abu* genes have fluctuations in expression during molting, which can potentially explain their transcriptional changes. The previously reported changes in *abu* gene expression upon mutations, bacterial infection, and ER stressors cannot be observed anymore in tightly synchronized populations. Further, reduction of *abu* gene may cause susceptibility to pathogenic bacteria indirectly through alterations of pharyngeal morphology rather than immune responses (George-Raizen et al., 2014). Therefore, great caution should be taken while interpreting the potential roles of non-canonical UPR in immunity.

Upon bacterial infection, *C. elegans* worms also respond by activating autophagy. Autophagy has been shown to be required for resistance to different bacteria, including *P.aeruginosa* (Kirienko, Ausubel et al., 2015), *S.typhimurium* (Curt, Zhang et al., 2014) and *S. aureus* (Visvikis et al., 2014). Also, as mentioned, infection also induces autophagy transcriptional regulator HLH-30 (the homolog of vertebrate TFEB) (Visvikis et al., 2014).

1.9 Commensal bacteria in *C. elegans*

C. elegans is very special among model organisms because they feed on live bacteria, which can be both the food source and pathogens to the worms. Live bacteria can greatly influence the worms' physiology independently of pathogenicity through metabolites and nutrient content. In the laboratory, *C. elegans* worms are normally cultured with a single strain of *E. coli* bacteria. OP50, the standard food source for *C. elegans* (Brenner, 1974), actually cannot be found in the natural habitat of the worms (Samuel, Rowedder et al., 2016). It was selected because it is an uracil auxotroph, which forms thin lawns on the uracil deficient nematode growth media (NGM) plates to allow easy manipulation and visualization of the worms (Macneil & Walhout, 2013). It is possible to culture the worms with other benign bacteria without causing infection. Culturing *C. elegans* with different bacteria can greatly affect physiology of the worms. Diet-induced phenotypes include numbers of offspring, developmental rate, metabolic profile and lifespan (Macneil & Walhout, 2013). For example, when grown on *Bacillus*

subtilis, which exists in the natural habitat of the worms and is the more preferable food than OP50, worms live longer than on *E. coli* OP50. Nitric oxide (NO) produced by *B. subtilis* was found to be the signaling molecule for activation of HSF-1 and DAF-16 transcription factors in the worms to extend lifespan (Donato, Ayala et al., 2017).

A living bacteria diet is metabolically active, and therefore is able to metabolize or modify drugs or other chemicals which are added to treat the worms (Macneil & Walhout, 2013). Chemicals can be inactivated or metabolized into biologically active agents. Also, it is possible that some factors exert their effects on the worms indirectly by altering physiology of the bacterial food source. For example, metformin can extend lifespan in different model organisms, including *C. elegans*. Interestingly, the lifespan extension can only be seen when the animals are fed with live bacteria. It was later found that metformin actually inhibits folate synthesis in the bacteria, and reduced folate intake causes extended lifespan in *C. elegans* (Cabreiro, Au et al., 2013).

The laboratory conditions may not perfectly model the natural habitat of the worms, since in the wild the worms proliferate on decaying organic material, where an extremely diverse microbiome can be found. Metagenomics of wild *C. elegans* isolates' gut content reveals thousands of operational taxonomic units of bacteria, including species from phyla of *Proteobacteria*, *Bacteroidetes*, *Firmicutes*, and *Actinobacteria*. When culturing with these bacteria individually, the worms show vastly different developmental timing, body size and stress reporter induction, suggesting that the natural commensal bacteria of *C. elegans* profoundly affect its physiology, and some induces stresses like pathogens (Samuel et al., 2016).

1.10 Functions of the nucleolus

The nucleolus is a special compartment in the nucleus of eukaryotic cells. This organelle is a non-membrane bound highly dynamic structure (Boisvert, van Koningsbruggen et al., 2007). It is best known for its role in ribosomal RNA (rRNA) synthesis and ribosome assembly. Ribosomal DNA (rDNAs), which encodes for precursor ribosomal RNA (pre-rRNA), is contained in the nucleolus. Pre-rRNA is transcribed within the nucleolus by RNA polymerase I (Hernandez-Verdun, Roussel et al., 2010). The pre-rRNA is then further processed by nucleolar factors, including

methyl transferase, pseudouridine synthase and nuclease, into mature 28S (26S in *C. elegans*) and 18S rRNA. These operations occur co-transcriptionally or immediately after transcription. Methyl transferases, such as fibrillarin, add methyl groups to ribose and the bases of the RNA. Pseudouridine synthase converts uridine to pseudouridine. Nuclease cleaves and removes linker RNA within the pre-rRNA. The modified rRNA is then assembled with 5S rRNA and ribosomal protein components, which are synthesized outside the nucleolus, into pre-ribosomal units. These complexes are then exported into the cytoplasm (Hernandez-Verdun et al., 2010).

Although ribosome biogenesis is the most well-known function of the nucleolus, in the last two decades, a number of studies suggest that the nucleolus has some unexpected functions in addition to ribosome biogenesis. One such unexpected functions is messenger RNA (mRNA) splicing. Splicing factors can be found in the nucleolus (Bubulya, Prasanth et al., 2004, Lin, Chu et al., 2017). Nucleolar specific splicing events have also been observed (Falaleeva, Pages et al., 2016). Signal recognition particle (SRP) maturation also requires the nucleolus. SRP is a cytosolic and highly conserved ribonucleoprotein, which recognizes signal peptides and delivers specific proteins to the ER for targeting to the plasma membrane or secretion. The SRP core proteins and the SRP RNA are imported into the nucleolus, in which the assembly process takes place (Boisvert et al., 2007). Processing of certain transfer RNAs (tRNA) and small nuclear RNAs (snRNAs) also occurs in the nucleolus. These RNA species also require modifications, such as methylation and pseudouridylation, similar to rRNA (Boisvert et al., 2007).

Nucleoli are easily recognizable in *C. elegans* under differential interference contrast (DIC) microscopy. The organelle exists as a discrete circular structure within the nucleus (Fig. 3). The nucleolar size of germ cells, and intestinal cells are relatively large, with diameters ranging from 3 to 7 μm , partially due to the high activity of translation and ribosome biosynthesis in these tissues (Lee, Lee et al., 2012). On the other hand, neuronal nucleoli are much smaller, presumably because neurons do not need high level of protein translation. Hypodermal cells are ideal for studying nucleolar size in the worms because they exist as a single layer of cells with nucleoli of intermediate sizes, ranging from 2 μm to 3 μm in diameter (Lee et al., 2012, Tikku, Jain et al., 2016). Genetic screens were done to identify *C. elegans* mutants with abnormal nucleolar morphology.

These mutants were named *ncI* (abnormal NuCLEoli) (Hedgecock & Herman, 1995). *ncI-1* is a negative regulator of nucleolar size and will be discussed in more detail later in this thesis. *ncI-2*, a mutant with defects in germline nucleoli, has not yet been molecularly characterized (Lee et al., 2012).

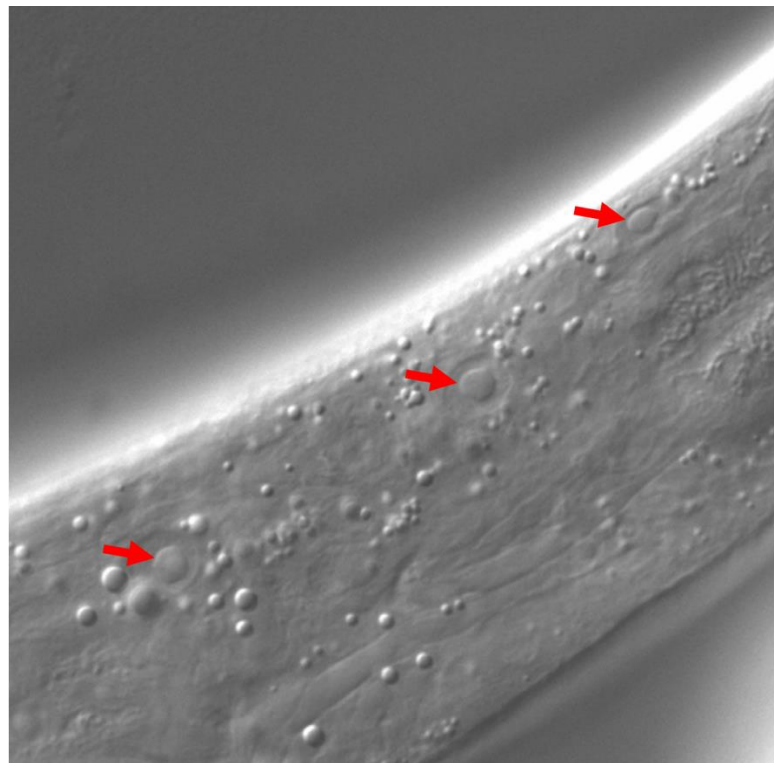


Figure 3. Nucleolar morphology in hypodermis of *C. elegans*. The image of wild-type *C. elegans* was acquired with DIC microscopy. Red arrows indicate nucleoli.

Because the nucleolus is the primary controller of ribosome biogenesis and protein synthesis, it is therefore reasonable to postulate that it has a significant role in different diseases and other physiological processes. Indeed, dysregulation of the nucleolus is a common feature of cancerous cells, which usually possess enhanced ribosome biogenesis and other anabolic activities (Boisvert et al., 2007). Many aggressive cancers show abnormal and enlarged nucleolar morphology. Nucleolar proteins, such as fibrillarin, also become more abundant in these cancer cells (Rodriguez-Corona, Sobol et al., 2015). In cells from patients with Hutchinson-Gilford progeria syndrome (HGPS), a rare form of genetic pre-mature ageing pathology, nucleoli are hyper-activated and expanded. As a consequence, global protein synthesis is elevated (Buchwalter & Hetzer, 2017). Interestingly, on the other hand, longevity-inducing interventions or mutations reduce nucleolar size and ribosome biogenesis (Demontis, Patel et al., 2014, Neumuller, Gross et al., 2013, Sheaffer, Updike et al., 2008, Tiku et al., 2016). The nucleolus is also a target for viruses. Viral proteins, such as human immunodeficiency virus (HIV) Rev protein (Daelemans, Costes et al., 2004), influenza A virus NS1 protein (Melen, Tynell et al., 2012) and herpes simplex virus-1 (HSV-1) US11 (Greco, Arata et al., 2012), preferentially localize to the nucleolus. These viral nucleolar proteins facilitate replication of the viruses and are necessary for the optimal fitness of the parasites.

1.11 Functions of fibrillarin

Fibrillarin is an evolutionarily conserved nucleolar protein. It was named fibrillarin because it exists mainly in fibrillar centers (FCs) and dense fibrillar component (DFC) of nucleoli, where rDNA transcription occurs (Rodriguez-Corona et al., 2015). The size of fibrillarin ranges from 34 to 38 kDa in different species. In *C. elegans*, it is around 36 kDa (Tiku et al., 2016). Fibrillarin is a methyl transferase, which uses S-adenosylmethionine (SAM) as a methyl donor. Fibrillarin mediates methylation of the 2-hydroxyl group of ribose targets on pre-rRNA and is indispensable for the maturation of rRNA and ribosome biogenesis. This process is highly complicated and is carried out in more than 100 sites for each pre-rRNA molecule. The precise location is directed by small nucleolar ribonucleoproteins (snoRNPs), which use a class of specialized RNA called small nucleolar RNA (snoRNA) to guide the modification machinery.

Fibrillarin also methylates histone H2A at the 35S ribosomal DNA locus. This epigenetic mark can facilitate the transcription of pre-rRNA by RNA polymerase I (Rodriguez-Corona et al., 2015).

In *C. elegans*, fibrillarin is encoded by *fib-1*. The gene is contained in the operon CEOP5428 which encodes fibrillarin (FIB-1) and RPS-16 (Lee et al., 2012). Deletion of *fib-1* is lethal and reduction by RNAi also leads to larval arrest. Intriguingly, FIB-1/fibrillarin levels affects lifespan. Various long-lived mutants possess small nucleoli and reduced levels of FIB-1/fibrillarin, which leads to reduced ribosome biogenesis. A modest reduction of FIB-1/fibrillarin in wildtype animals is sufficient to increase their lifespan. Interestingly, the lifespan extending effects and the small nucleolus phenotype of the long-lived mutants are reversed by deleting *ncf-1* (Tiku et al., 2016). NCL-1 is a cytoplasmic ring finger, B-box zinc finger and NHL repeat protein, which is homologous to Brat (brain tumor) in fruit flies and TRIM2/3/32 of mammals. Deletion of the *brat* gene causes enlarged nucleoli (Lee et al., 2012). In worms, NCL-1 inhibits *fib-1* expression by inhibiting *fib-1* translation (Yi, Ma et al., 2015). Deletion of *ncf-1* abolishes long-lived phenotypes of all long-lived mutants tested, and therefore this gene acts as a convergent factor of longevity. The *ncf-1* mutants also show increased nucleolar size and abundance of fibrillarin (Tiku et al., 2016).

As mentioned in the previous section, the nucleolus is involved in different pathology, and fibrillarin, as a major nucleolar protein, inevitably participates in such conditions. Fibrillarin is required for biogenesis of the machinery necessary for protein translation and ultimately cell proliferation. Fibrillarin has been shown to be overexpressed in numerous kinds of cancer, including adenocarcinoma, leukaemia and breast cancer (Rodriguez-Corona et al., 2015). Fibrillarin is also a common target for viral proteins. Binding of ORF3 protein from nut rosette virus to fibrillarin is required for viral ribonucleoprotein function (Kim, Macfarlane et al., 2007). Tat protein from HIV (Ponti, Troiano et al., 2008) and NS1 protein from influenza A also bind to fibrillarin to modulate antiviral responses of the hosts (Melen et al., 2012).

1.12 Introduction to mRNA splicing

Splicing is a modification of mRNA commonly found in eukaryotic cells. It occurs co-transcriptionally or immediately after transcription inside the nucleus. Non-coding regions called introns are removed, and exons, the protein coding sequences, are joined together to form the mature mRNA (Berget, Moore et al., 1977, Chow, Gelinas et al., 1977). Discovery of splicing is regarded as one of the most significant discoveries in modern molecular biology as it explains how the information is transferred between different layers of the central dogma. Splicing is catalyzed by the spliceosome, which is composed of a large variety of splicing factors (Wani & Kuroyanagi, 2017). Some of these splicing factors will be discussed more detailly in the next section.

One significant consequence of splicing is an increase in the numbers of possible transcripts encoded by a genome. In many cases, splicing creates multiple different proteins with different functions from the same pre-mRNA by varying the exon composition. This phenomenon is termed alternative splicing. Certain exons can be skipped while some introns can be included. In some rare scenario, splicing can also occur inter-molecularly. Trans-splicing is a unique form of splicing, where exons from two different pre-mRNA molecules are joined together, creating a novel mRNA molecule (Burgess, 2013). Alternative splicing greatly enhances complexity of the genome. Indeed, splicing tends to be more prominent in higher organisms. In human, over 95% of the transcripts undergoes certain forms of alternative splicing, while in *C. elegans* only 25% of the transcripts is alternatively spliced (Wani & Kuroyanagi, 2017). In simple lifeforms like prokaryotic cells, splicing is a rare event (Reinhold-Hurek & Shub, 1992).

1.13 Functions of PUF60/RNP-6

Poly(U) Binding Splicing Factor 60 (PUF60) is an RNA binding protein involved in pre-mRNA splicing and transcriptional regulation. Splicing is achieved by cooperation of five different small nuclear ribonucleoproteins (snRNPs) (U1-U5) and a large variety of associated factors (Maniatis & Tasic, 2002). 5' splice donor sites are recognized by the U1 snRNP. 3' splice acceptors are recognized by U2 auxiliary factor (U2AF), which

recognizes a long polypyrimidine sequence located at the 3' end of the introns. The activity of U2AF facilitates the recruitment of the U2 snRNP. Another factor, splicing factor one/branch-point binding protein (SF1/BBP) facilitates the recognition of the highly conserved branch-point sequence in the middle of the introns (Reed, 2000).

The initial characterization of PUF-60 was done in 1999 when it was first discovered as a 60-kDa splicing factor with poly-U binding affinity that works cooperatively with U2AF to promote splicing by facilitating association of the U2 snRNP with primary transcripts.(Page-McCaw, Amonlirdviman et al., 1999). PUF60 also interacts physically with splicing factor 3b (SF3b) (Rahmutulla, Matsushita et al., 2014). PUF60 is also known as far-upstream element binding protein. The far-upstream element (FUSE) regulates expression of c-myc. PUF60 binds to FUSE binding protein (FBP), which is a transcription factor that stimulates c-myc expression. Binding of PUF60 to FBP hinders functions of FBP and therefore inhibits c-myc expression (Duncan, Bazar et al., 1994). Myc proteins are transcription factors that activate expression of proliferation promoting genes (Dang, 2012). The function of PUF60 is conserved in invertebrates. Mutations in the PUF60 homolog of *Drosophila*, Half Pint (Hfp), also lead to aberrant splicing of mRNAs (Van Buskirk & Schupbach, 2002) and also increased abundance of d-myc protein (Quinn, Dickins et al., 2004).

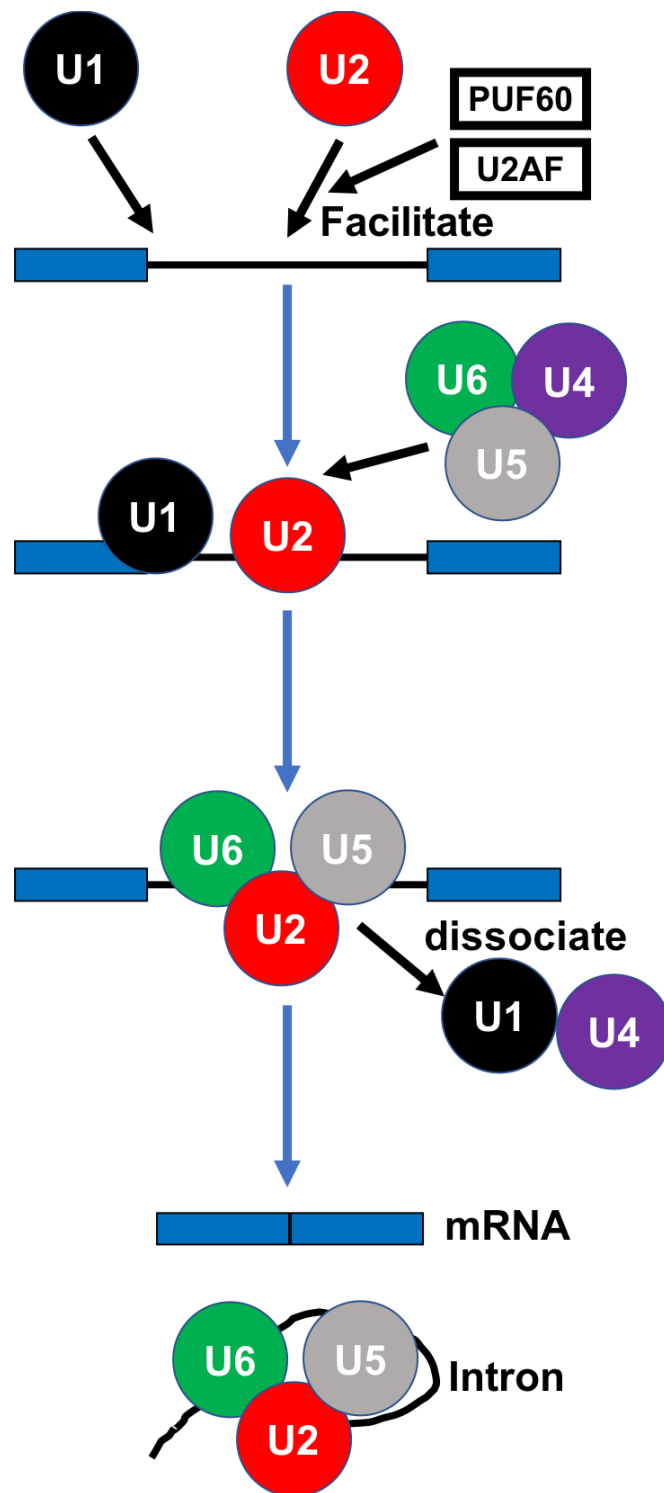


Figure 4. Pre-mRNA splicing by the snRNPs. snRNPs are sequentially recruited to the RNA molecule and evidences suggest RNP-6 is involved in the recruitment of U2 complex.

PUF60 is widely implicated in human diseases. Auto anti-PUF60 antibodies are highly produced in patients with autoimmune diseases, including Sjögren's syndrome and dermatomyositis (Fiorentino, Presby et al., 2016). Titre of serum anti-PUF60 antibodies correlates with disease severity, suggesting the auto antibodies contribute to pathogenesis (Fiorentino et al., 2016). PUF60 is an essential gene, and homozygous knockout leads to embryonic lethality (Matsushita, Kitamura et al., 2015). Heterozygous loss of function causes a rare genetic disease called Verheij syndrome. Sequencing of RNA from the patients' cells reveals aberrant splicing patterns. Developmental phenotypes could be observed in most of the patients. Examples include short stature, spinal segmentation anomalies, congenital heart disease, ocular colobomata and hand anomalies (Low, Ansari et al., 2017). PUF60 is also involved in viral infection. PUF60 promotes hepatitis B viral RNA transcription and splicing (Sun, Nakashima et al., 2017).

In the nematode *C. elegans*, splicing is also regulated by the conserved snRNPs and associated factors. However, one interesting discrepancy is that there is no consensus branch-point sequence at the middle of the introns or long polypyrimidine sequence at the 3' end (Zorio & Blumenthal, 1999). U2AF instead recognizes an alternative consensus UUUUCAGR sequence at the 3' splice acceptor site (Hollins, Zorio et al., 2005). Intriguingly, splicing plays a critical role in regulation of ageing in *C. elegans*. Splicing homeostasis deteriorates during ageing. Dietary restriction and mTOR inhibition extend lifespan partially by maintaining good splicing capacity. Also, overexpressing splicing factor SFA-1 is sufficient to extend lifespan (Heintz, Doktor et al., 2017).

The homolog of PUF60 is encoded by *mp-6* in *C. elegans*. This gene is poorly studied in *C. elegans*. At the amino acid sequence level, RNP-6 is a relatively conserved protein, especially the two RNA recognition motifs (RRMs). The transcript undergoes differential splicing, yielding three different isoforms with molecular weight of 37, 39 and 81 kDa. Interestingly, alternative splicing of *mp-6*, which itself is a splicing factor, is controlled by another splicing factor, called *sym-2* (Barberan-Soler & Zahler, 2008).

1.14 Aims of the study

C. elegans has been a useful model for studying innate immunity. As discussed in the earlier sections, the worm has a very conserved innate immune system. Nevertheless, despite years of research, our knowledge of innate immunity in *C. elegans* is limited and fragmentary, especially how host responses are initiated. Benign bacteria have virtually the same chemical composition as pathogenic bacteria, making simple detection of PAMPs unlikely to be the sole mechanism. Similar situation also exists in higher organisms. Microbiome is well tolerated by our immune system although it also possesses immunostimulatory PAMPs. Exactly how pathogens can stimulate host responses remains to be elucidated. Understanding the molecular mechanism of immune responses in *C. elegans* then should shed light on how higher organisms, including humans, detect and fight infections.

As we mentioned in the earlier sections, RNA binding proteins, such as fibrillarin and PUF60/RNP-6 play essential roles in RNA metabolism. RNA is an essential component of all life. RNA binding proteins are responsible for biogenesis and quality control of various RNA species, which affect every biological process. Therefore, it is reasonable to speculate that RNA metabolism also plays a critical role in the regulation of innate immunity in *C. elegans*.

In this study, we aim to identify novel regulators of innate immunity in *C. elegans*. We are particularly interested to investigate how immune responses are initiated. Special focus is given to two candidate genes, namely *fib-1* and *rnp-6*. Both of them encode RNA binding proteins. Pathogenic infection disrupts core cellular processes. It has been reported that disturbing different organelles, such as mitochondrial functions (Pellegrino et al., 2014), proteasomal activity, cytoskeletal dynamics (Melo & Ruvkun, 2012) and ribosomal translation (McEwan, Kirienko et al., 2012), induces immune-responses. The potential involvement of the nucleolus in innate immunity against bacterial infections remains largely unexplored. We therefore aim to: 1) investigate how fibrillarin and the nucleolus behave and affect host responses during infection. Also, the functions of splicing in general and RNP-6 in particular is poorly studied in *C. elegans*. We intend to 2) determine the role of *rnp-6* and splicing in infection responses

and identify the downstream signaling pathways. Finally, we also aim to 3) extend the findings to mammalian cell culture system in order to test whether these functions are evolutionarily conserved.

CHAPTER 2

MATERIALS AND

METHODS

Materials and Methods

2.1 Maintenance of *C. elegans* cultures

The worms were maintained using the standard protocols, which are modified from the original methods (Brenner, 1974). The animals were grown on NGM plates, which consists of 3 g/L NaCl, 2.5 g/L peptone and 17 g/L agar in H₂O supplemented with 1mM MgSO₄, 1mM CaCl₂, 5 µg/mL cholesterol and 25mM/L potassium phosphate buffer. *E.coli* strain OP50, which serves as the food source for the worms, was grown in lysogeny broth (LB) at 37°C overnight with gentle shaking to obtain a saturated culture. The culture was seeded and spread on NGM plates. After drying, animals were put on the bacterial lawn and incubated at 20°C.

The strains used for the experiments were: N2 (wildtype), *ncl-1(e1865)*, *ncl-1(e1942)*, *daf-16(mu86)*, *hlh-30(tm1978)*, *adls2122(lgg-1::gfp; rol-6(su1006))* (Kang, You et al., 2007), *cguls001 (FIB-1::GFP)* (Lee, Lo et al., 2010), *ife-2(ok306)*, *ifg-1(cxTi9279)*, *pmk-1(km25)*, *agls17 (myo-2p::mCherry + irg-1p::GFP)* (Estes, Dunbar et al., 2010), *rnp-6(dh1127)*, *rnp-6(dh1125)*, *rnp-6(dh1127);pmk-1(km25)*, *tir-1(tm3036)*, *lin-15(n765);ybls2167[eft-3::RET-1E4E5(+1)E6-GGS6-mCherry* *eft-3::RET-1E4E5(+1)E6-(+2)GGS6-EGFP* *lin-15(+)* *pRG5271Neo*] X (Heintz et al., 2017) and *rnp-6(dh1127);lin-15(n765);ybls2167[eft-3::RET-1E4E5(+1)E6-GGS6-mCherry* *eft-3::RET-1E4E5(+1)E6-(+2)GGS6-EGFP* *lin-15(+)* *pRG5271Neo*] X.

2.2 *C. elegans* killing assay

The protocols for *C. elegans* killing assay are based on the previously published protocols (Powell & Ausubel, 2008) with some modifications. *S. aureus* (Strain MW2-WT), *E. faecalis* (Strain ATCC 29212) and *P. aeruginosa* (strain PA14) were used to infect *C. elegans*. For each bacterium, a single colony was inoculated into the appropriate medium. *S. aureus*, *E. faecalis* and *P. aeruginosa* were inoculated in tryptic soy broth (TSB) medium, brain heart infusion (BHI) medium and LB respectively. The bacteria were grown at 37°C with gentle shaking overnight. For each bacterium, 20 µl of the overnight bacterial cultures were seeded on the killing assay plates, tryptic soy

agar (TSA) plates with 10 µg/mL nalidixic acid (Sigma, NAL) for *S. aureus*, BHI plates with 10µg/mL NAL for *E. faecalis* and modified NGM, which has an enriched peptone content (3.5 g/L instead of 2.5 g/L), for *P. aeruginosa*. After drying, the seeded killing assay plates were then incubated at 37°C overnight. On the next day, the plates were allowed to equilibrate to room temperature before transferring worms. 20-25 age synchronized young adult worms were transferred to the killing plates with 3 replicate plates for each condition. The plates were then incubated at 25°C. Survival was monitored every 12 hours for *S. aureus* and *P. aeruginosa* and every 24 hours for *E. faecalis*. Worms that did not respond to gentle touch by a worm pick are defined as dead and were removed from the plates. Worms that crawled off the plate or had severe ruptured vulva phenotypes were censored from the analysis.

2.3 RNAi in *C. elegans*

Standard feeding protocol was used (Hammell & Hannon, 2012). The dsRNA expressing HT115 bacteria were from the Vidal (Rual, Ceron et al., 2004) and Ahringer library (Kamath & Ahringer, 2003). The bacteria were grown in LB medium with 100 µg/mL ampicillin overnight at 37°C with gentle shaking. The culture was then concentrated for 5 times and spread on RNAi plates, which are NGM plates supplemented with 100 µg/mL ampicillin and 0.4 mM Isopropyl β-D-1-thiogalactopyranoside (IPTG). The seeded plates were then incubated at room temperature for at least 12 hours to allow expression of the dsRNA. For egg on RNAi, young adults were transferred to the RNAi plates spread with the designated RNAi bacteria. The worms were then allowed to lay eggs for 3-6 hours before being removed from the plates. For L3 on RNAi (temporal *fib-1* RNAi), egg laying was done on normal NGM plates, and the larvae were allowed to feed and grow on the same plates until larval stage L3. The L3 larvae were then transferred to the RNAi plates.

2.4 Immunoblotting

Standard protocols of western blot were employed for detection of proteins. Worms were picked into ice-cooled M9 buffer. Laemmli lysis buffer with 5% 2-mercaptoethanol was then added to the buffer, and the mixture was immediately snap-frozen in liquid nitrogen. For mammalian cell samples, cells were lysed using

radioimmunoprecipitation assay (RIPA) buffer. 20 µg of protein was mixed with Laemmli lysis buffer with 5% 2-mercaptoethanol. The samples were then heated to 95°C for 10 minutes for denaturation of proteins. Denatured samples were then sonicated in a sonicating water bath for 10 minutes and loaded on 4-15% MiniPROTEAN® TGXTM Precast Protein Gels (Bio-Rad). Electrophoresis was conducted at constant voltage of 200V for around 40 minutes. Separated proteins were then transferred to PVDF membranes using Trans-Blot® TurboTM Transfer System (BioRad). The membranes were then blocked at room temperature in 5% Bovine serum albumin (BSA) or 5% milk in Tris-buffered Saline and Tween20 (TBST) for at least 1 hour. Primary antibody incubation was performed at 4°C overnight. On the next day, the membranes were washed with TBST for 45 minutes. After that, secondary antibodies were added, and the membranes were incubated at room temperature for 1 hour. The membranes were then washed again with TBST for 45 minutes. The membranes were imaged with ChemiDoc Imager (BioRad). Western Lightning® Plus Enhanced Chemiluminescence Substrate (PerkinElmer) was used as the chemiluminescence reagent.

Antibodies used in this study:

Target	Manufacturer	Reference	Dilution
Anti-Fibrillarin	Novus Biologicals	NB300-269	1:1000
Anti-Histone H3	Abcam	ab1791	1:4000
Anti-β-Actin	Abcam	ab8224	1:5000
Anti-GAPDH	Santa Cruz	sc47724	1:2500
Anti-Ubiquitin	Cell Signaling	P4D1	1:1000
Anti-Puromycin	Merck Millipore	12D10	1:10000
Anti-Phospho-p38 MAPK	Cell Signaling	9211	1:1000
Anti-GFP	Takara	632381	1:2000
Anti-Mouse HRP	ThermoFisher	G-21040	1:5000
Anti-Rabbit HRP	ThermoFisher	G-21234	1:5000

2.5 *C. elegans* sample preparation for RNA analysis

C. elegans samples used for polymerase chain reactions (PCRs) and RNA sequencing were prepared as described below. Egg laying was done, and the animals were allowed to grow at 20°C for around 72 hours to obtain age synchronized young adults. The adults were then washed in M9 buffer and transferred to 10cm TSA plates spread with either *S. aureus* or heat-inactivated *E. coli* OP50. These plates were also supplemented with 10 µg/mL NAL. *S. aureus* and *E. coli* OP50 were grown in TSB and LB medium respectively. Heat inactivation of *E. coli* culture was achieved by first concentrating the bacteria 10 times. The concentrated culture was then boiled for 10 seconds. 100 µl of the culture was spread on a LB plate, which was then incubated at 37°C overnight. Absence of colonies indicates a complete inactivation of the bacteria. 500 µl of *S. aureus* and heat-inactivated *E. coli* OP50 were then spread on the TSA plates, which were then incubated at 37°C for 6 hours. After that, the plates were allowed to equilibrate to room temperature before seeding *C. elegans*. TSA plates with heat-inactivated OP50 serve as the non-infection control here. The animals were incubated on the plates at 25°C for 4 hours. The worms were then washed off with M9 buffer before lysis with QIAzol Lysis Reagent (Qiagen).

2.6 RNA extraction and cDNA synthesis

C. elegans were lysed with QIAzol Lysis Reagent. RNA was extracted using the standard chloroform extraction method (Rio, Ares et al., 2010). The RNA was purified using RNeasy Mini Kit (QIAGEN). DNA impurities were removed by DNase digestion using RNase-Free DNase Set (Qiagen). Concentration and purity of the RNA samples were analyzed by NanoDrop 2000c (peqLab). cDNA synthesis was done using iScript cDNA synthesis kit (Bio-Rad). For all the kits mentioned, standard protocols provided by the manufacturer were followed.

2.7 Quantitative PCR

Power SYBR Green master mix (Applied Biosystems) was used for quantitative PCR (qPCR). The reagents and samples were pipetted onto a 384 well plate using JANUS

automated workstation (PerkinElmer). The reactions were run on a ViiA7 384 Real-Time PCR System machine (Applied Biosystems). *snb-1* was used as the endogenous control for normalization. Quantification was performed using the comparative CT method (Schmittgen & Livak, 2008).

qPCR primers used in this study:

Target	Forward	Reverse
<i>fib-1</i>	CAAACGTTGTCCCAATTGTCTG	GGAAGTTTTGGGCATTGAGAG
<i>ilys-2</i>	GTTGGATCGCTTTCTTGTGG	CGTCAGCACATCTCTTCCAG
<i>irg-1</i>	TGATCTTGTTCCGTACCCATG	ATCCTCTCCAGTTTCGTTTCATC
<i>spp-1</i>	GGTGTTTTCTGTGATGTCTGC	ATAGTCCAGCAAAGAGTTCCG
<i>nlp-34</i>	TCATCGCTTGCCTGTTGG	CATGGGCGGTAGTATGGG
<i>lys-3</i>	CCAAGATATGATTAGAAAGTGCGAAG	ACTAAACGTGTTCCAGCCTC
<i>lgg-1</i>	ACCCAGACCGTATTCCAGTG	ACGAAGTTGGATGCGTTTTTC
<i>irg-2</i>	TGTTGACGAGTTTTACTTCCG	CAATTGTGCCTTCAGTTTTTCATG
<i>hlh-30</i>	GGCAGCGACAAAATTCACAG	TCATCTTCCATGCCCATGAG
<i>fmo-2</i>	TGCCAAACAAGTCTACCTAGTC	TGTAGAGTGAGAAGAAACGCG
<i>cllec-7</i>	TGTTTATGGGACGATTGACG	TCCTGTCAATGCACCTTGTAC
<i>cllec-218</i>	GTTGGCAAGTGAAGGAAATGG	TGATATTTACGAGGACAGAAGCAG
#1 (pre-rRNA)	CTGTGTTTACACCCGAATGATTCTAG	CTAATCGTGAGATGGGACACTCATACA
#2 (pre-rRNA)	CGCAGACATATAGTCTAGCGAG	GATCCATAGATATTGCTGATGATTC
#5 (pre-rRNA)	AACGCATAGCACCAACTG	TCCGAAGAGAAGCCTAAG
#6 (pre-rRNA)	AATACTGGGATTTCGTCTA	GAGTTCAGGTTGAGATTAG
<i>nlp-30</i>	TTCTCGCCTGCTTCATGG	GTCCATAACCTCCATATCCGC
<i>C18D11.6</i>	AGTGGAAGCTAGTCAAACGC	GTGAAATCCCCAACCGAATG
<i>M01G2.9</i>	CAGTATTGAAGGCGCATGTTC	TGATACTTTGTTAGCCCTCCATTG
<i>hpo-15</i>	CGCTCTCCCATATTTCTCACTC	TCTGCGACCACTCAAATAACC
<i>frm-7</i>	CTGCCAATGTGCTTTGAGTG	TCCAGTTTCCGCTTCACC
<i>fbxa-24</i>	GAAGTACATTTCAAGGTTGCCG	GCATTTAATTACAAAGTTTGCAATTATCG
<i>F47B8.4</i>	TTGAGTATACATTGAATAAAATAGCATTG	TCAGTTCTAATACGACGCCTTG
<i>F18G5.6</i>	GAATTGAAGAGCTGAGAATGGC	TGGTGTTGGTATTGCTGAGTC
<i>F11E6.11</i>	ACAGCTCTTTTGTCATCTTTTCAG	AGCAATCGGGCATTATACTTCC
<i>C07A4.3</i>	AAGAATGTATCCGTCAGTGCC	AGATGAGAGGATTGCGTTGG
<i>M03B6.5</i>	TGGAGCTTTCTGATTATATCCTAG	ATTGAATTCCACTTTCTTCATCGTC
<i>lip1-2</i>	TTACCAACTCAGAGTGCAGC	GCCATTTTCATCCCAACTGAAC
<i>H11E01.2</i>	CTGCGTACTGGGCTACATTC	GAGATAGGACAAAGTGGGAGTG
<i>cyp-37B1</i>	AAGAATGTATCCGTCAGTGCC	AGATGAGAGGATTGCGTTGG
<i>cpz-2</i>	GAAATCGGAAATGTGCTAGAGC	GTGTAGTTGGTAAGGGAGAAGC
<i>R10E8.8</i>	AATCTTATAAAACAGGGATCGATTATACG	TCAGGTGCATTTCCGTATTTCG
<i>rnp-6</i>	CAGAAACAGCAACAGGAGAATC	GAAGCATATCTTCGCGGATTTTC
<i>snb-1</i>	GAATCATGAAGGTGAACGTGG	CCAATACTTGCGCTTCAGGG

The design of qPCR primers for pre-rRNA was adapted from a recent publication (Zhou, Feng et al., 2017).

2.8 RNA sequencing and bioinformatic analysis

Sample preparation was described in the sections “2.5 *C. elegans* sample preparation for RNA analysis” and “2.6 RNA extraction and cDNA synthesis”. Library preparation was done using 1 µg of total RNA as an input. We followed the protocol of Illumina TruSeq stranded RiboZero. After purification and validation (2200 TapeStation; Agilent Technologies), all 12 libraries (3 biological replicates, with control N2, control *rnp-6(dh1127)*, infected N2 and infected *rnp-6(dh1127)* in each biological replicate) were pooled which was then quantified by using the KAPA Library Quantification kit (Peqlab) and the 7900HT Sequence Detection System (Applied Biosystems). The libraries were then sequenced on one lane of an Illumina HiSeq4000 sequencing system using a paired end 2x75nt sequencing protocol. The data generated was subsequently analyzed. Alignment of the reads was done using the Hisat version 2.0.4 software against the Wormbase genome (WBcel235_89). For differential gene expression analysis between different samples, the stringtie version 1.3.0 was used followed by Cufflinks version 2.2. The dispersion between each condition was calculated (genotypes and infection), and differentially expressed genes (DEGs) (q-value<0.05) were identified. The DAVID (Database for Annotation, Visualization and Integrated Discovery) bioinformatics resources database was used for Gene Ontology (GO) annotation and enrichment analysis.

2.9 rRNA analysis

100 animals were harvested for each sample. The Worms were washed in M9 buffer and lysed in QIAzol Lysis Reagent. Total RNA was extracted as described in the section “2.6 RNA extraction and cDNA synthesis”. The RNA samples, each extracted from equal number of worms, were analyzed on an Agilent 2200 TapeStation System analyzer using the High Sensitivity RNA ScreenTape System protocol provided by the manufacturer (Agilent).

2.10 Puromycin incorporation assay

Worms were incubated in S-basal medium, which consists of 5.85 g/L NaCl, 1 g/L K_2HPO_4 and 6 g/L KH_2PO_4 in H_2O , supplemented with 0.5 mg/mL puromycin and *E.coli* OP50 as the food source at 20°C with shaking for 3 hours. For the cycloheximide control, 2 mg/mL of the chemical was included in the incubation mixture. After the incubation, 30 animals per condition were harvested using the same method described for worm immunoblotting in the earlier section. The samples were then analyzed using western blot for detection of incorporated puromycin.

2.11 Mammalian cell cultures

HeLa cells and THP-1 cells were obtained from American Type Culture Collection (ATCC). All cells were maintained at 37°C with 5% CO_2 in a humid atmosphere. HeLa cells were cultured in Dulbecco's modified Eagle's medium (DMEM) supplemented with 10% fetal calf serum (FCS). THP-1 cells were maintained in Roswell Park Memorial Institute (RPMI) medium supplemented with 10% FCS. Bone marrow derived macrophages (BMDMs) were isolated from 8-12 weeks old female C57BL/6J mice provided by the animal facility of Center for Molecular Medicine, University of Cologne, Germany. Briefly, femurs were obtained from mice sacrificed by cervical dislocation. Bone marrow cells were flushed out from the bone using RPMI medium. The cells were then centrifuged, washed and re-suspended in RPMI supplemented with 10% FBS. Differentiation was done by incubating the cells in medium consisted of RPMI with 10% FBS supplemented with 20% murine fibroblast L929 culture supernatant for 7 days. Cells which failed to differentiate remained in suspension and were removed by replacing the medium.

THP1 cells were differentiated into macrophages using the following protocol. The cells were incubated in 10% FCS RPMI medium supplemented with 25ng/ml of 12-O-tetradecanoylphorbol-13-acetate (PMA) for 24 hours.

2.12 Fibrillarin knockdown and overexpression in mammalian cell cultures

siRNA against fibrillarin was purchased from Dharmacon (GE Healthcare Life Sciences). Dharmafect-2 (GE Healthcare Life Sciences) was used to deliver the siRNA into HeLa cells and BMDMs using the manufacturer's protocol. Human fibrillarin-GFP fusion expression plasmid was ordered from Addgene (Catalog Number: 26673). Lipofectamine 3000 (ThermoFisher Scientific) was used as the transfection reagent for the plasmid following the manufacturer's protocol.

2.13 Infection of mammalian cells

S. aureus (MW2-WT), *E. faecalis* (ATCC 29212), *S. Typhimurium* (SL1344), and *L. monocytogenes* (EGDe) were used for infection at multiplicity of infection (MOI) 50 and MOI 10 for HeLa and macrophages (THP-1 derived and BMDM) respectively. Late logarithmic phase grown bacterial cultures were diluted in cell culture media (DMEM or RPMI) with 10% FCS to the desired MOI. The mixture was then incubated with the cells for 10 minutes at room temperature and then for 30 minutes at 37°C with 5% CO₂ in a humid atmosphere. After the incubation, the bacteria containing medium was removed, and the residual extracellular bacteria were killed by incubation with medium with 10% FCS and 50µg/ml gentamicin for 2 hours. After that, medium with lower concentration of gentamicin (10µg/ml) was used for continued culture.

2.14 Cell viability assays

Lactate dehydrogenase (LDH) release assay and trypan blue exclusion assay were used to measure viability of cells. LDH Cytotoxicity Assay Kit (CytoTox 96 Non-Radioactive Cytotoxicity Assay; Promega) was used for measuring released LDH. At the indicated time points after infection, cell culture medium was harvested, and LDH in the medium released by dead cells was measured according to the manufacturer's protocol. For the trypan blue method, dead cells were first washed off with phosphate-buffered saline (PBS). Viable cells were then dissociated by incubation with 0.5% trypsin. Cells were then mixed with trypan blue and counted using a hemocytometer. Cells that did not uptake trypan blue were counted as alive.

2.15 Bacterial burden assay

HeLa and BMDM cells were infected as described with *S. aureus*. At the indicated time-points, infected cells were washed with PBS and then lysed with 0.3% Triton X-100 in PBS at room temperature for 5 minutes. The lysate was then diluted in a 10-fold series, and the dilutions were plated on BHI plates. Colony-forming units (CFUs) were counted after overnight incubation at 37°C. To obtain bacterial burden per cell, the results were normalized to the number of cells seeded.

2.16 Immunocytochemistry

GFP expressing *S. aureus* was used to infect HeLa cells using the same protocol described. 250 nM lysotracker deep red (Invitrogen) was added to the cell cultures 24 hours after infection for visualization of lysosomes. The cells were incubated with the reagent for 15 minutes at 37°C with 5% CO₂ in a humid atmosphere. Excessive lysotracker was removed by washing with pre-warmed sterile PBS. 4% paraformaldehyde in PBS was used for cell fixation at room temperature for 15 minutes. The fixed samples were then washed with PBS and mounted on standard imaging glass slides with ProLong Gold mounting medium containing DAPI (ThermoFisher Scientific). Olympus IX81 inverted confocal microscope was used for image acquisition. Olympus Fluoview-10 ASW 4.2 was used for image processing and calculating Pearson's correlation.

2.17 Enzyme-linked immunosorbent assay (ELISA)

At the indicated time points, supernatants from infected and uninfected cells were harvested and immediately frozen in liquid nitrogen. ELISA of IL-6, IL-8 and IL10 was performed to gauge the levels of the cytokines using DUOSet ELISA kits from R&D Biosystems for human IL-6, IL-8 and IL-10, following the manufacturer's protocol.

2.18 *tos-1* alternative splicing PCR assay

Worms were treated as described in “2.5 *C. elegans* sample preparation for RNA analysis”. cDNA was synthesized from infected and control worms in the same way as described in the “2.6 RNA extraction and cDNA synthesis” section. DreamTaq DNA Polymerases (ThermoFisher) was used to amplify the *tos-1* segment.

Forward primer sequence: ATCTACGGATTTCGAGTCGTCACCATC.

Reverse primer sequence: GAAGAAATCTTCCAGTCCGAAGGG.

The primer design is based on a recent publication (Ma, Tan et al., 2011). The annealing temperature was 57°C. PCR reactions were cycled for 35 cycles. The products were analyzed by agarose electrophoresis, and DNA was visualized by staining with Roti®-GelStain (Carl Roth).

CHAPTER 3
ROLES OF FIBRILLARIN
IN HOST RESPONSES
DURING INFECTION

Roles of fibrillarin in host responses during infection

3.1 Introduction

As discussed in the introduction of the thesis, one of the two focuses is fibrillarin, an evolutionarily conserved nucleolar protein responsible for methylation modification of rRNA (Rodriguez-Corona et al., 2015). Fibrillarin was found to be downregulated in multiple stress resistant long-lived mutants (Tiku et al., 2016). These mutants, such as the IIS mutants (Garsin et al., 2003) and gonadally ablated mutants (Wu, Cao et al., 2015), display enhanced resistance to pathogenic insults as well. However, the role of fibrillarin and the nucleolus in host response to infection has not yet been characterized. We reasoned that downregulation of fibrillarin may alter host responses. We investigated the effects of fibrillarin on infection responses in both *C. elegans* and mammalian cells. Results suggest that the nucleolus and fibrillarin play a critical role in the initiation of protective responses from the host in both nematodes and mammalian cells, suggesting that this effect is evolutionarily highly conserved.

3.2 Results

3.2.1 FIB-1/fibrillarin reduction enhances resistance against bacterial infection in *C. elegans*

FIB-1/fibrillarin is a highly conserved nucleolar methyltransferase necessary for the maturation of rRNA. It has been recently reported that long-lived mutants of *C. elegans* have reduced levels of FIB-1 protein and smaller nucleoli. Further, knocking-down *fib-1* is already sufficient to extend lifespan in worms (Tiku et al., 2016). Lifespan extending conditions often also induce resistance to stresses, including infections. Therefore we tested whether *fib-1* reduction could confer infection resistance. Worms were grown on normal NGM plates with OP50 bacteria. RNAi was initiated by transferring the worms to RNAi plates 30 hours before the experiment in order to prevent the deleterious effects of *fib-1* reduction on development. This treatment led to a significant reduction of FIB-1 protein with no obvious developmental phenotype (Fig. 6A). Intriguingly, when these worms were infected, they showed enhanced resistance

against multiple pathogens, namely *S. aureus* (Fig. 5A), *E. faecalis* (Fig. 5B) and *P. aeruginosa* (Fig. 6B). Interestingly, the effect was specific to pathogenic stress because *fib-1* knockdown did not affect resistance to other stresses, including heat (Fig. 6C), cold (Fig. 6D) and oxidative stress (Fig. 6E). Bacterial intake, indicated by pharyngeal pumping rate, was unaffected by *fib-1* knockdown (Fig. 6F), suggesting the observed effects are not due to dietary restriction or differential ingestion of the bacteria. The protection conferred by *fib-1* knockdown was not due to increased aversion behavior, because similar level of resistance was observed using full lawn plates, whose entire agar surface was covered by bacteria (Fig. 6G,H). Next, *ncl-1* loss-of-function mutants were tested for their resistance. NCL-1 is a negative regulator of FIB-1, and the mutants possess elevated level of FIB-1 (Tiku et al., 2016, Yi et al., 2015). *ncl-1* mutants showed higher susceptibility to infection (Fig. 5C,D). This suggests that increased levels of FIB-1 in the *ncl-1* mutants compromised survival upon infection.

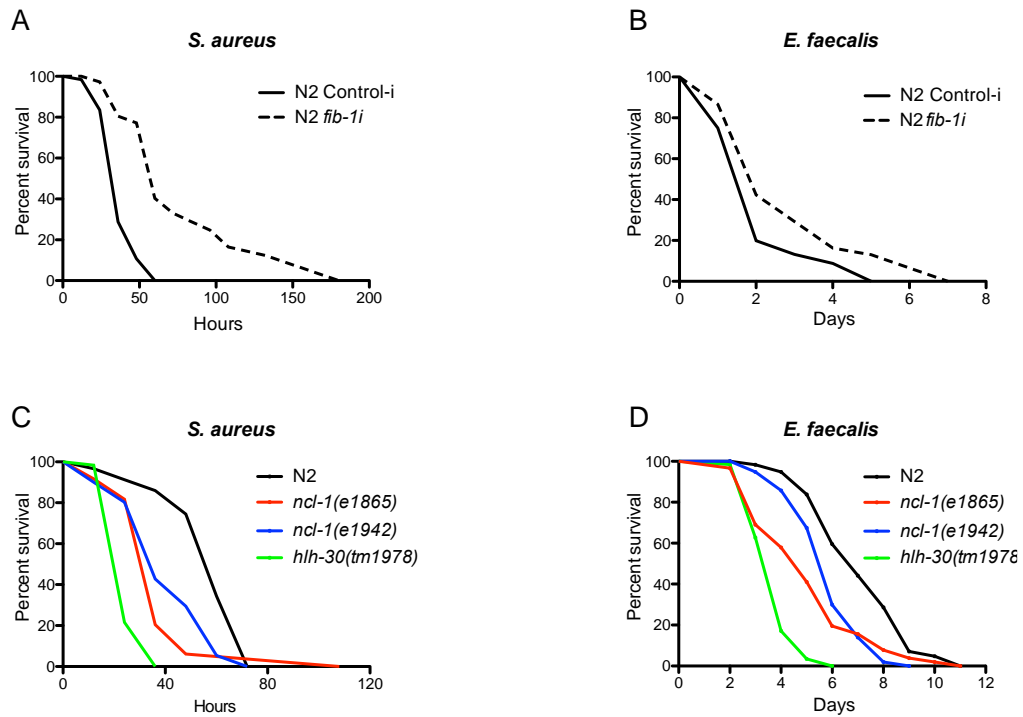


Figure 5. (A,B) Temporal RNAi against *fib-1* prolongs survival of wildtype N2 *C. elegans* upon *S. aureus* and *E. faecalis* infection ($P < 0.0001$). (C,D) *ncl-1* mutants (*e1865* and *e1942*) are sensitive compared to wildtype N2 worms upon infection with *S. aureus* and *E. faecalis* ($P < 0.0001$). *hlh-30(tm1978)*, a well-established sensitive mutant, served as a control and reference for the experiments. P-values were calculated by log-rank test.

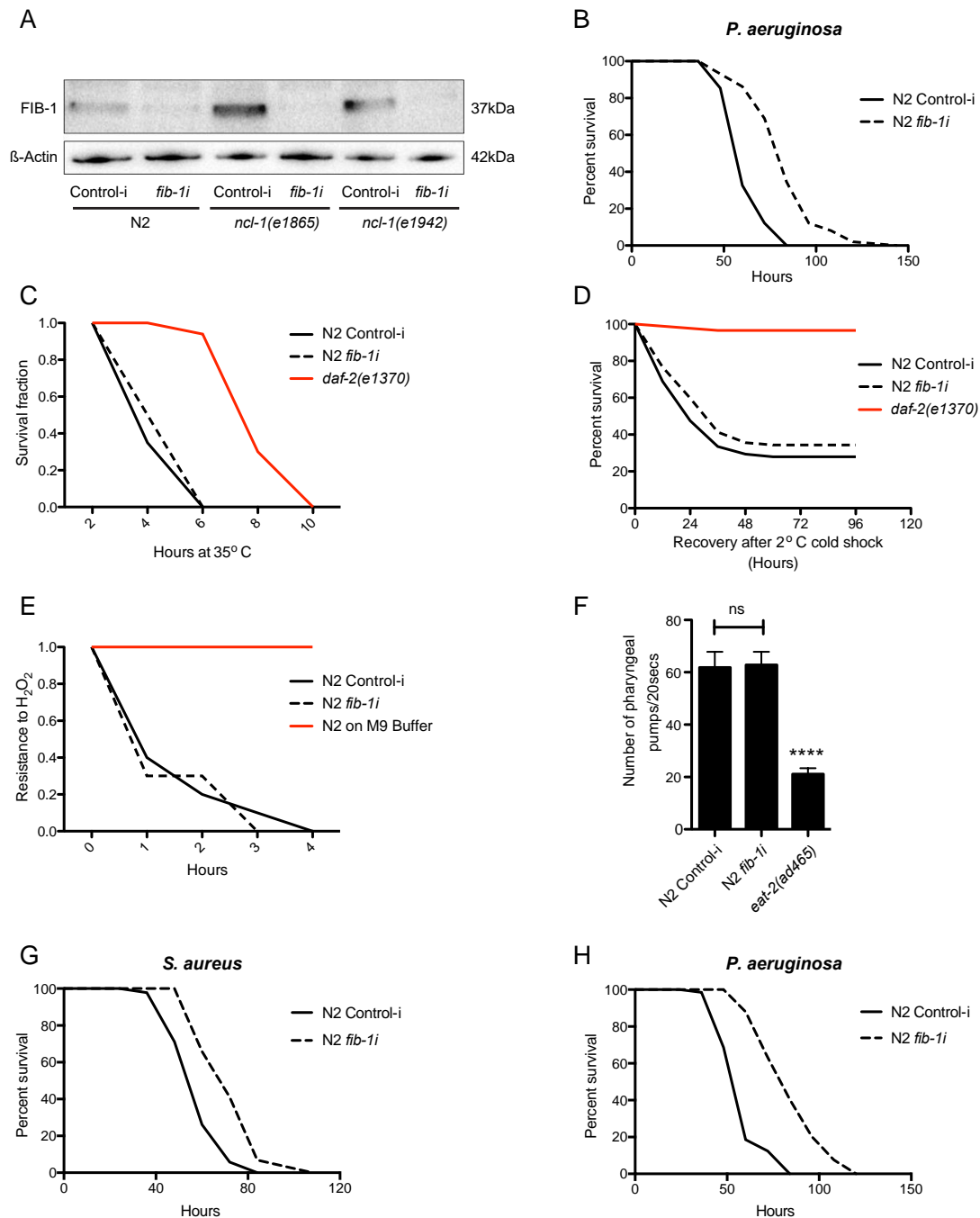


Figure 6. (A) FIB-1 protein was significantly reduced after the temporal (30 hours) RNAi treatment. (B) *fib-1* RNAi prolongs survival of wildtype N2 worms upon *P. aeruginosa* infection ($P < 0.0001$, log-rank test). (C,D,E) *fib-1* RNAi does not affect heat resistance, cold shock recovery, or oxidative stress tolerance in wildtype worms. (F)

Pharyngeal pumping rate is not affected by *fib-1* RNAi. Error bars represent mean \pm s.d. **** $P < 0.001$, unpaired t-test. (G,H) Survival assay using full lawn bacterial plates which eliminate behavioral avoidance ($P < 0.0001$, log-rank test).

3.2.2 Bacterial infection induces FIB-1/fibrillarin reduction and nucleolar shrinkage

Since FIB-1 levels affect infection resistance, it was hypothesized that infection may perturb FIB-1. Western blot was performed to detect the endogenous levels of FIB-1 of infected *C. elegans*. After 12-hours of infection with *S. aureus*, *E. faecalis* (Fig. 7A) and *P. aeruginosa* (Fig. 8A), FIB-1 protein levels were significantly down-regulated in wildtype animals. Infected *ncf-1* mutants also exhibited a reduction of FIB-1, although the level of reduction was milder, and the relative levels remained significantly higher compared to infected wildtype animals (Fig. 7A,B). Similar results were also obtained using a FIB-1::GFP translational fusion reporter. After infection, FIB-1::GFP was greatly reduced, suggesting a decrease of FIB-1 abundance (Fig. 7C). Infection induced FIB-1 reduction is likely to be a post-transcriptional response, as no significant changes in *fib-1* mRNA level were detected using qRT-PCR (Fig. 8B). Because FIB-1 is an essential nucleolar protein, reduction of FIB-1 can lead to a perturbation of the nucleolus. Morphology of nucleoli of infected worms was examined under DIC microscopy. As expected, nucleoli shrunk significantly after 12-hours of infection with *S. aureus* and *E. faecalis* (Fig. 7D,E). This phenomenon seems to be driven by active bacteria because heat killed bacteria did not induce nucleolar shrinkage (Fig. 8C,D). Unlike wildtype, nucleolar size of *ncf-1* mutants appeared to remain as the uninfected size (Fig. 7D,E). Since the nucleolus is the site of rRNA transcription and maturation, and FIB-1 is indispensable for this process, we hypothesized that rRNA levels would also be affected by pathogen infection. Indeed, *S. aureus* infection caused a reduction of mature rRNA levels (Fig. 7F).

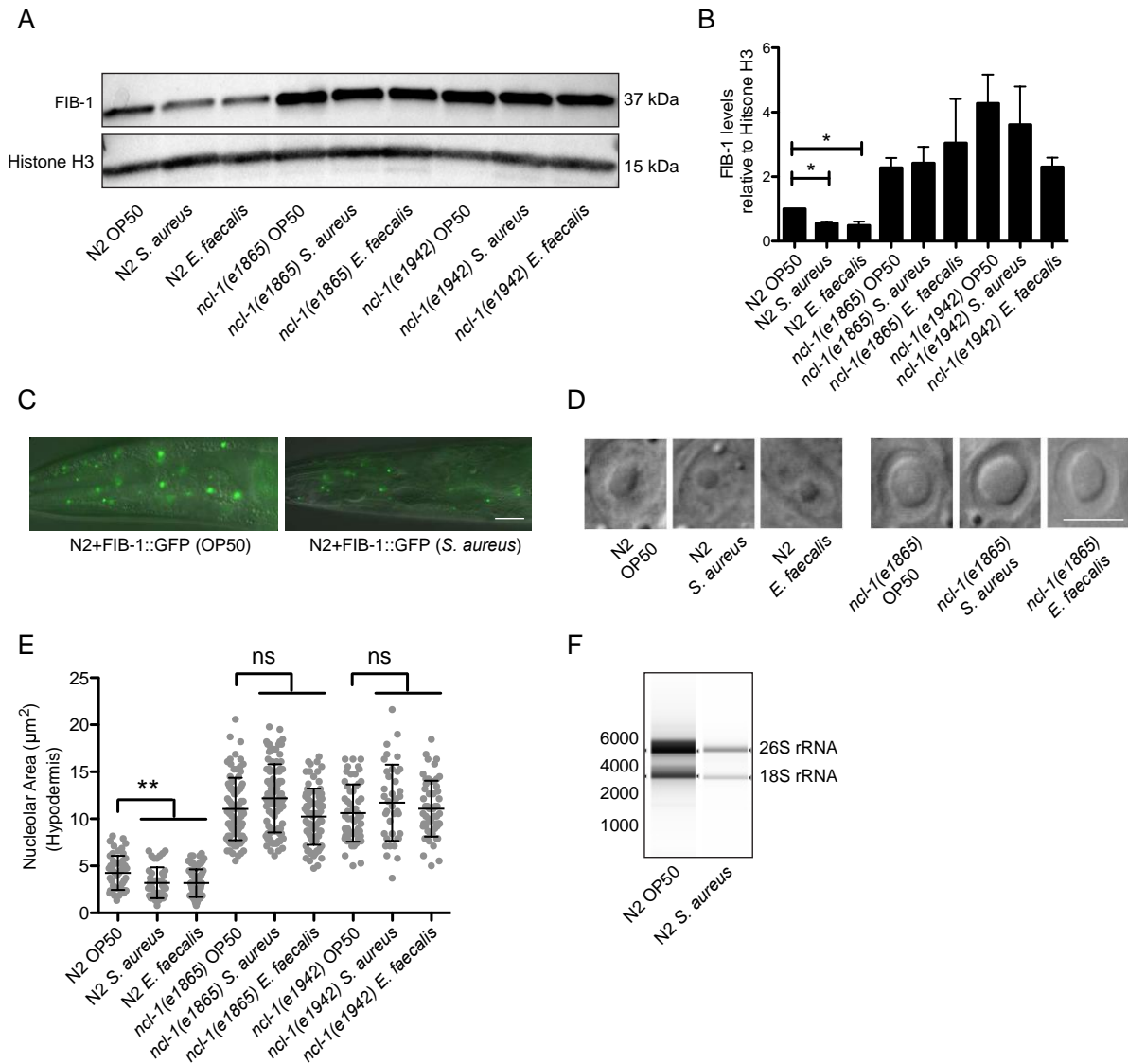


Figure 7. (A,B) Decrease of FIB-1 protein levels in wildtype N2 and the *ncd-1* mutants infected with *S. aureus* or *E. faecalis*. Error bars represent mean \pm s.e.m. of three independent biological replicates. (C) Expression of FIB-1 translational GFP reporter decreases after infection of *S. aureus*. (D,E) Nucleolar size of hypodermal cells is reduced after 12-hour of infection with *S. aureus* or *E. faecalis* in wildtype N2 worms while nucleolar size of hypodermal cells in the *ncd-1* mutants remains largely unaffected. Error bars represent mean \pm s.d. (F) Wildtype *C. elegans* infected with *S. aureus* possesses less 26S and 18S mature rRNA. RNA was extracted from equal number of uninfected and infected worms. The RNA was then analyzed using a bioanalyzer. Scale bars represent 20 μm (C) and 5 μm (D). * $P < 0.05$, ** $P < 0.01$, ns non-significant, unpaired t-test.

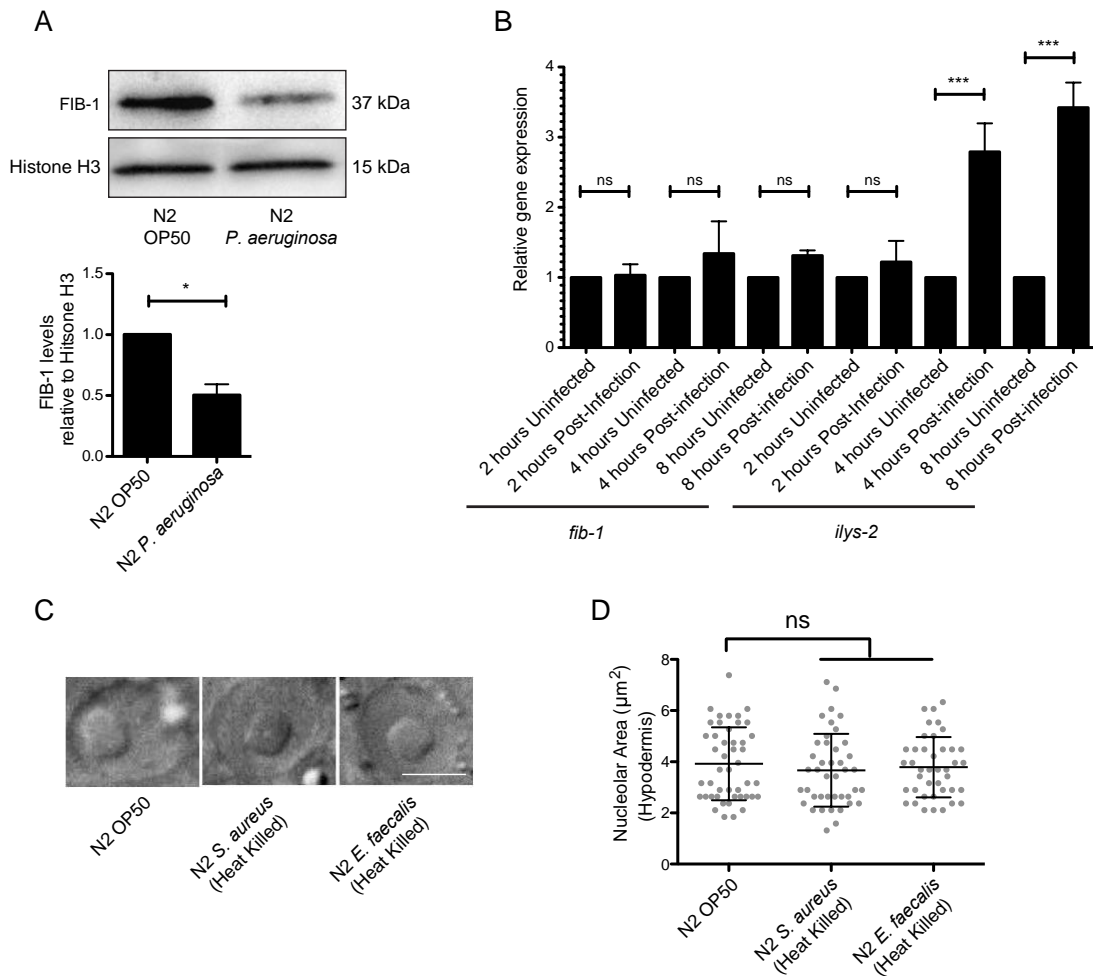


Figure 8. (A) After infection with *P. aeruginosa*, FIB-1 protein abundance is significantly reduced in wildtype animals. Error bar represents mean \pm s.e.m. of three independent biological replicates. * $P < 0.05$, unpaired t-test (B) *S. aureus* infection does not change the transcript levels of *fib-1* while expression of *ilys-2*, an infection responsive gene, is highly induced. Error bars represent mean \pm s.e.m. from three independent biological replicates *** $P < 0.001$, one-way ANOVA. (C,D) Unlike active bacteria, heat-killed *S. aureus* and *E. faecalis* do not alter nucleolar size of hypodermal cells. Error bars represent mean \pm s.d. ns non-significant, unpaired t-test. Scale bar represents 5 μ m.

3.2.3 FIB-1/fibrillarin reduction also confers resistance to infection sensitive mutants

It has been shown in previous studies that some *C. elegans* mutants show increased sensitivity upon bacterial infection, suggesting the genes play an indispensable role in innate immunity (Garsin et al., 2003, Kim et al., 2002, Visvikis et al., 2014). We sought to investigate whether these established mediators of innate immunity interact with *fib-1*. RNAi knockdown of *fib-1* was performed on mutants of *pmk-1*, *hlh-30* and *daf-16*. Interestingly, *fib-1* reduction was able to confer resistance against both *S. aureus* (Fig. 9A,B,C) and *E. faecalis* (Fig. 10A) in all these mutants, suggesting *fib-1* regulates innate immunity independently or acting downstream of these known regulators. *pmk-1* encodes the worm's ortholog of p38 MAP kinase, which is a key evolutionarily conserved signal transducer of innate immunity (Kim et al., 2002). *hlh-30*, which encodes the ortholog of mammalian TFEB, is an essential transcription factor for induction of immune response genes and autophagy during infection in both worms and mammalian macrophages (Visvikis et al., 2014). *fib-1* RNAi did not affect HLH-30::GFP fusion reporter localization (Fig. 11A,B) nor autophagic flux (Fig. 11C). In both control and infected animals, autophagic flux was the same after *fib-1* RNAi as indicated by the cleavage of the autophagosomal membrane protein LC3/LGG-1 (Fig. 11C). Next, the potential involvement of ubiquitin-proteasome system (UPS) was examined. No difference in the abundance of ubiquitinated proteins was observed after reduction of FIB-1 under both control and infected conditions (Fig. 11D). These results suggest that the enhanced survival by *fib-1* reduction is unlikely due to improved proteolytic mechanisms. Further, *fib-1* reduction also rescued the reduced survival of the *ncl-1* mutants (Fig. 9D, Fig. 10B,C). All in all, these results suggest that FIB-1 is a novel mediator of host response, probably functioning independently or downstream of the established pathways.

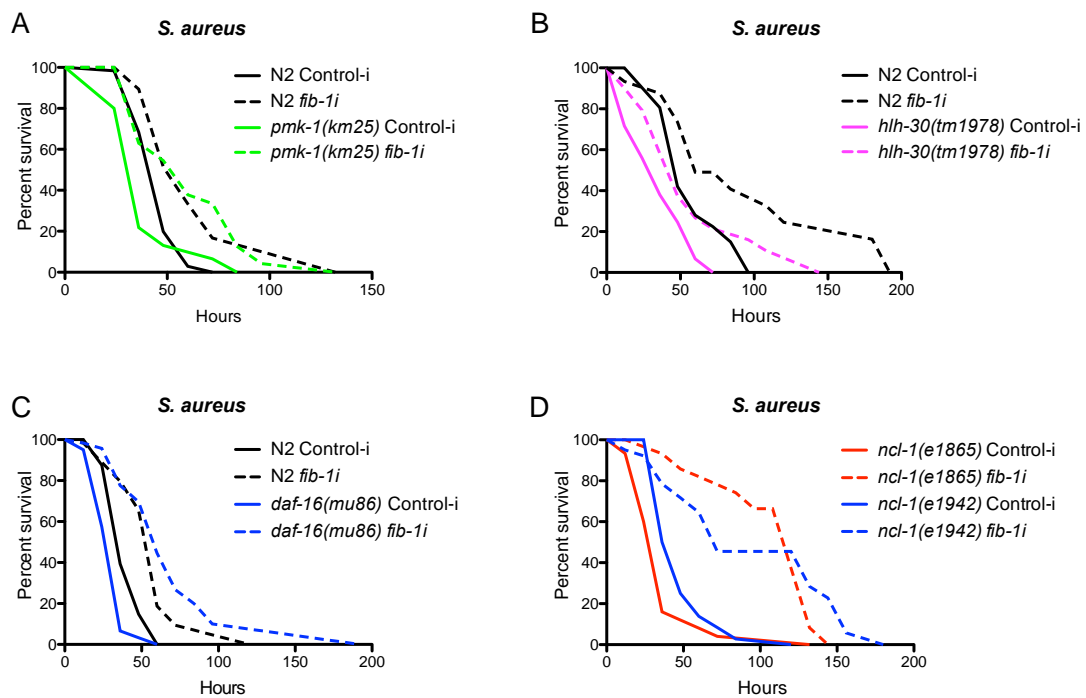


Figure 9. (A,B,C,D) *fib-1* RNAi promotes the survival of the sensitive mutants *pmk-1(km25)* ($P=0.0001$), *hlh-30(tm1978)* ($P=0.0021$), *daf-16(mu86)* ($P<0.0001$) and *ncl-1(e1865* and *e1942)* ($P<0.0001$) upon *S. aureus* infection. P-values were calculated by log-rank test.

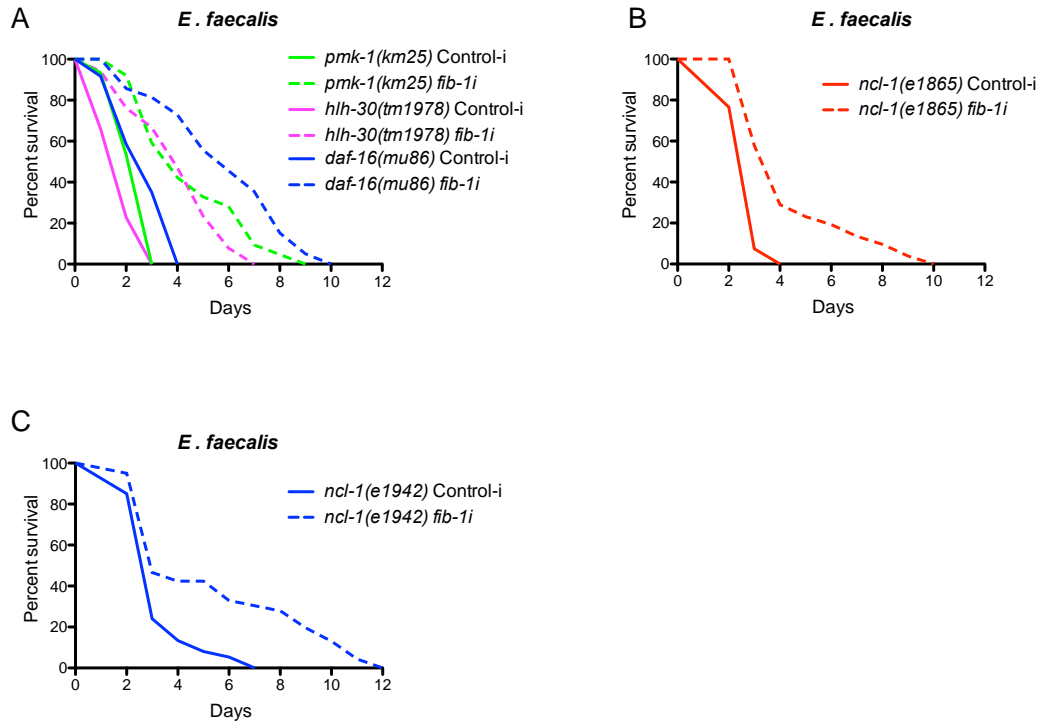


Figure 10. (A,B,C) *fib-1* RNAi promotes the survival of the sensitive mutants *pmk-1(km25)* ($P < 0.0001$), *hllh-30(tm1978)* ($P < 0.0001$), *daf-16(mu86)* ($P < 0.0001$) and *ncl-1(e1865* and *e1942)* ($P < 0.0001$) upon *E. faecalis* infection. P-values were calculated by log-rank test.

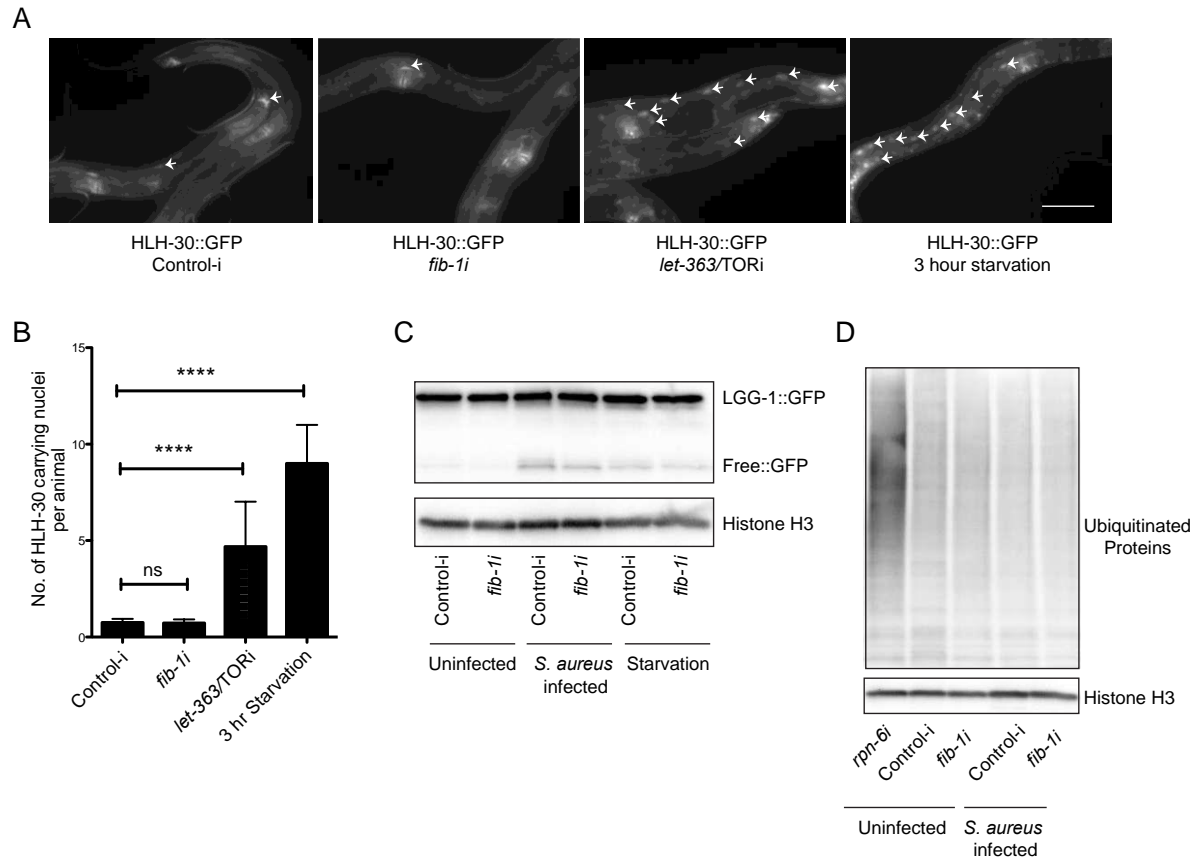
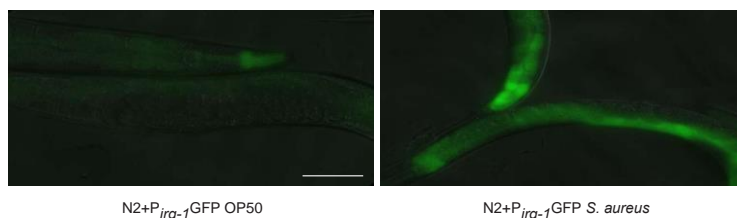


Figure 11. (A,B) *fib-1* RNAi does not affect HLH-30::GFP localization. The positive control, *let-363/TOR* RNAi and 3 hours of starvation induce HLH-30::GFP localization into the nucleus. HLH-30::GFP signal is indicated by the white arrows. (C) Western blots detection of LC3/LGG-1::GFP and cleaved GFP in control and *fib-1* RNAi animals upon infection with *S. aureus*. No obvious effects of *fib-1* RNAi on LGG-1::GFP cleavage can be observed. Infection increases the abundance of the free GFP band suggestive of enhanced autophagic flux. Starvation serves as a positive control here. (D) Western Blot detection of ubiquitinated protein levels in control and *fib-1* RNAi treated animals under control or infected conditions. Again, no effects for *fib-1* RNAi on the abundance of ubiquitinated proteins. *rpn-6* RNAi serves as a positive control.

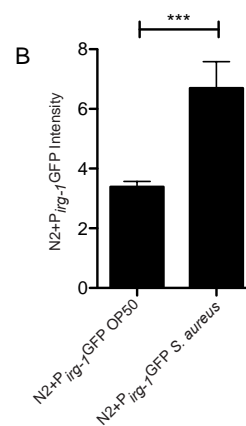
3.2.4 FIB-1/fibrillarin reduction leads to reduced translation

Fibrillarin mediates the critical steps of ribosome maturation. We therefore investigated how ribosome biogenesis and translation are affected by *fib-1* knockdown and whether translation could be the mechanistic explanation for the resistance phenotype. First, we utilized the *irg-1* transcriptional reporter. Expression of *irg-1* is induced by the transcription factor ZIP-2 upon infection. Pathogen induced translational blockage leads to a global reduction of protein synthesis, but also triggers preferential translation of ZIP-2 in a manner dependent on its upstream 5' UTR. Therefore, an increase in *irg-1* expression would indicate suppression of translation. We observed a moderate induction of the reporter after infection of *S. aureus* (Fig. 12A,B). As a control, cycloheximide treatment also activated *irg-1* reporter expression in a similar manner (Fig. 13A). Similar induction of the reporter was also observed upon *fib-1* reduction by RNAi (Fig. 12C,D). Induction of *irg-1* was confirmed using RT-qPCR (Fig. 12E). Although *irg-1* was induced, other infection related genes were not affected by *fib-1* RNAi (Fig. 13B), suggesting it is specific for *irg-1* and unlikely to be a generalized inflammatory response. All these data support *fib-1* reduction decreases translation. Indeed, *fib-1* knockdown induced translation suppression as indicated by a reduction of puromycin incorporation (Fig. 12G,H). It was also observed that mature rRNA levels decreased (Fig. 12F), and pre-rRNA levels increased upon *fib-1* knockdown (Fig. 13C). This can be explained by a blockage in rRNA maturation resulted by FIB-1 reduction. This also suggests that the reduction of the levels of mature rRNA levels occurs post-transcriptionally. Next, we tested whether reduced translation is sufficient to confer resistance. For this, *ifg-1* and *ife-2* partial loss of function mutants were used. *ifg-1* encodes the eIF4G, and *ife-2* encodes the cap binding initiation factor eIF4E. Both proteins are translation initiation factors. The mutants exhibited enhanced resistance compared to wild-type (Fig. 12I, Fig. 13D), suggesting reducing translation can confer resistance. Moreover, *fib-1* RNAi only slightly enhanced the survival of the *ifg-1* mutants (Fig. 12J,K). Collectively, these results indicate that the resistance conferred by *fib-1* reduction might mechanistically overlap with the resistance conferred by translational reduction.

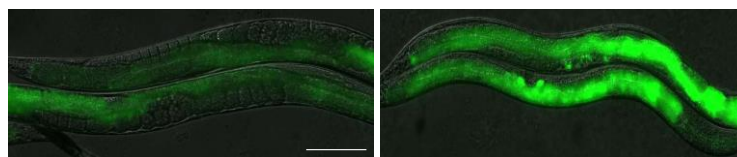
A

N2+P *ifg-1* GFP OP50N2+P *ifg-1* GFP *S. aureus*

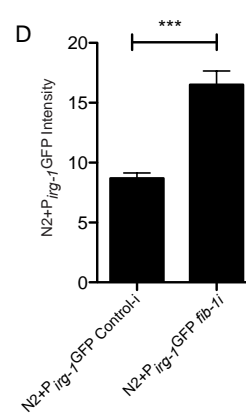
B



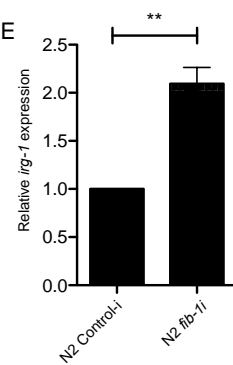
C

N2+P *ifg-1* GFP Control-iN2+P *ifg-1* GFP *fib-1i*

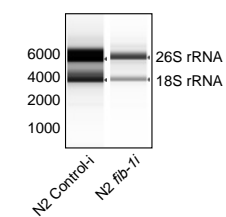
D



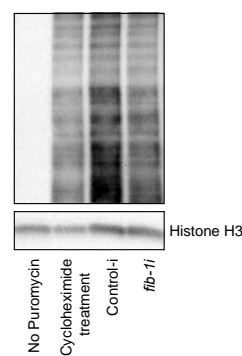
E



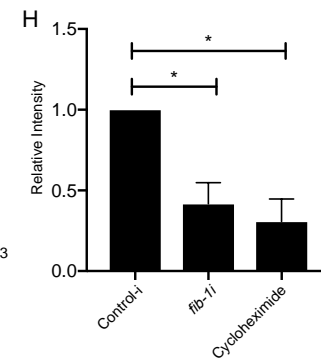
F



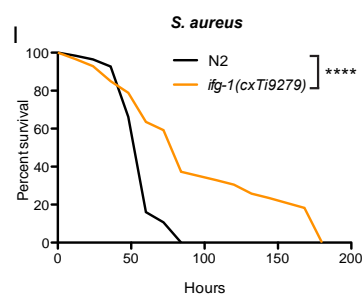
G



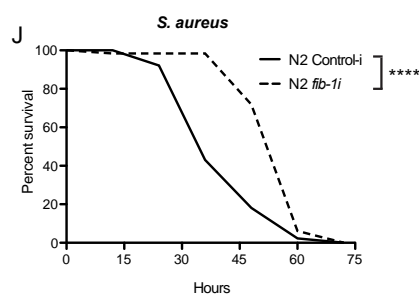
H



I



J



K

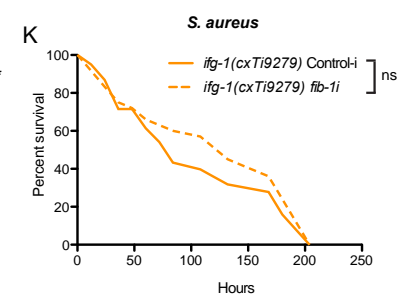
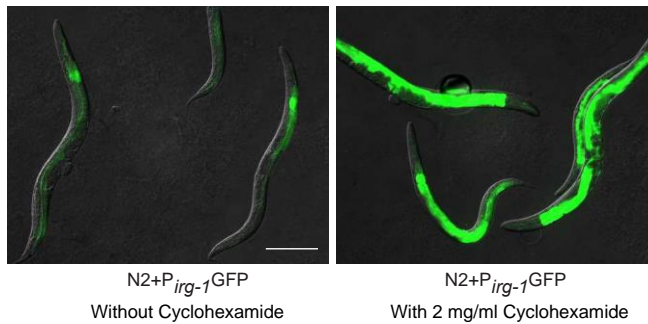
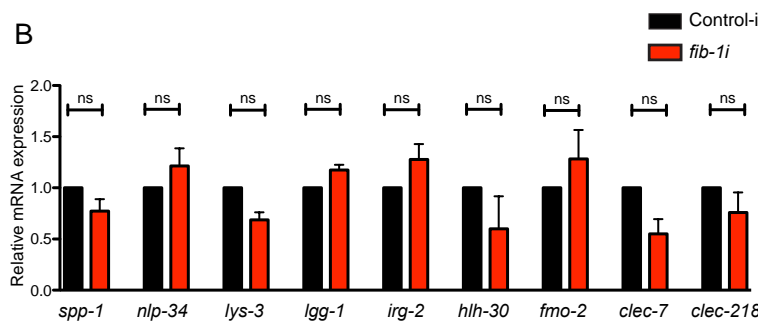


Figure 12. (A,B) P_{irg-1} GFP transcriptional reporter is induced after 12-hour *S. aureus* infection. Error bars represent mean \pm s.e.m. (C,D,E) *fib-1* knockdown induces P_{irg-1} GFP transcriptional reporter and the transcript levels of *irg-1*. Error bars represent mean \pm s.e.m. (F) *fib-1* RNAi leads to a reduction of 26S and 18S mature rRNA levels in worms. Total RNA extracted from equal number of animals was analyzed using a bioanalyzer. (G,H) *fib-1* RNAi treatment reduces puromycin incorporation in worms. No puromycin and cycloheximide treatments serve as controls here. Error bars represent mean \pm s.e.m. (I) *ifg-1(cxTi9279)* shows improved survival upon *S. aureus* infection ($P < 0.0001$, log-rank test). (J,K) *fib-1* knockdown significantly enhances the survival in wildtype N2 animals ($P < 0.0001$, log-rank test) but not in the *ifg-1(cxTi9279)* mutant ($P = 0.74$, log-rank test) upon *S. aureus* infection. Scale bars represent 100 μ m. * $P < 0.05$, ** $P < 0.01$, *** $P < 0.001$, **** $P < 0.0001$, ns non-significant, unpaired t-test.

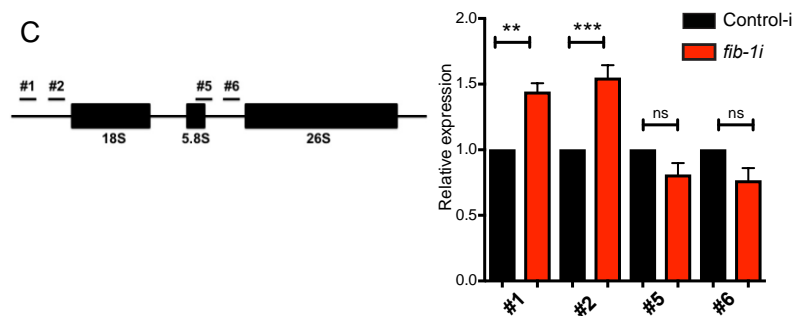
A



B



C



D

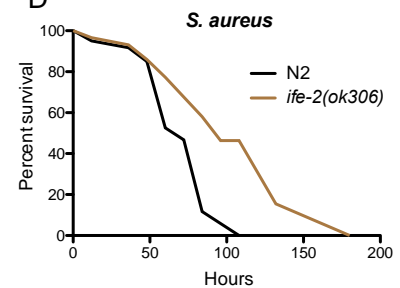


Figure 13. (A) Cycloheximide (2mg/ml) treatment induces P_{irg-1}GFP transcriptional reporter. (B) *fib-1* RNAi does not generally induce expression of infection responsive genes. Error bars represent mean \pm s.e.m. from three independent biological replicates, ns non-significant one-way ANOVA. (C) qRT-PCR detection of pre-rRNA species. *fib-1* RNAi increases the abundance of pre-rRNA species. The illustration shows the annealing sites of the primers used. *snb-1* was used for normalization. Error bars represent mean \pm s.e.m. **P<0.01, ***P<0.001. One-way Anova was used for statistics (D) *ife-2(ok306)* shows enhanced resistance upon *S. aureus* infection (P=0.0034, log-rank test). Scale bar represents 200 μ m.

3.2.5 Fibrillarin reduction protects against bacterial infection in mammalian cells

The above data suggest that reduction of fibrillarin is a protective host response in *C. elegans*. We wondered whether mammalian fibrillarin may have similar functions in innate immunity during bacterial infection.

To begin with, we checked whether bacterial infection also leads to a reduction of fibrillarin in human cells. Indeed, human cervical cancer cell line HeLa cells infected with *S. aureus* exhibited decreased levels of fibrillarin (Fig. 14A). Similar effects can also be observed in BMDM, which are primary macrophage cells differentiated from murine bone marrow, infected with *S. aureus*, *E. faecalis* (Fig. 14B), *S. typhimurium* and *L. monocytogenes* (Fig. 14C). Infection by these bacteria diminished fibrillarin after 24 hours of infection. Because infection leads to shrinkage of nucleoli in infected *C. elegans*, nucleolar size of infected mammalian cells was also imaged. For this experiment, THP-1 derived macrophages were chosen because of their clear and non-fragmented nucleolar morphology. After 24 hours of infection with *S. aureus*, a modest reduction of nucleolar size could be observed (Fig. 14D,E). All in all, these data suggest that reduction of fibrillarin and shrinkage of nucleoli are an evolutionarily conserved host response to infection.

Next, the potential regulation of resistance by fibrillarin reduction was investigated. siRNA against fibrillarin was transfected into BMDM and HeLa cells before infection (Fig. 15A). After infection with *S. aureus*, cell survival of fibrillarin knockdown HeLa cells was significantly improved compared to control siRNA transfected cells as assayed by LDH cytotoxicity assay (Fig. 15B) and trypan blue exclusion assay (Fig. 15C). Similar results were also observed in BMDM after knockdown of fibrillarin (Fig. 14F). Fibrillarin knockdown also improved clearance of intracellular *S. aureus* in BMDM (Fig. 14G). On the other hand, over-expression of fibrillarin in HeLa cells slightly increased the number of dead cells after infection (Fig. 15D). The effects of fibrillarin knockdown and overexpression cannot be explained by differential bacterial uptake by the cells as bacterial burden was comparable at the beginning of the infection (Fig. 15E,F). In addition, fibrillarin knockdown prior to infection suppressed infection induced production of pro-inflammatory cytokines IL-6 and IL-8 (Fig. 14H), but further

stimulated the secretion of anti-inflammatory cytokine IL-10 (Fig. 14I) in BMDM. Similar results were also obtained with HeLa cells (Fig. 15G). This indicates that fibrillarin reduction promotes immune homeostasis and reduced inflammation. Improved survival and better clearance of bacterial cells can be due to augmented intracellular bacteriolytic activity. To test this possibility, GFP labelled *S. aureus* was used to infect HeLa cells. Increased colocalization of the intracellular GFP labelled bacteria and lysosomes was observed in fibrillarin siRNA transfected BMDM compared to control siRNA transfected cells (Fig. 14J,K), which indicates increased digestion of bacteria and might explain the better intracellular bacterial clearance and enhanced cell survival upon fibrillarin knockdown.

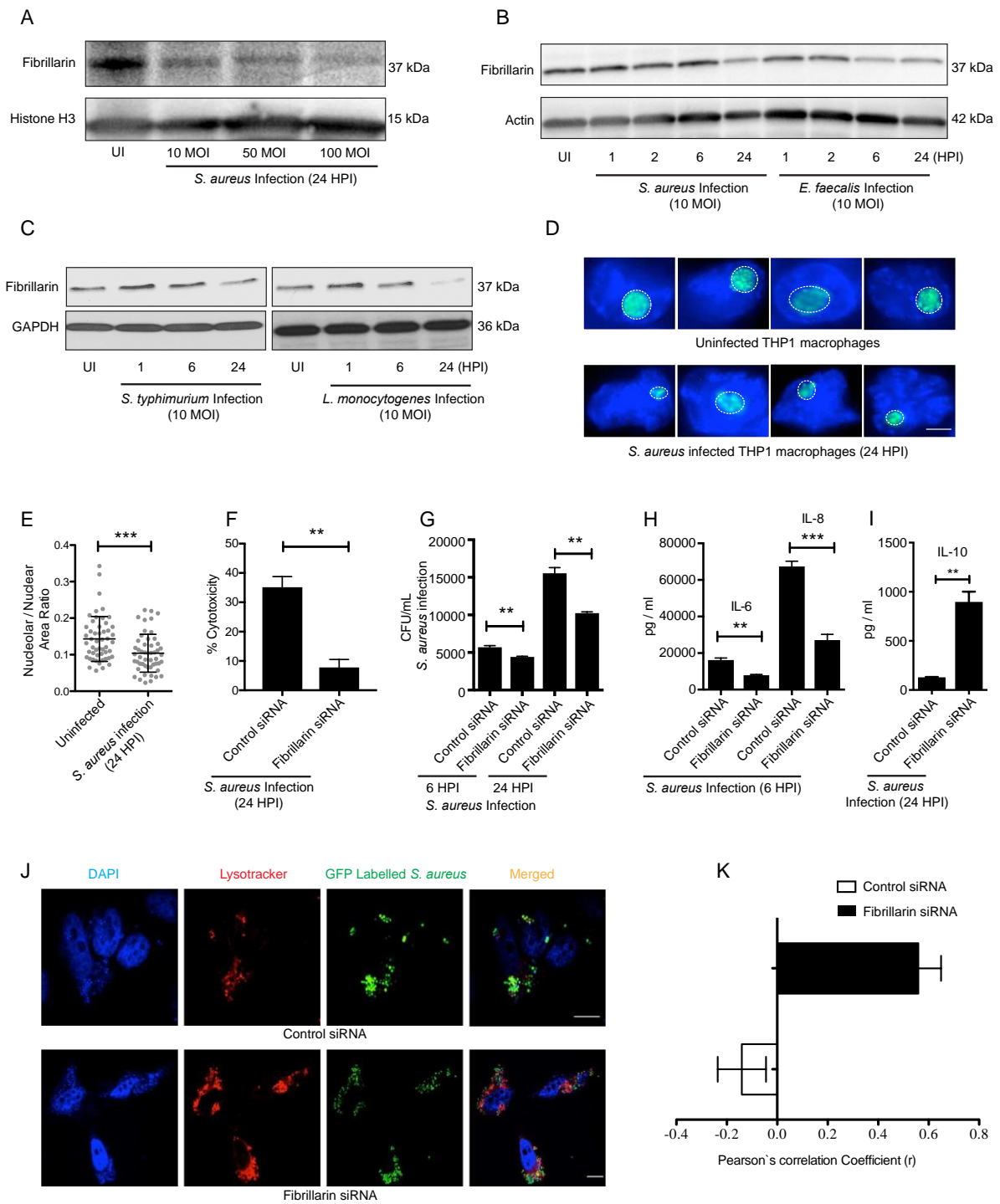


Figure 14. (A) Reduction of fibrillarin protein levels after *S. aureus* infection in HeLa cells. (B,C) BMDM also shows a reduction of fibrillarin 24 hours post-infection with *S. aureus*, *E. faecalis*, *S. typhimurium* and *L. monocytogenes*. (D,E) A shrinkage of nucleoli was observed after 24-hour infection with *S. aureus* in THP-1 derived macrophages. Error bars represent mean \pm s.d. (F) LDH release assay suggests fibrillarin knockdown reduces cell death after 24 hours of *S. aureus* infection (MOI 10) in BMDM. Error bars represent mean \pm s.e.m., unpaired t-test (G) Lower intracellular bacteria counts indicate fibrillarin siRNA leads to a better clearance of the bacteria after 6 and 24 hours of *S. aureus* infection (MOI 10) in BMDM. Error bars represent mean \pm s.e.m., unpaired t-test. (H) Pro-inflammatory cytokines IL- 6 and 8 in supernatant from *S. aureus* infected BMDM were quantified using ELISA method. Fibrillarin transfected cells show reduced secretion of IL-6 and 8. Error bars represent mean \pm s.e.m. (I) ELISA results show an increased production of anti-inflammatory cytokine IL-10 after 24 hours of infection with *S. aureus* in fibrillarin siRNA transfected BMDM. Error bars represent mean \pm s.e.m, **P<0.01 unpaired t-test. (J,K) GFP expressing *S. aureus* was used to infect HeLa cells. The cells were stained with lysotracker and show enhanced co-localization of bacterial cells with lysosomes, when treated with fibrillarin siRNA. **P<0.01, ***P<0.001, unpaired t-test. Scale bars represent 4 μ m (D) and 10 μ m (J). UI – Uninfected, HPI – Hours Post Infection, MOI – Multiplicity of Infection

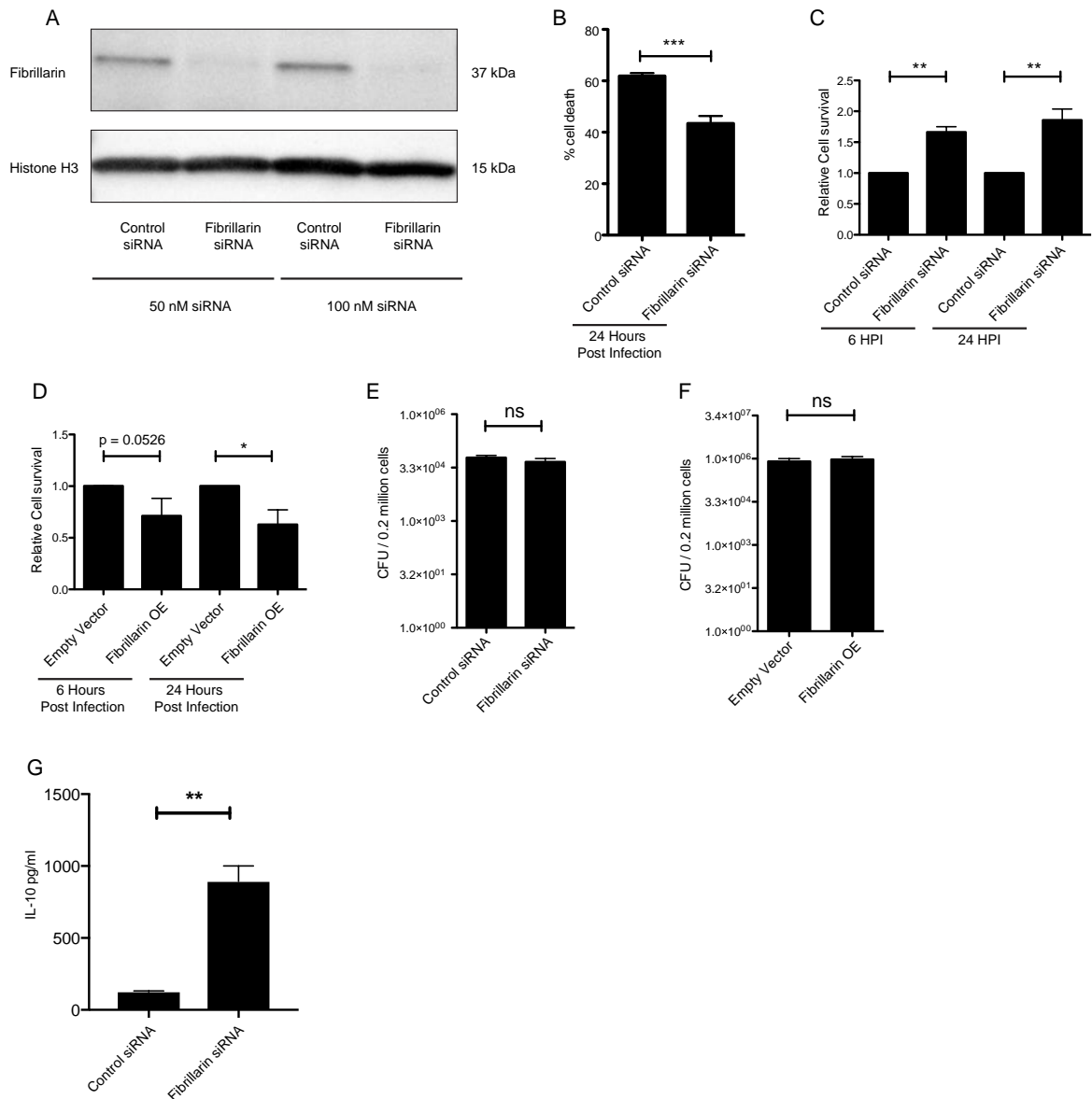


Figure 15. (A) 50 and 100 nM fibrillarin siRNA significantly reduces abundance of fibrillarin protein in HeLa cells. (B) Fibrillarin knockdown reduces cell death in *S. aureus* infected HeLa cells as measured by LDH release assay (**P<0.001, unpaired t-test, error bars represent mean \pm s.e.m.). (C) Fibrillarin knockdown protects HeLa cells from cell death after 6 and 24 hours of *S. aureus* infection as assayed by trypan blue exclusion assay. Error bars represent mean \pm s.e.m., one-way ANOVA. (D) Over-expression of fibrillarin in HeLa cells moderately reduces cell survival after 6 and 24 hours of *S. aureus* infection. Error bars represent mean \pm s.e.m. *P<0.05, one-way

ANOVA. (E,F) Fibrillarin knockdown and over-expression do not affect bacterial uptake in HeLa cells. Intracellular CFU was immediately assayed after infection and is comparable in both control and fibrillarin siRNA transfected cells. Error bars represent mean \pm s.d., ns non-significant, unpaired t-test. (G) Fibrillarin knockdown enhances IL-10 production in *S. aureus* infected HeLa cells. The measurement was done 24 hours post-infection. Error bars represent mean \pm s.e.m, **P<0.01 unpaired t-test.

3.3 Discussion

In this part of the study, we identified novel functions of fibrillarin in innate immunity.

Fibrillarin reduction confers resistance to worms infected with *S. aureus*, *E. faecalis*, and *P. aeruginosa*, suggesting reducing fibrillarin is sufficient to initiate protective host responses. On the other hand, *ncl-1*/TRIM2 mutants that overexpress fibrillarin (Tiku et al., 2016, Yi et al., 2015) are more sensitive. The results indicate that fibrillarin inhibits innate immunity against bacterial pathogens. Bacterial infection naturally induces reduction of fibrillarin levels in the host. Also, bacterial infection leads to a shrinkage of nucleoli in *C. elegans*. This suggests that a reduction in nucleolar size and fibrillarin levels is a beneficial host response triggered by bacterial infection. Innate immunity of *C. elegans* is mediated by a number of factors including PMK-1/p38 MAPK (Kim et al., 2002), HLH-30/TFEB (Visvikis et al., 2014) and DAF-16/FOXO (Garsin et al., 2003). Nevertheless, it is unlikely for these factors to act downstream of fibrillarin as the resistance conferred by fibrillarin reduction is not dependent on them. It still remains unclear how these different factors coordinate to mediate protective mechanisms and confer pathogen resistance. The results present in this study suggest that fibrillarin regulates bacterial infection resistance as a convergent factor downstream or parallel to these major players. Bacterial infection similarly reduces fibrillarin levels and nucleolar size in mammalian cells. Reduction of fibrillarin also improves survival and reduces inflammation in mammalian cells, meaning the roles of fibrillarin in immunity is conserved. Importantly, these results vividly demonstrated the incredible conservation of the regulators of innate immunity in *C. elegans* and also the usefulness of using the worms as a model for studies of innate immunity

Cellular organelles, including lysosome, ER, and mitochondria have long been known as signaling hubs that help manage infection. However, the role of nucleoli in mediating innate immunity against bacteria is relatively unstudied. Reduction of fibrillarin and nucleolar size suggests a general decrease in nucleolar functions, and this is sufficient to trigger protective responses. This puts nucleoli as one of the signaling hubs functioning in the signal transduction pathway. Theoretically, the nucleoli or fibrillarin can be targeted with systemic siRNA delivery or small molecules to fight infection, especially prophylactically, as we demonstrated reduction of fibrillarin before infection greatly improves resistance in both worms and mammalian cells. For example, prophylactic antibiotics is commonly taken before surgery or by people with weakened immune system (Rosen, Getz et al., 2016). Fibrillarin or nucleolus targeting drugs can potentially replace prophylactic antibiotics. This can reduce the use of antibiotics and slow down the rise of antibiotic resistant bacteria. Nucleolar size has already been proposed as a biomarker for longevity (Tiku et al., 2016). Also, as shrinkage of nucleoli is a protective host response, it could be possibly used as a prognosis marker for bacterial infection.

Further, it would be very interesting to investigate what is the up-stream stimulus for fibrillarin reduction. Also, how fibrillarin levels are regulated is another important question. Possible ways to regulate fibrillarin could include proteolytic mechanisms, such as proteosomal or autophagic degradation. In terms of downstream effectors, our results do not support that the currently well-studied effectors, namely PMK-1/p38 MAPK, HLH-30/TFEB and DAF-16/FOXO, play an important role. The down-stream mechanistic details still remain to be seen. Our results from epistasis experiments suggest suppression of translation may be involved, since mutants that diminish translation rate trigger pathogen resistance, and fibrillarin knockdown only slightly improves survival of such mutants, suggesting overlapping mechanisms. Nevertheless, it should be mentioned that the possible involvement of other nucleolar functions cannot be excluded. Other than ribosome biogenesis, the nucleolus also modifies tRNA, snRNA and also SRPs, and their roles in innate immunity would be an intriguing question to study. Pathogens commonly disrupt core cellular processes in order to disable such pathways and processes, which would otherwise help mount a defense response. It has been reported that disruption of major cellular processes including

mitochondrial functions, proteasomal activity and microtubular dynamics can activate transcription of immune-responsive genes (Melo & Ruvkun, 2012, Pellegrino et al., 2014), corroborating the notion of effector-triggered immunity. Reduction of fibrillarin seems to follow the same framework. Nucleolar functions and translation, like other essential cellular processes, are supposed to be closely monitored. Our work presents a novel connection between the nucleolus and anti-bacterial innate immunity. This also demonstrates a vital role played by translation and nucleolar functions in imparting effector-triggered immunity.

Although genetic epistasis indicates the involvement of translation, it remains to be seen what really triggers protection downstream of translation. It is well-known that viral infection leads to a rapid decrease of translational activity (Li, MacDonald et al., 2015). The reason can be easily understood. Viruses are obligate parasites, which must hijack the host's translational machinery to replicate, and therefore reducing translation can efficiently reduce viral replication rate. However, the role of reduction of translation in bacterial infection is less well-understood since bacteria possess its own translation machinery. It is proposed that a reduction of translation may lead to preferential translation of selected genes, which are required for protection. Similar situation can be seen in both human and *C. elegans*. Reduction of translation by exotoxin A leads to preferential translation of *zip-2* transcript in *C. elegans* (Dunbar et al., 2012). It is possible that reduction of fibrillarin also leads to more production of some beneficial proteins, while general translation decreases. Proteomics and transcriptomics of infected cells or worms with fibrillarin knockdown should help to address these questions. By comparing the data from the two omics approaches, the differentially produced proteins could be identified.

Interestingly, in murine macrophages, depletion of fibrillarin dampened the production of pro-inflammatory cytokines, namely IL-6 and IL-8, upon *S. aureus* infection, which also correlated with diminished cell death. On the other hand, anti-inflammatory cytokine IL-10 was induced by fibrillarin reduction. Consistently, fibrillarin knockdown in *C. elegans* does not induce a general transcriptional inflammatory response, but only specifically stimulates *irg-1* expression. Very often, the severity of infection is guided by inflammation, but not directly by the bacteria. Although an appropriate inflammatory response is required to defend against infection, overt inflammation

causes massive collateral damage and compromises survival of the host. For example, highly pathogenic avian influenza virus and *Staphylococcus* bacteria induce cytokine storm and sepsis, which are uncontrollable inflammation devastating to the survival of the hosts (Chousterman, Swirski et al., 2017). Therefore, for a beneficial and controllable immune response, pathogen resistance mechanisms usually encompass also negative regulators of inflammation, which are required to elicit optimal protection. Our data suggests reduction of fibrillarin is one of such anti-inflammatory mechanisms. Novel therapies for sepsis and cytokine storm are needed and under heavy research. Reduction of fibrillarin may potentially be used clinically in the future to alleviate inflammation.

Digestion of bacteria by fusion of the pathogen containing phagosomes with lysosomes plays a vital role in eliminating infection (Siqueira, Ribeiro et al., 2018). Interestingly, we observed an increased co-localization of intracellular bacteria with lysosomes in cells after fibrillarin knockdown, suggesting more efficient removal of intracellular bacteria by lysosomal mechanism. This is consistent with the data from the bacterial burden assay, in which the fibrillarin RNAi transfected cells showed less intracellular bacteria. This intriguing observation points towards a potential role of fibrillarin in regulating lysosomal biogenesis or acidification. Further, the enhanced capacity to remove bacteria and the resulted lower bacteria burden may explain the observed reduction in pro-inflammatory cytokine levels and increased cell survival. On the other hand, in *C. elegans*, fibrillarin RNAi does not significantly change the lysosomal pathway as assayed with cleavage of LGG-1::GFP. This raises the interestingly possibility that the effects of fibrillarin on lysosomal functions maybe species specific. Another possible explanation would be such effect is specific to specialized immune cells, such as macrophages, which are missing in *C. elegans*.

It is well-known that many long-lived mutants of *C. elegans* are also resistant to pathogenic stress. Examples are IIS mutants (Garsin et al., 2003) and *glp-1* mutants (Wu et al., 2015). Recently, it has been identified these long-lived mutants also have reduced fibrillarin level (Tiku et al., 2016). This raises the question of whether the mutants have enhanced resistance because of their lower level of fibrillarin. Current results do not address this point. Conceivably, epistasis between fibrillarin and the various longevity mutations could be tested.

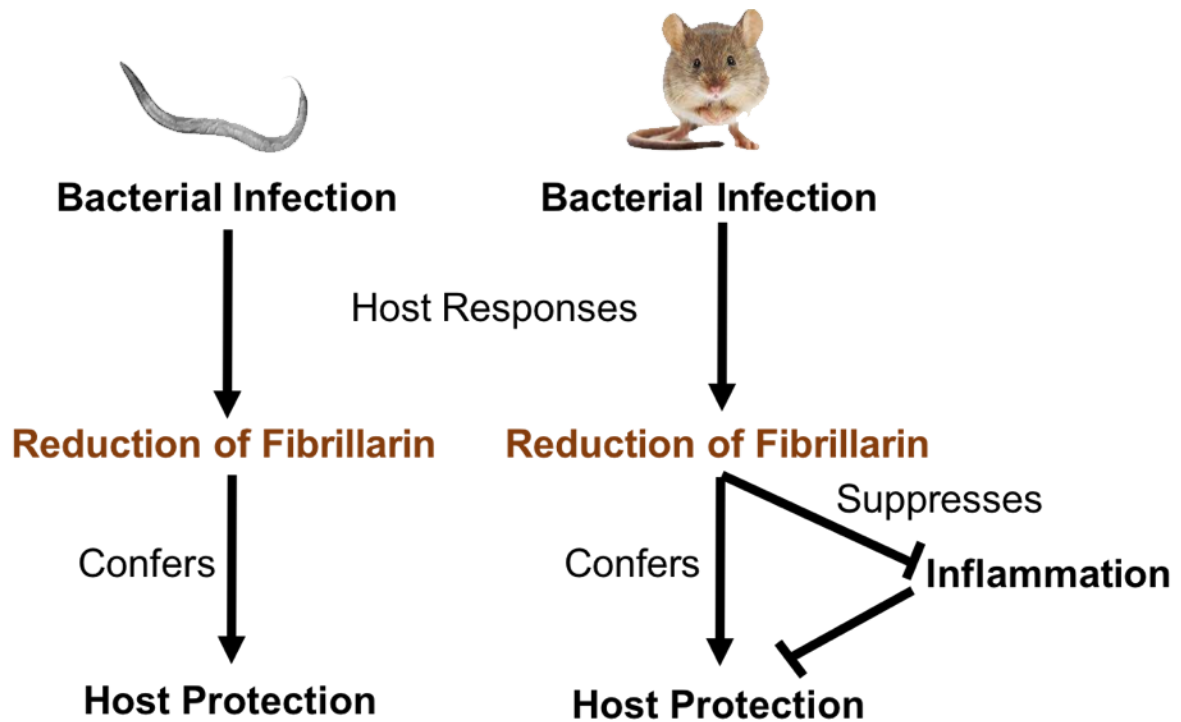


Fig 16. A summary of the roles played by fibrillarin in innate immunity. In both nematodes and mammals, bacterial infection leads to reduction of fibrillarin. Reduction of fibrillarin is sufficient to confer protection to the host in both nematodes and mammals. Reducing fibrillarin in mammals also suppresses inflammation.

3.4 Work contribution

The experiments present in this chapter were a collaboration between me, Dr. Varnesh Tiku (MPI-AGE), Dr. Parul Methrotra (MPI-AGE) and Dr. Raja Ganesan (CECAD, University of Cologne). I and Dr. Varnesh Tiku initiated the project, and I was involved in experimental design and data analysis of all the experiments.

All qPCR experiments, the puromycin incorporation assay, rRNA analysis, LGG-1::GFP cleavage and ubiquitin western blots, were performed by me independently.

C. elegans survival assays were performed together by me and Dr. Varnesh Tiku. Survival of the animals were scored at different time points, which were shared by us. For nucleolar size measurement, HLH-30::GFP localization, FIB-1::GFP reporter imaging and fibrillarin western blots in *C. elegans*, sample preparation (e.g. synchronization of animals, RNAi treatment, infection and harvesting) was done by me. Imaging and western blotting were done by Dr. Varnesh Tiku. Dr. Varnesh Tiku also performed the *irg-1* transcriptional reporter experiments, pharyngeal pumping rate measurement, and also the stress resistance assays.

All experiments involving HeLa cells were performed together by me and Dr. Parul Methrotra. Nucleolar size measurement in THP-1 derived macrophages was performed by Dr. Varnesh Tiku. The BMDM experiments were performed by Dr. Raja Ganesan.

CHAPTER 4

ROLES OF RNP-6 IN

INNATE IMMUNITY

Roles of RNP-6 in innate immunity

4.1 Introduction

This chapter focuses on *rnp-6*, which encodes the nematode's homolog of the mammalian splicing factor PUF60. Despite other cellular processes have been intensively studied in the context of infection, the effects of pathogens on splicing is relatively unexplored. Using different approaches, we identified an interesting link between splicing and immunity. Recently, Dr. Wenming Huang (MPI-AGE) from our laboratory identified a novel mutation in *rnp-6*, which causes longevity and resistance to cold stress (unpublished data). Interestingly, we found that the activity of RNP-6 inhibits immunity while reducing RNP-6 or splicing activity in general is sufficient to activate immune responses. These data suggest a tight connection exists between initiation of immune responses and splicing, which is previously underappreciated.

4.2 Results

4.2.1 Infection alters splicing pattern

As discussed in the previous section, infection leads a perturbation of rRNA maturation. It is unknown whether infection also affect other RNA metabolism pathways. Splicing is an essential modification for mRNA, and its roles in innate immunity are relatively unexplored. To begin with, we tested whether infection with *S. aureus* affects splicing of the splicing reporter strain of *ret-1*, which consists of a pair of reporter minigenes of *ret-1* exon 5 with different frameshifts. Both minigenes are driven by the ubiquitous promoter of *eft-3*. Inclusion of exon 5 leads to GFP expression, whereas expression of mCherry indicates skipping of the exon (Heintz et al., 2017). Interestingly, the ratio of GFP to mCherry signals decreased dramatically after *S. aureus* infection when compared to control (Fig. 17A,B), suggesting infection promotes skipping of exon 5. Next, splicing of *tos-1* was also examined using RT-PCR method. *tos-1* stands for target of splicing-1 and is a sensitive endogenous reporter for in vivo studies of splicing (Ma, Gao et al., 2012, Ma et al., 2011). Similar to what we observed in *ret-1*, infection also induced a shift of splicing isoforms in *tos-1* (Fig. 17 C,D). *S. aureus* induced

exclusion of a region between exon 1 and 2, resulting in increased abundance of the smaller transcript. These data suggest an interesting connection between infection and splicing.

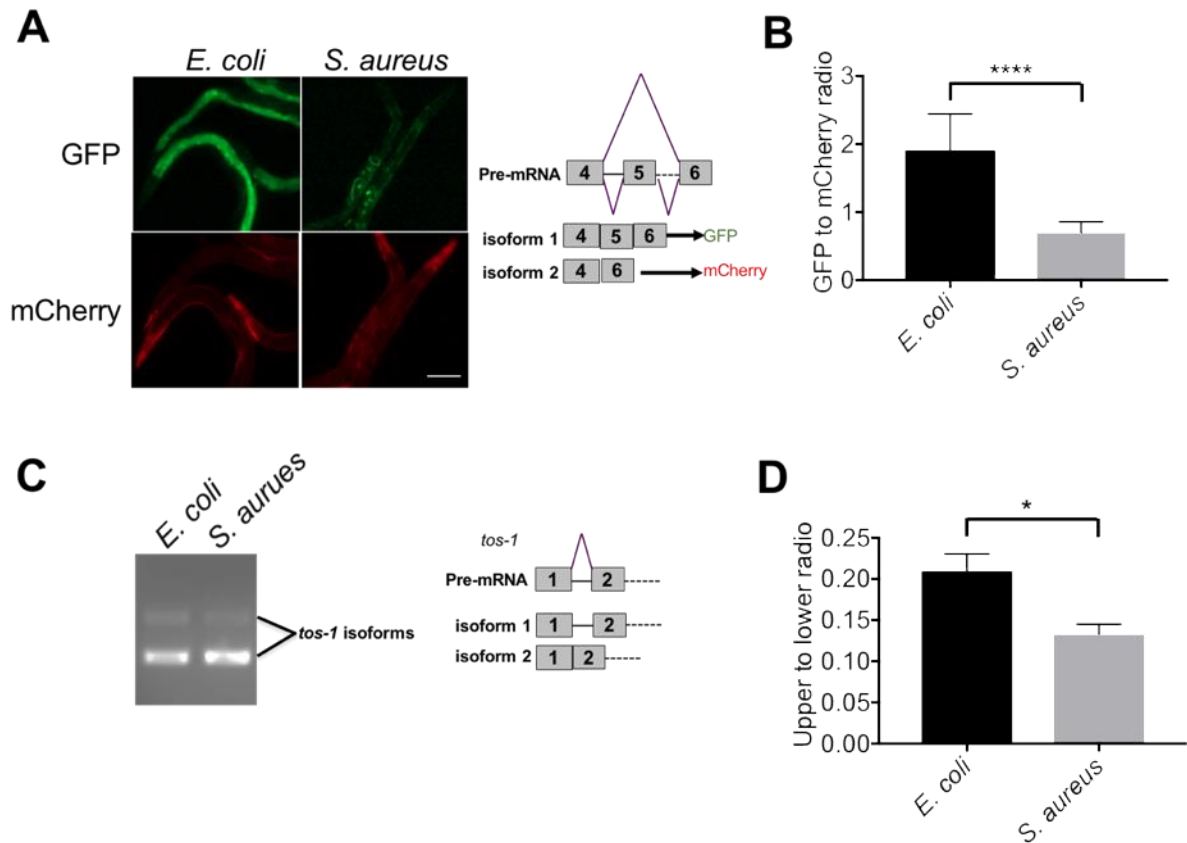


Fig 17. (A,B) The *ret-1* splicing reporter strain shows reduced expression of GFP and increased expression of mCherry after a 12-hour infection of *S. aureus*. The scale bar represents 50 μ m. Error bars represent mean \pm s.d. (C,D) RT-PCR shows that splicing of endogenous *tos-1* transcript is altered after 4 hours of infection with *S. aureus*. Error bars represent mean \pm s.e.m. * $P < 0.05$, **** $P < 0.0001$, unpaired t-test. The experiments were done three times independently.

4.2.2 A mutation in the splicing factor *rnp-6* causes immunodeficiency

Because of the interesting connection between infection and splicing, we tested whether mutants of splicing factors can impact host responses to infection. A novel point mutation of *rnp-6* was tested. *rnp-6* encodes the homolog of mammalian PUF60, which is a splicing factor with poly-U binding affinity that works cooperatively with U2AF for efficient splicing. The mutation *rnp-6(dh1127)* is a missense mutation with the conversion of glycine to aspartate, which is located in the second RRM. Intriguingly, the mutated glycine and also its surrounding amino acids are highly conserved across different species (Fig. 18), suggesting it is an important functional motif. The mutant was originally identified from an ethyl methanesulfonate (EMS) mutagenesis screening for cold resistant mutants, which can survive after a prolonged incubation at 2°C. The mutant shows resistance to stresses and also longevity at 20°C (Dr. Wenming Huang, unpublished data).

Survival assays of *rnp-6(dh1127)* were conducted with different pathogenic bacteria, namely *S. aureus* (Fig. 19A), *E. faecalis* (Fig. 19B) and *P. aeruginosa* (Fig. 19C). The *rnp-6* mutants showed reduced survival on all three bacteria. This effect is specific to pathogenic bacteria as the mutant had a normal lifespan when cultured with OP50 under 25°C (Fig. 20A). Using another strain *rnp-6(dh1125)*, which together with *rnp-6(dh1127)* are two independent strains carrying the same point mutation and created by Clustered Regularly Interspaced Short Palindromic Repeats (CRISPR) technology, we confirmed that the *rnp-6* mutation is causative for the reduced survival phenotype (Fig. 20B,C,D). Reduced survival can be potentially explained by a failure to mount defensive responses. To test this possibility, qRT-PCR was performed. Interestingly, in *rnp-6(dh1127)*, induction of many infection responsive genes was severely hampered upon *S. aureus* infection, including genes encoding anti-microbial proteins *nlp-30*, *nlp-34*, *ilys-2* and *spp-1*, detoxification proteins *cyp-37B1*, *hpo-15*, *lip1-2* and *cpz-2*, and also many other infection responsive genes (Fig. 19D). However, the transcript level of *rnp-6* remained constant after *S. aureus* infection whereas expression of *ilys-2* significantly increased (Fig. 20E). These data suggest that the mutation in *rnp-6(dh1127)* disrupts immune responses, and therefore leads to reduced survival upon infection.

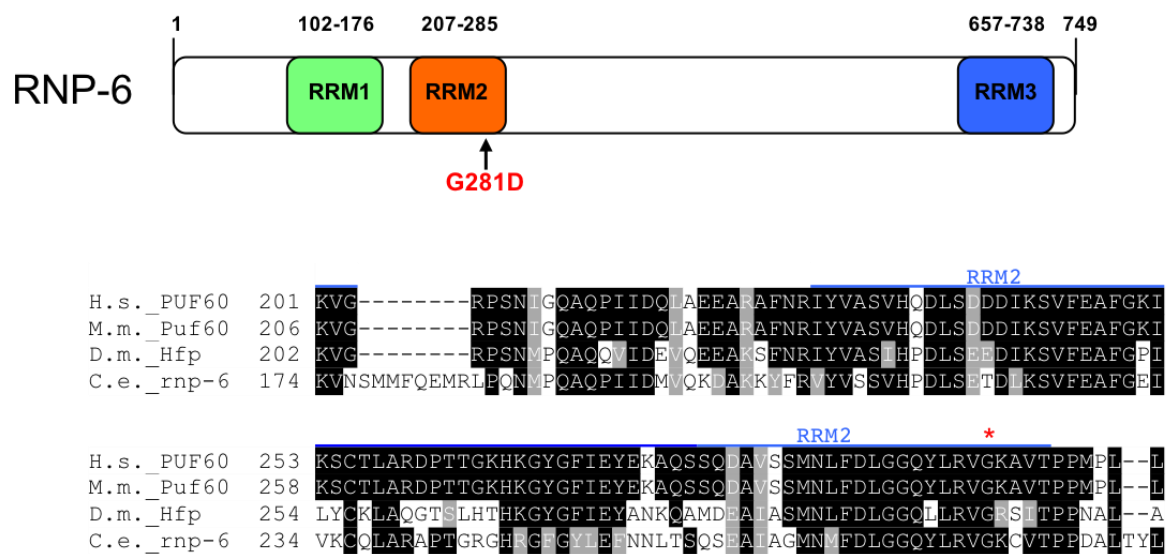


Fig 18. Depiction of the primary structure of RNP-6. The mutation is located at the second RRM. The missense mutation causes a conversion of glycine change to aspartic acid at the site highly conserved across evolution (amino acid 281 in *C. elegans* and amino acid 300 in human, indicated by the red star).

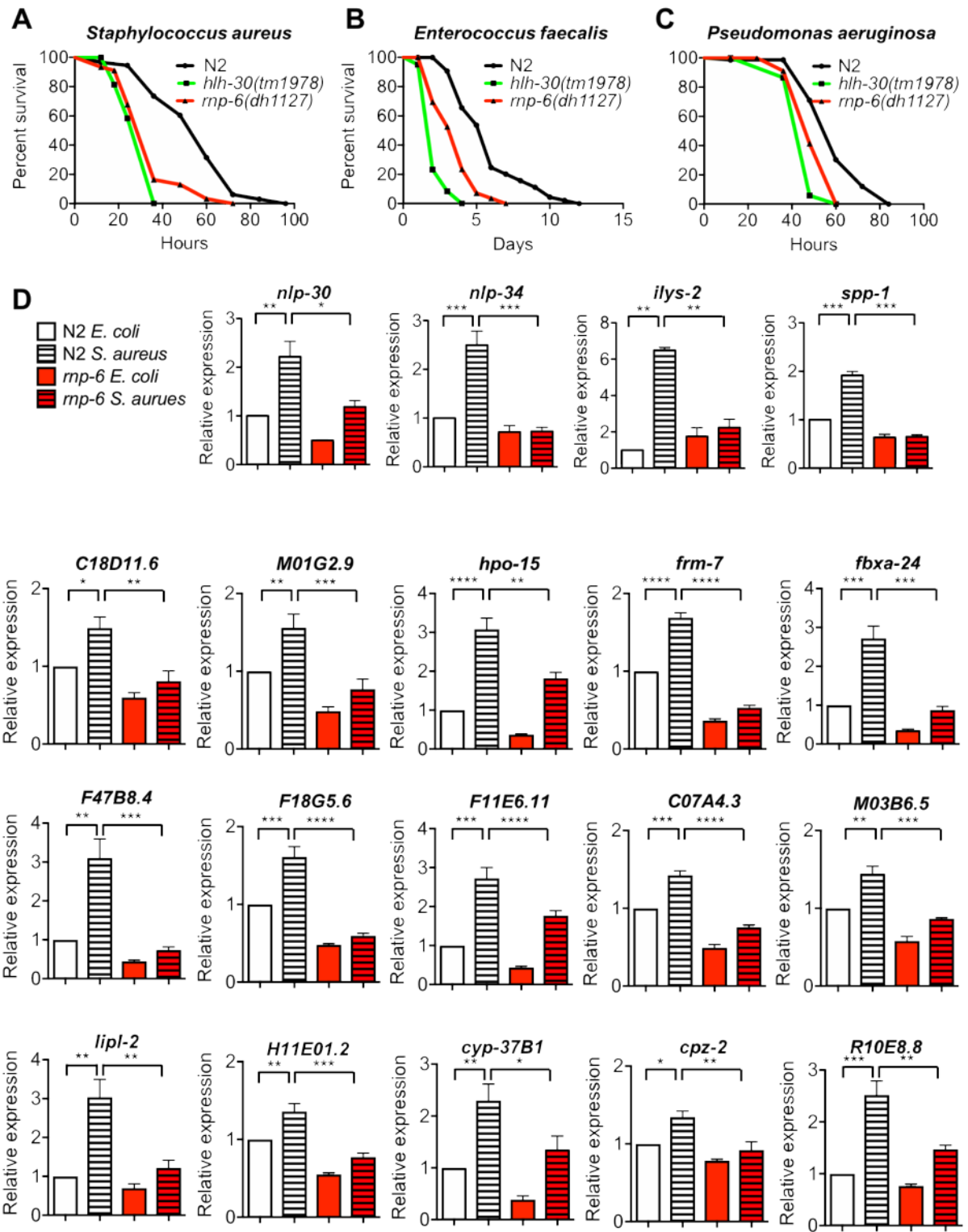


Figure 19. (A,B,C) *rnp-6(dh1127)* shows compromised survival upon infection of *S. aureus* ($P<0.0001$, log-rank test), *E. faecalis* ($P<0.0001$, log-rank test) and *P. aeruginosa* ($P=0.0022$, log-rank test). The mutants of *hlh-30(tm1978)* serve as a control for infection sensitivity. (D) qRT-PCR results of infection responsive genes in N2 wild-type and *rnp-6(dh1127)* animals. When infected with *S. aureus*, induction of the genes is blunted in the *rnp-6(dh1127)* mutants when compared to N2 (* $P<0.05$, ** $P<0.01$, *** $P<0.001$, **** $P<0.0001$). Error bars represent mean \pm s.e.m. from three independent biological replicates. Statistics: one-way ANOVA.

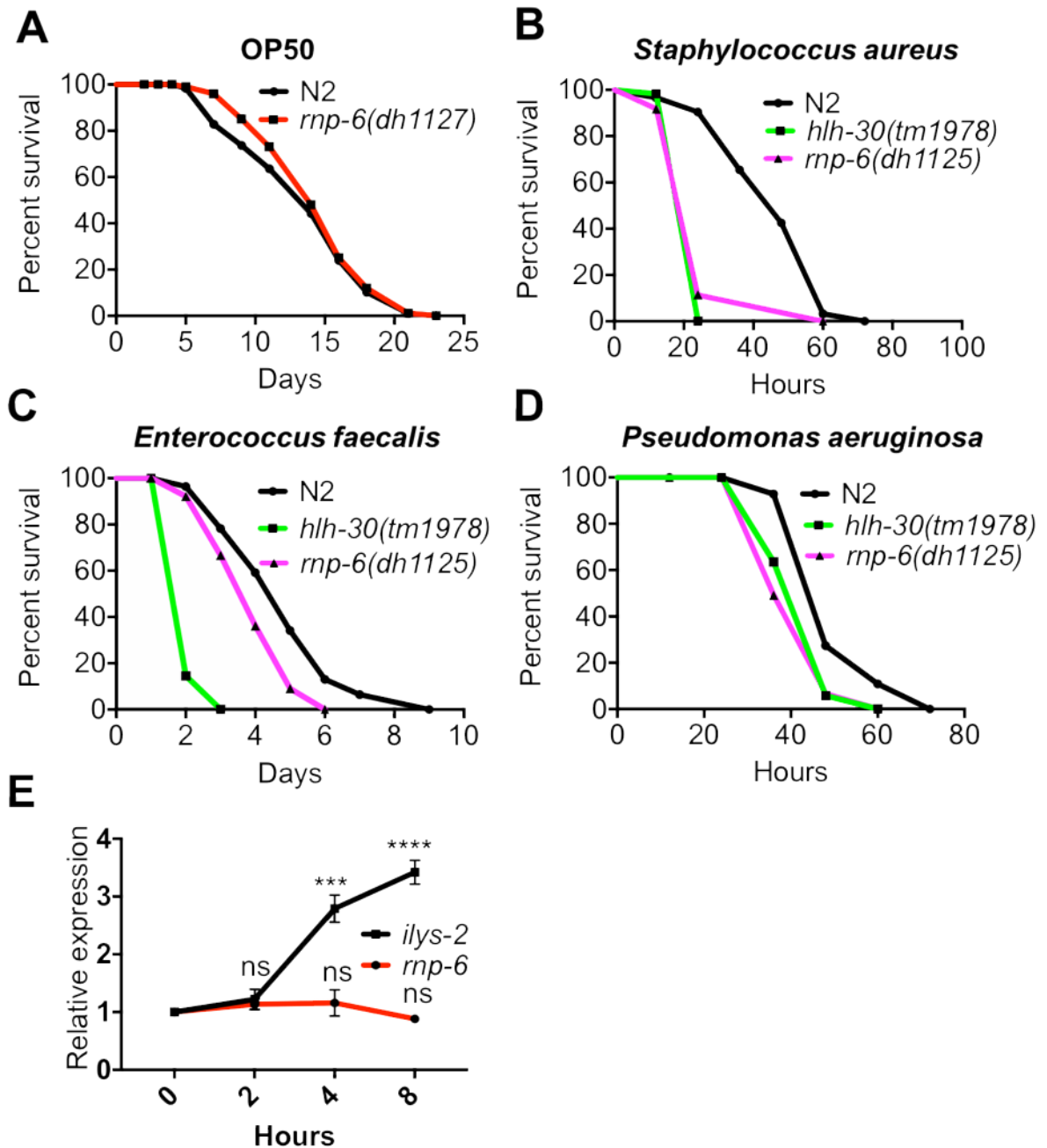


Figure 20. (A) *rnp-6(dh1127)* shows a normal lifespan when cultured with *E. coli* OP50 at 25°C ($P=0.3102$, log-rank test). (B,C,D) *rnp-6(dh1125)* shows reduced survival while infected with *S. aureus* ($P=0.0008$, log-rank test), *E. faecalis* ($P=0.0049$, log-rank test) and *P. aeruginosa* ($P<0.0001$, log-rank test). The mutants of *hlh-30(tm1978)* serve as a control for infection sensitivity. (E) qRT-PCR results of *rnp-6* transcript levels. The level of *rnp-6* expression remains constant after infection with *S. aureus*, while immune

response gene *ilys-2* serves as a positive control for immune induction. *** $P < 0.001$, **** $P < 0.0001$, ns non-significant. Error bars represent mean \pm s.e.m. from three independent biological replicates, ns non-significant. Statistics: one-way ANOVA.

4.2.3 Transcriptomic profiling reveals substantial effects of the *rnp-6* mutation on infection induced transcriptional and splicing changes

To gain further insight into the roles of *rnp-6* in infection responses, we performed RNA-sequencing of *S. aureus* infected N2 and *rnp-6(dh1127)* animals. As expected, when comparing the infected samples with the control samples, the DEGs are highly enriched for immune and defense response genes. This is true for both N2 and *rnp-6(dh1127)* (Fig. 21, 22). We also compared the transcriptome of N2 and *rnp-6(dh1127)* under both control and infected conditions. In both cases, the *rnp-6* mutation resulted in numerous DEGs, which are enriched with defense response genes (Fig. 23, 24). This is consistent with the idea that *rnp-6(dh1127)* mutation compromises immune responses. Interestingly, under non-infected condition, DEGs of immune response are still significantly enriched, suggesting the *rnp-6* mutation might also affect the basal expression of these genes.

Next, we sought to take a more careful look on the infection responsive genes that are dependent on *rnp-6*. Among the 665 genes that are upregulated upon infection in wild-type animals, 117 are significantly down in infected *rnp-6(dh1127)* (Fig. 25) (Table. 1). GO term analysis also found that among these *rnp-6* dependent genes, defense response genes are highly enriched (Table. 2), suggesting *rnp-6(dh1127)* greatly diminishes the induction of defense response genes upon infection. On the other hand, 1529 genes are significantly downregulated in wild-type animals upon infection. Within this set of genes, 158 are upregulated in infected *rnp-6(dh1127)* when compared to infected wild-type (Fig. 26) (Table. 3). These genes are highly enriched for GO terms of organic acid metabolism (Table. 4), such as organic acid metabolic process, carboxylic acid metabolic process, oxoacid metabolic process, fatty acid metabolic process and monocarboxylic acid metabolic process.

Since *rnp-6* encodes a splicing factor, we also analyzed the differentially spliced transcripts. We reasoned that genes whose splicing is affected by infection only in N2 but not in *rnp-6(dh1127)* might be the mediators of innate immunity downstream of *rnp-6*. We took the list of genes that undergo alternative splicing upon infection in wild-type animals and deduced the genes from the list that also have alternative splicing in *rnp-6(dh1127)* upon infection. We also prioritized genes that have the same splicing pattern in *rnp-6(dh1127)* and N2 under non-infection condition as this would mean that the alternative splicing events are specific to infection. By doing this, we ended up with a list of 147 genes (Fig. 27) (Table. 5). GO term analysis reveals an enrichment of genes implicated in developmental process, including regulation of cell cycle, regulation of developmental growth and regulation of cell division (Table. 6).

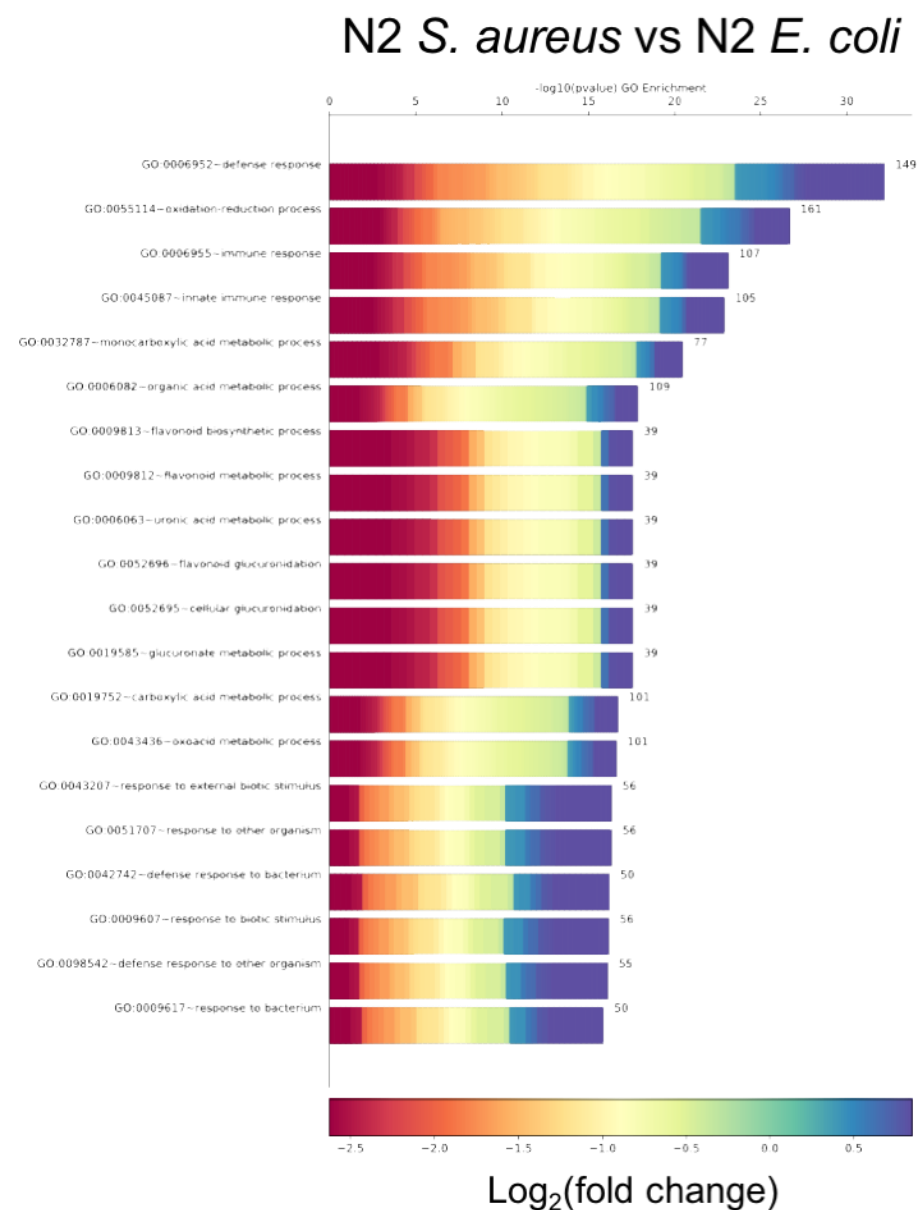


Figure 21. GO enrichment analysis. The DEGs upon infection in wild-type N2 worms were analyzed using DAVID. The enrichment score (x axis), fold change (colour coding) and number of genes are shown.

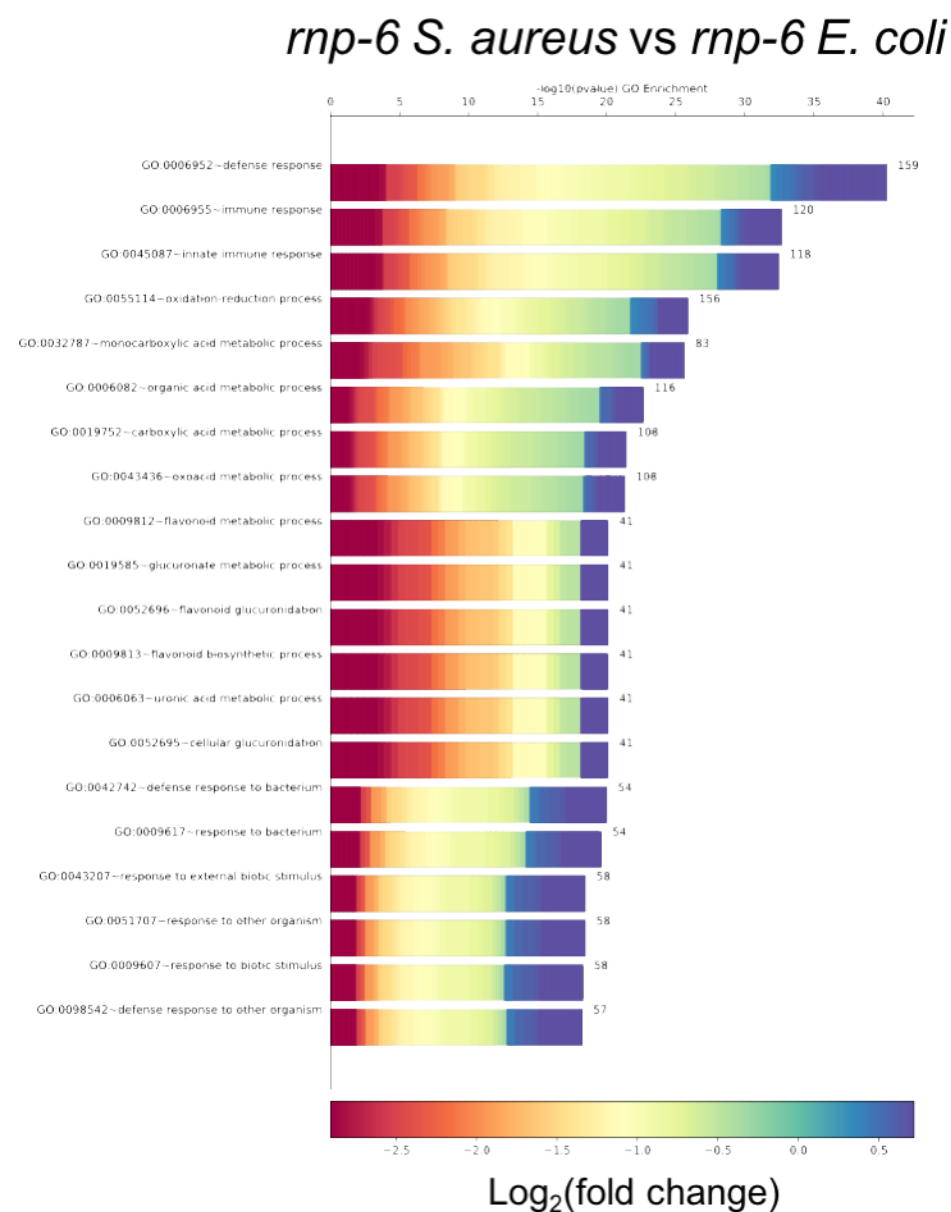


Figure 22. GO enrichment analysis. The DEGs upon infection in *rnp-6(dh1127)* worms were analyzed using DAVID. The enrichment score (x axis), fold change (colour coding) and number of genes are shown.

rnp-6 S. aureus vs N2 *S. aureus*

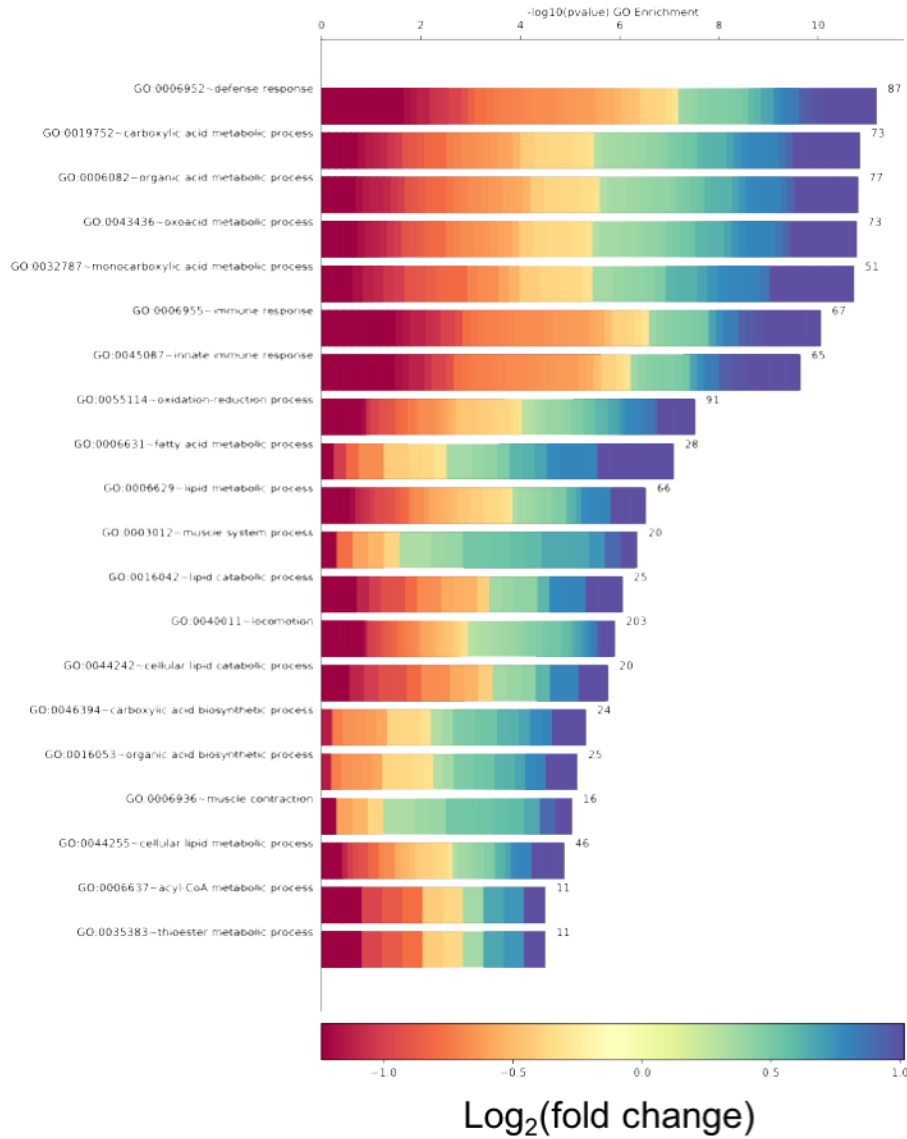


Figure 23. GO enrichment analysis. The DEGs in infected *rnp-6(dh1127)* worms compared to infected wild-type N2 worms were analyzed using DAVID. The enrichment score (x axis), fold change (colour coding) and number of genes are shown.

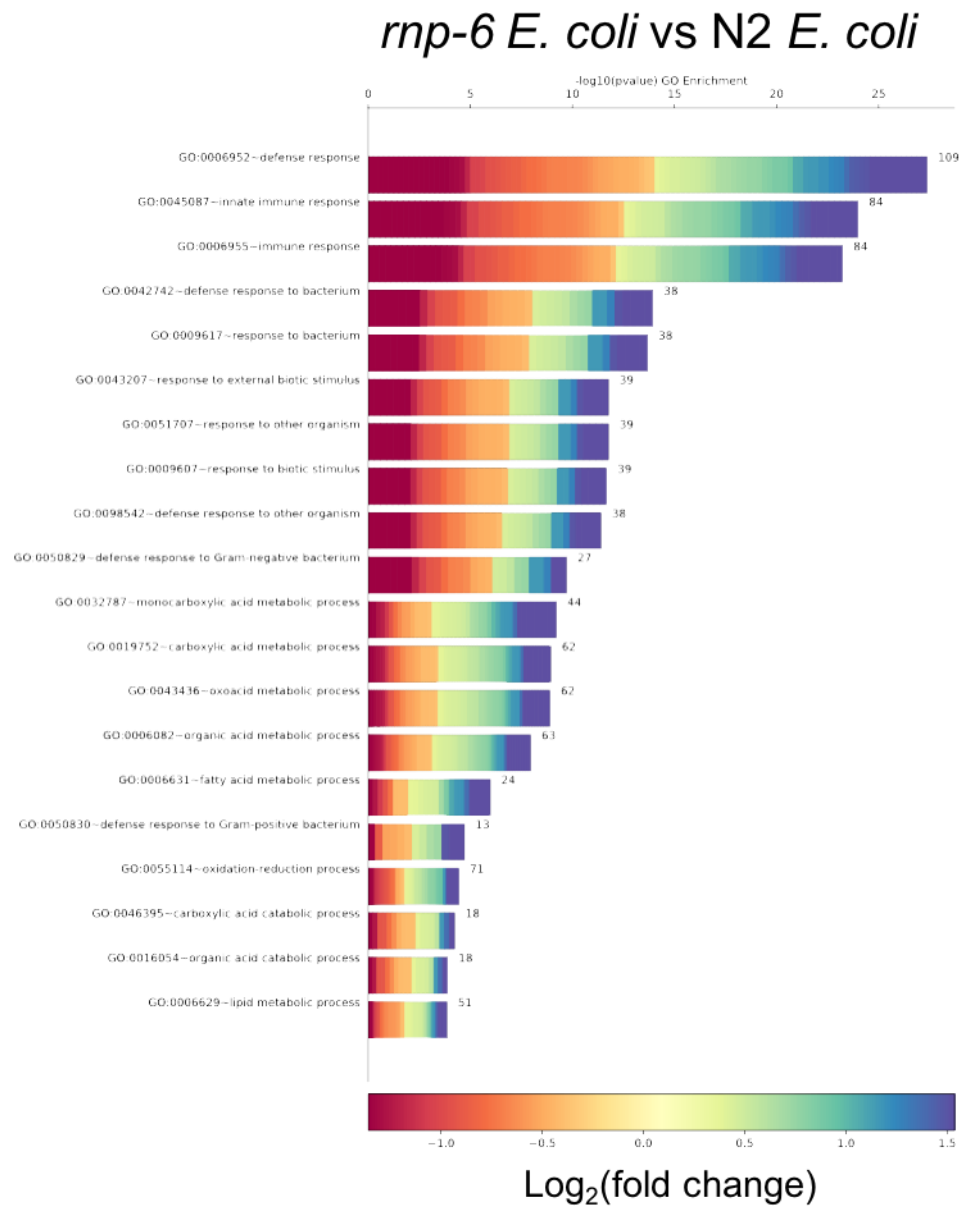


Figure 24. GO enrichment analysis. The DEGs caused by *rnp-6*(*dh1127*) under non-infection condition were analyzed using DAVID. The enrichment score (x axis), fold change (colour coding) and number of genes are shown.

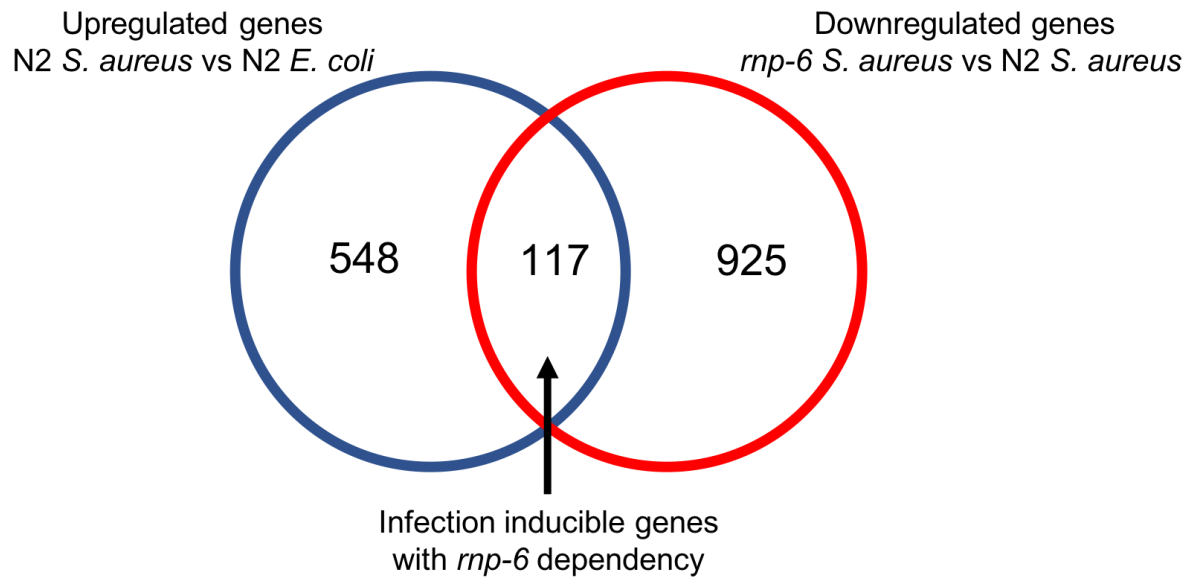


Figure 25. The Venn diagram showing the numbers of upregulated genes from the comparison of infected N2 versus non-infected N2 and downregulated genes from the comparison of infected *rnp-6*(*dh1127*) versus infected N2.

Gene ID	Gene Name	Gene ID	Gene Name
WBGene00000372	<i>cyp-13A7</i>	WBGene00012443	<i>Y15E3A.4</i>
WBGene00000558	<i>cnc-4</i>	WBGene00012750	<i>faah-6</i>
WBGene00000789	<i>cpz-2</i>	WBGene00012778	<i>Y42A5A.3</i>
WBGene00000981	<i>dhs-18</i>	WBGene00012819	<i>Y43F8B.9</i>
WBGene00001105	<i>dsl-3</i>	WBGene00013008	<i>cllec-146</i>
WBGene00001391	<i>far-7</i>	WBGene00013145	<i>cutl-2</i>
WBGene00001493	<i>frm-7</i>	WBGene00013694	<i>Y106G6A.1</i>
WBGene00001577	<i>gem-4</i>	WBGene00015048	<i>faah-2</i>
WBGene00001591	<i>glc-1</i>	WBGene00015131	<i>B0303.11</i>
WBGene00001819	<i>haf-9</i>	WBGene00015388	<i>C03F11.2</i>
WBGene00001906	<i>his-32</i>	WBGene00015392	<i>nspc-7</i>
WBGene00001908	<i>his-34</i>	WBGene00015597	<i>fbxa-162</i>
WBGene00001923	<i>his-49</i>	WBGene00016061	<i>hpo-15</i>
WBGene00001925	<i>his-51</i>	WBGene00016669	<i>ilys-2</i>
WBGene00001926	<i>his-52</i>	WBGene00016670	<i>ilys-3</i>
WBGene00001927	<i>his-53</i>	WBGene00016883	<i>C52E2.4</i>
WBGene00001939	<i>his-65</i>	WBGene00017340	<i>F10D7.3</i>
WBGene00002016	<i>hsp-16.2</i>	WBGene00017361	<i>F10E9.12</i>
WBGene00002018	<i>hsp-16.41</i>	WBGene00017582	<i>F18G5.6</i>
WBGene00002026	<i>hsp-70</i>	WBGene00017964	<i>F31F7.1</i>
WBGene00003766	<i>nlp-28</i>	WBGene00018044	<i>F35D11.3</i>
WBGene00003768	<i>nlp-30</i>	WBGene00018731	<i>F53A9.8</i>
WBGene00003828	<i>nuc-1</i>	WBGene00018803	<i>fbxa-24</i>
WBGene00003878	<i>pept-3</i>	WBGene00019068	<i>faah-3</i>
WBGene00004727	<i>sax-1</i>	WBGene00019187	<i>H11E01.2</i>
WBGene00004779	<i>ser-4</i>	WBGene00019376	<i>lipl-4</i>
WBGene00004993	<i>spp-8</i>	WBGene00019409	<i>K05F1.8</i>
WBGene00005228	<i>srh-2</i>	WBGene00019788	<i>M116.1</i>
WBGene00006681	<i>twk-29</i>	WBGene00019902	<i>R05G6.10</i>
WBGene00006684	<i>twk-32</i>	WBGene00020075	<i>math-35</i>
WBGene00007365	<i>C06B3.6</i>	WBGene00020256	<i>T05C3.6</i>
WBGene00007398	<i>C07A4.3</i>	WBGene00020446	<i>T12B3.3</i>
WBGene00007409	<i>C07B5.4</i>	WBGene00020672	<i>T22B7.3</i>
WBGene00007682	<i>C18D11.6</i>	WBGene00021167	<i>cyp-32B1</i>
WBGene00007725	<i>C25F9.5</i>	WBGene00021497	<i>Y40C5A.4</i>
WBGene00007766	<i>C27C7.1</i>	WBGene00021852	<i>Y54F10AM.8</i>
WBGene00007919	<i>cup-16</i>	WBGene00021977	<i>Y58A7A.3</i>
WBGene00008425	<i>D2045.8</i>	WBGene00022181	<i>pho-9</i>
WBGene00008485	<i>ugt-43</i>	WBGene00022200	<i>fard-1</i>
WBGene00009008	<i>F21D5.3</i>	WBGene00022326	<i>fbxa-14</i>
WBGene00009226	<i>cyp-37B1</i>	WBGene00022781	<i>pmt-1</i>

WBGene00009692	<i>F44E5.5</i>	WBGene00022893	<i>ZK1290.13</i>
WBGene00009773	<i>lipI-2</i>	WBGene00023501	<i>F11E6.11</i>
WBGene00009785	<i>F46C5.10</i>	WBGene00044078	<i>tag-243</i>
WBGene00009805	<i>F47B8.4</i>	WBGene00044455	<i>F23F12.13</i>
WBGene00009899	<i>efl-3</i>	WBGene00044478	<i>K06B9.6</i>
WBGene00009957	<i>F53B2.8</i>	WBGene00044728	<i>Y53F4B.45</i>
WBGene00010174	<i>F56H9.2</i>	WBGene00044807	<i>R106.5</i>
WBGene00010422	<i>H32K16.2</i>	WBGene00077490	<i>M03A1.8</i>
WBGene00010545	<i>cbp-2</i>	WBGene00077757	<i>E02H4.7</i>
WBGene00010717	<i>K09C8.7</i>	WBGene00173345	<i>21ur-12912</i>
WBGene00010822	<i>M01G12.9</i>	WBGene00195005	<i>ZK809.10</i>
WBGene00010837	<i>M03B6.5</i>	WBGene00201370	<i>C07A12.14</i>
WBGene00011213	<i>R10E8.8</i>	WBGene00219801	<i>C05E4.16</i>
WBGene00011423	<i>ipla-7</i>	WBGene00219860	<i>C51F7.4</i>
WBGene00011596	<i>T07G12.5</i>	WBGene00220048	<i>R106.6</i>
WBGene00011727	<i>T12A7.6</i>	WBGene00220051	<i>R160.11</i>
WBGene00011951	<i>T23F6.3</i>	WBGene00206419	<i>R106.5</i>
WBGene00012420	<i>Y7A9D.1</i>		

Table 1. A list of infection inducible genes that are *rnp-6* dependent. The genes are from the intercept of the Venn diagram in Figure. 25.

Term	Count	P-Value
Defense response	9	1.6E-3
Defense response to other organism	5	4.2E-3
Response to other organism	5	4.6E-3
Response to external biotic stimulus	5	4.6E-3
Response to biotic stimulus	5	4.7E-3
Oxidation-reduction process	9	6.5E-3
Lipid metabolic process	7	1.1E-2
Defense response to Gram-positive bacterium	3	1.5E-2
Defense response to bacterium	4	1.8E-2
Response to bacterium	4	1.9E-2
Transmembrane transport	10	2.0E-2
Ion transport	9	2.0E-2
Anion transport	5	2.3E-2

Table 2. GO term enrichment analysis of the genes from Table.1 using DAVID.

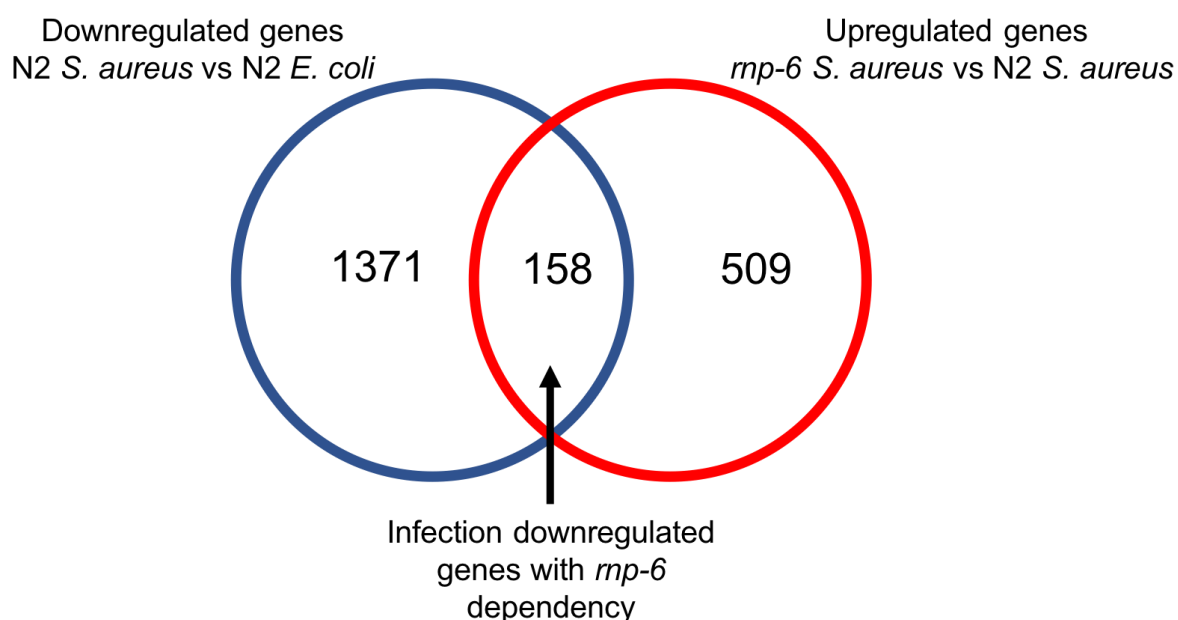


Figure 26. The Venn diagram showing the numbers of downregulated genes from the comparison of infected N2 versus non-infected N2 and upregulated genes from the comparison of infected *mp-6(dh1127)* versus infected N2.

Gene ID	Gene Name	Gene ID	Gene Name
WBGene00000083	adt-2	WBGene00010426	H37A05.2
WBGene00000175	aqp-7	WBGene00010593	gsnl-1
WBGene00000373	cyp-14A5	WBGene00010646	K08C7.1
WBGene00000656	col-80	WBGene00010834	mct-3
WBGene00000671	col-96	WBGene00010959	nduo-1
WBGene00000673	col-98	WBGene00010960	atp-6
WBGene00000675	col-101	WBGene00010988	metr-1
WBGene00000677	col-103	WBGene00011006	ugt-47
WBGene00000699	col-125	WBGene00011474	aldo-1
WBGene00000708	col-135	WBGene00011487	T05E12.6
WBGene00000716	col-143	WBGene00011713	T11F9.12
WBGene00000733	col-160	WBGene00011831	T19B10.2
WBGene00000768	cor-1	WBGene00012163	VZK822L.2
WBGene00000779	cpn-3	WBGene00012247	W04E12.2
WBGene00000977	dhs-14	WBGene00012253	cllec-50
WBGene00001000	dim-1	WBGene00012382	ttr-16
WBGene00001116	dyc-1	WBGene00012538	Y37A1B.5
WBGene00001244	elo-6	WBGene00012583	cllec-4
WBGene00001385	far-1	WBGene00012757	Y41C4A.11
WBGene00001387	far-3	WBGene00013227	Y56A3A.6
WBGene00001397	fat-5	WBGene00013293	Y57G11A.5
WBGene00001398	fat-6	WBGene00013489	col-42
WBGene00001399	fat-7	WBGene00014003	ZK593.3
WBGene00001468	flr-4	WBGene00014254	cyp-13A10
WBGene00001581	gfi-1	WBGene00014666	C05D12.3
WBGene00001650	gon-1	WBGene00014732	F09F3.8
WBGene00001725	grl-16	WBGene00014941	Y67H2A.9
WBGene00002268	lec-5	WBGene00015709	cyp-33A1
WBGene00003055	lon-1	WBGene00015780	C14F11.4
WBGene00003090	lys-1	WBGene00015791	C15C7.5
WBGene00003169	mec-5	WBGene00015913	C17F4.7
WBGene00003175	mec-12	WBGene00015956	C18B2.5
WBGene00003369	mlc-1	WBGene00016027	C23H5.8
WBGene00003511	mxl-3	WBGene00016095	C25E10.5
WBGene00003573	ncx-8	WBGene00016172	C27H5.2
WBGene00003602	nhr-3	WBGene00016759	C49A9.5
WBGene00003652	nhr-62	WBGene00016786	cyp-35A4
WBGene00003658	nhr-68	WBGene00016845	C50F7.5
WBGene00003891	osm-11	WBGene00016892	C53A3.2
WBGene00003934	pat-10	WBGene00016943	acdh-1
WBGene00003959	pcp-4	WBGene00017060	D2063.1

WBGene00004062	pmp-5	WBGene00017065	D2092.4
WBGene00004172	pqn-92	WBGene00017681	slc-17.5
WBGene00004513	rrn-1.2	WBGene00017691	ilys-5
WBGene00004997	spp-12	WBGene00017772	clec-1
WBGene00005644	srp-3	WBGene00017892	F28B4.3
WBGene00005655	srr-4	WBGene00017969	F32A5.3
WBGene00006404	tag-10	WBGene00018138	fol-2
WBGene00006408	tag-18	WBGene00018293	F41E6.12
WBGene00006418	tag-38	WBGene00018353	fbxa-182
WBGene00006764	unc-27	WBGene00018701	pccb-1
WBGene00006801	unc-68	WBGene00018707	oac-31
WBGene00006876	vab-10	WBGene00018910	F56A4.2
WBGene00006928	vit-4	WBGene00019017	F57F4.4
WBGene00006938	wee-1.1	WBGene00019105	asp-8
WBGene00007660	pals-6	WBGene00019489	K07E1.1
WBGene00007687	C18E9.7	WBGene00019540	K08D12.6
WBGene00007964	cyp-25A2	WBGene00019727	zig-12
WBGene00008032	C39E9.8	WBGene00019738	clec-265
WBGene00008205	sams-1	WBGene00020128	R193.2
WBGene00008393	D1086.6	WBGene00020237	phat-4
WBGene00008436	DH11.2	WBGene00020836	lgc-34
WBGene00008566	acox-1.3	WBGene00020886	ttr-6
WBGene00008567	acox-1.4	WBGene00020891	T28C12.4
WBGene00008575	scl-24	WBGene00021448	Y39D8A.1
WBGene00008602	oac-14	WBGene00021625	Y47D7A.13
WBGene00008629	cpt-5	WBGene00021779	Y51H7C.1
WBGene00008741	F13D12.6	WBGene00021895	clec-84
WBGene00008803	lips-10	WBGene00022610	ZC416.6
WBGene00008824	F14H3.5	WBGene00022645	ZK6.11
WBGene00009048	cth-1	WBGene00044316	F41G3.21
WBGene00009237	F28H7.3	WBGene00045416	Y37H2A.14
WBGene00009628	tatn-1	WBGene00047764	21ur-975
WBGene00009645	F42G10.1	WBGene00049765	21ur-4346
WBGene00009812	suca-1	WBGene00171449	21ur-10648
WBGene00009982	F53F1.4	WBGene00173414	21ur-13288
WBGene00010066	F54F7.6	WBGene00195050	T22D1.17
WBGene00010085	F55B11.3	WBGene00219215	F13B12.15
WBGene00010256	hrg-3	WBGene00235310	R02D1.2

Table 3. A list of infection downregulated genes with *mp-6* dependency. The genes are from the intercept of the Venn diagram in Figure. 26.

Term	Count	P-Value
Organic acid metabolic process	13	3.8E-5
Carboxylic acid metabolic process	12	8.6E-5
Oxoacid metabolic process	12	8.8E-5
Fatty acid metabolic process	6	9.8E-4
Monocarboxylic acid metabolic process	8	1.0E-3
Oxidation-reduction process	13	1.5E-3
Actin cytoskeleton organization	8	2.0E-3
Actin filament-based process	8	2.5E-3
Muscle structure development	7	4.8E-3
Carboxylic acid biosynthetic process	5	5.8E-3
Myofibril assembly	6	7.7E-3
Organic acid biosynthetic process	5	7.9E-3
Actomyosin structure organization	6	8.7E-3
Striated muscle cell development	6	8.9E-3
Muscle cell development	6	9.3E-3
Striated muscle cell differentiation	6	9.3E-3
Lipid metabolic process	9	9.8E-3
Sensory perception of mechanical stimulus	3	1.1E-2
Muscle system process	4	1.1E-2
Muscle cell differentiation	6	1.3E-2
Fatty acid beta-oxidation using acyl-CoA dehydrogenase	3	1.4E-2
Cellular lipid metabolic process	7	1.6E-2
Homeostatic process	7	1.7E-2
Small molecule biosynthetic process	5	1.9E-2
Lipid homeostasis	3	2.4E-2
Cellular component assembly involved in morphogenesis	6	2.5E-2
Cytoskeleton organization	8	2.7E-2
Mechanosensory behavior	3	2.8E-2
Long-chain fatty acid biosynthetic process	2	3.0E-2
Chemical homeostasis	5	3.3E-2
Long-chain fatty acid metabolic process	2	3.7E-2
Fatty acid beta-oxidation	3	3.8E-2
Locomotion	21	3.8E-2
Fatty acid biosynthetic process	3	3.9E-2
Response to mechanical stimulus	3	4.3E-2
Monocarboxylic acid biosynthetic process	3	4.3E-2
Lipid oxidation	3	4.6E-2
Fatty acid oxidation	3	4.6E-2
Lipid localization	11	4.9E-2

Table 4. GO term enrichment analysis of the genes from Table. 3 using DAVID.

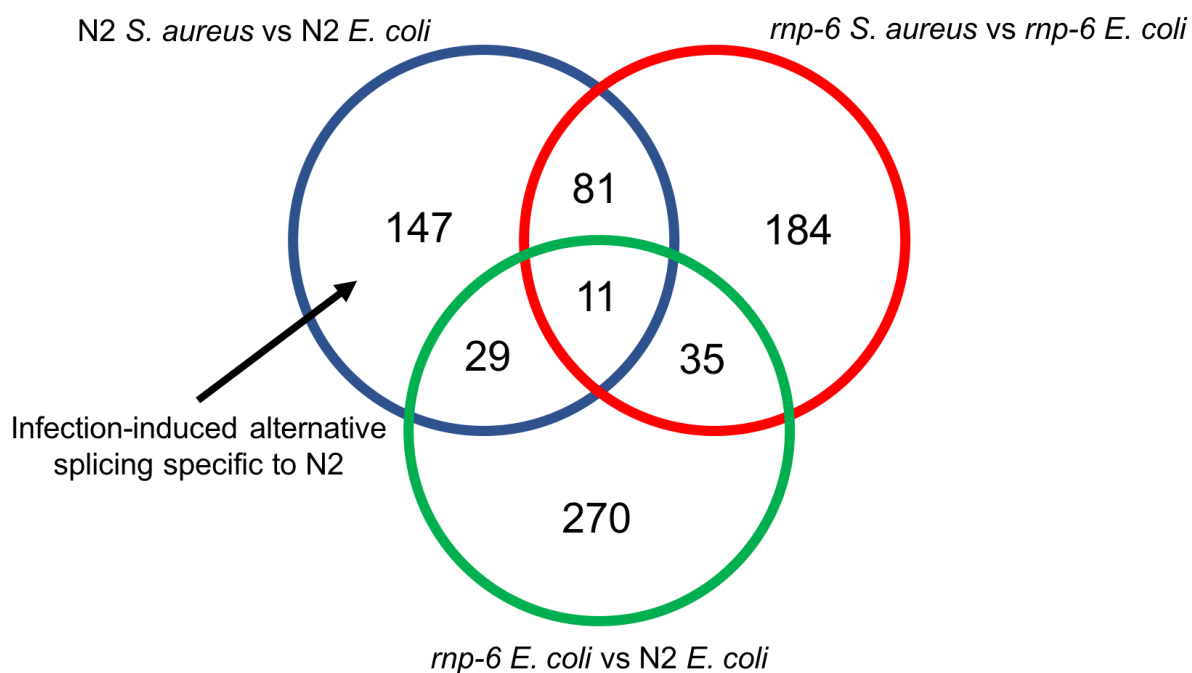


Figure 27. The Venn diagram showing the numbers of alternatively spliced genes from the comparison of infected N2 versus non-infected N2, infected *rnp-6(dh1127)* versus infected N2 and non-infected *rnp-6* versus non-infected N2.

Gene ID	Gene Name	Gene ID	Gene Name
WBGene00000201	arx-3	WBGene00010350	H01G02.3
WBGene00000218	asp-5	WBGene00010724	K09E9.1
WBGene00000383	cdc-14	WBGene00010867	tag-260
WBGene00000390	cdc-42	WBGene00011218	R10E11.6
WBGene00000465	cpg-1	WBGene00011239	pges-2
WBGene00000517	cki-2	WBGene00011397	T03E6.8
WBGene00000669	col-94	WBGene00011648	cni-1
WBGene00000776	cpl-1	WBGene00011856	T20D3.2
WBGene00000981	dhs-18	WBGene00012033	T26C5.3
WBGene00001160	efk-1	WBGene00012326	W07E11.1
WBGene00001398	fat-6	WBGene00012633	Y38H6C.21
WBGene00001595	gld-1	WBGene00012953	fbxa-216
WBGene00001622	glt-4	WBGene00013216	Y54G11A.7
WBGene00001999	hrp-1	WBGene00013597	gpi-1
WBGene00002008	hsp-4	WBGene00014666	C05D12.3
WBGene00002054	ifb-2	WBGene00014947	Y71A12B.14
WBGene00002132	inx-10	WBGene00015366	C03A7.2
WBGene00002213	kin-32	WBGene00015471	Imp-2
WBGene00002245	lag-1	WBGene00015692	ugt-25
WBGene00002269	lec-6	WBGene00015801	C15H9.5
WBGene00002272	lec-9	WBGene00016033	C24A3.2
WBGene00003055	lon-1	WBGene00016158	ari-1
WBGene00003169	mec-5	WBGene00016809	C50D2.6
WBGene00003235	mif-2	WBGene00017025	D1037.1
WBGene00003374	mlk-1	WBGene00017028	dex-1
WBGene00003497	mup-4	WBGene00017641	csr-1
WBGene00003567	ncx-2	WBGene00017881	asp-13
WBGene00003738	nid-1	WBGene00017934	F30B5.4
WBGene00003936	pat-12	WBGene00018094	F36F12.3
WBGene00003961	pct-1	WBGene00018222	F40A3.7
WBGene00003964	pdi-3	WBGene00018335	F42A9.6
WBGene00003996	pgp-2	WBGene00018435	btb-9
WBGene00004031	pis-1	WBGene00018879	F55D10.4
WBGene00004178	prg-1	WBGene00018897	zipt-2.4
WBGene00004248	pus-1	WBGene00018910	F56A4.2
WBGene00004414	rpl-3	WBGene00019298	K02D7.1
WBGene00004443	rpl-29	WBGene00019322	ahcy-1
WBGene00004444	rpl-30	WBGene00019521	dmd-7
WBGene00004447	rpl-33	WBGene00019697	M01B12.4
WBGene00004477	rps-8	WBGene00019720	M01H9.4
WBGene00004491	rps-22	WBGene00019746	M03A1.3

WBGene00004703	rsp-6	WBGene00019747	ipla-1
WBGene00004890	smp-2	WBGene00019779	endu-2
WBGene00004928	soc-1	WBGene00020131	gcy-28
WBGene00004951	spc-1	WBGene00020393	T10B5.7
WBGene00005025	sqv-7	WBGene00020891	T28C12.4
WBGene00006220	str-176	WBGene00020936	hrpf-1
WBGene00006438	nrfl-1	WBGene00021043	pck-1
WBGene00006801	unc-68	WBGene00021057	W06B4.2
WBGene00006888	vbh-1	WBGene00021236	pud-1.2
WBGene00006927	vit-3	WBGene00021344	Y37B11A.2
WBGene00006928	vit-4	WBGene00021503	ctsa-2
WBGene00006974	zen-4	WBGene00021594	tig-3
WBGene00007122	B0250.5	WBGene00021814	Y53G8AR.7
WBGene00007153	clcc-41	WBGene00021852	Y54F10AM.8
WBGene00007362	cyp-35C1	WBGene00022067	Y67D8C.3
WBGene00007622	C16C10.1	WBGene00022200	fard-1
WBGene00007624	hrde-1	WBGene00022300	Y76B12C.6
WBGene00007764	C27B7.7	WBGene00022313	Y77E11A.12
WBGene00008130	fbxa-140	WBGene00022331	fbxa-19
WBGene00008132	gale-1	WBGene00022351	Y82E9BR.19
WBGene00008218	nas-2	WBGene00022358	Y92H12A.2
WBGene00008400	drh-3	WBGene00022584	ZC266.1
WBGene00008430	hgap-2	WBGene00022592	klu-2
WBGene00008436	DH11.2	WBGene00022620	rde-8
WBGene00008570	kcnl-2	WBGene00044073	tag-244
WBGene00008901	nhr-27	WBGene00044107	F58G6.9
WBGene00008999	myrf-2	WBGene00044290	B0035.18
WBGene00009057	cept-1	WBGene00077714	R102.11
WBGene00009493	hrg-4	WBGene00169117	21ur-12350
WBGene00009563	F39H2.3	WBGene00219700	linc-6
WBGene00010130	vha-14	WBGene00219959	F52D2.14
WBGene00010263	wago-4	WBGene00255596	Y37B11A.8
WBGene00010308	F59B2.3		

Table 5. A list of infection specific alternatively spliced genes with *rnp-6* dependency. For the Venn diagram please refer to Figure. 27.

Term	Count	P-Value
Regulation of cell cycle	10	1.7E-3
Regulation of cell cycle process	8	2.7E-3
Regulation of developmental growth	11	7.4E-3
Cell cycle arrest	3	7.7E-3
Regulation of cell division	4	8.1E-3
Regulation of growth	11	1.0E-2
Mitotic cell cycle	9	1.4E-2
Mitotic cell cycle process	8	1.8E-2
Negative regulation of cell cycle	5	1.8E-2
Developmental growth	11	1.9E-2
Growth	13	2.0E-2
Positive regulation of multicellular organismal process	11	2.0E-2
Mitotic nuclear division	6	2.4E-2
Translation	9	3.0E-2
Positive regulation of growth	9	3.2E-2
Peptide biosynthetic process	9	3.2E-2
Regulation of multicellular organism growth	9	3.3E-2
Cell division	7	3.5E-2
Positive regulation of developmental process	10	3.5E-2
Hexose metabolic process	3	3.8E-2
Amide biosynthetic process	9	4.0E-2
Cytoskeleton-dependent cytokinesis	3	4.2E-2
Monosaccharide metabolic process	3	4.4E-2
Organonitrogen compound biosynthetic process	12	4.9E-2

Table 6. GO term enrichment analysis of the genes from Table. 5 using DAVID.

4.2.4 RNP-6 inhibits immunity

As discussed in the previous sections, a point mutation *rnp-6(dh1127)* compromises innate immunity. To further investigate the effects of RNP-6 activity on immunity, RNAi was used to knockdown *rnp-6* activity in wild-type N2 animals. Surprisingly, reduction of RNP-6 by RNAi was sufficient to improve survival upon *S. aureus* infection (Fig. 28A). We hypothesized that the effects could be due to pre-activation of immune responses induced by *rnp-6* RNAi prior to infection. To test this idea, qRT-PCR was performed on wild-type N2 worms subjected to RNAi against *rnp-6*. Indeed, several infection responsive genes, including *nlp-34*, *lys-3*, *irg-2*, *irg-1*, *M01G12.9*, *fmo-2* and *cyp-37B1*, were highly induced by *rnp-6* knockdown (Fig. 28B). Further, the conserved mediator of immune responses, PMK-1, was activated upon *rnp-6* RNAi as indicated by increased phosphorylation of the protein (Fig. 28C). These data strongly support the idea that RNP-6 activity negatively regulates immunity. In agreement with this interpretation, overexpression of RNP-6 significantly compromised survival upon *S. aureus* infection to an extent similar to *rnp-6(dh1127)* (Fig. 28D). Since RNAi knockdown enhanced immunity while *rnp-6(dh1127)* mutation compromised immunity, we suggest that the original mutation represents a gain of function that inhibits immunity and survival during infection.

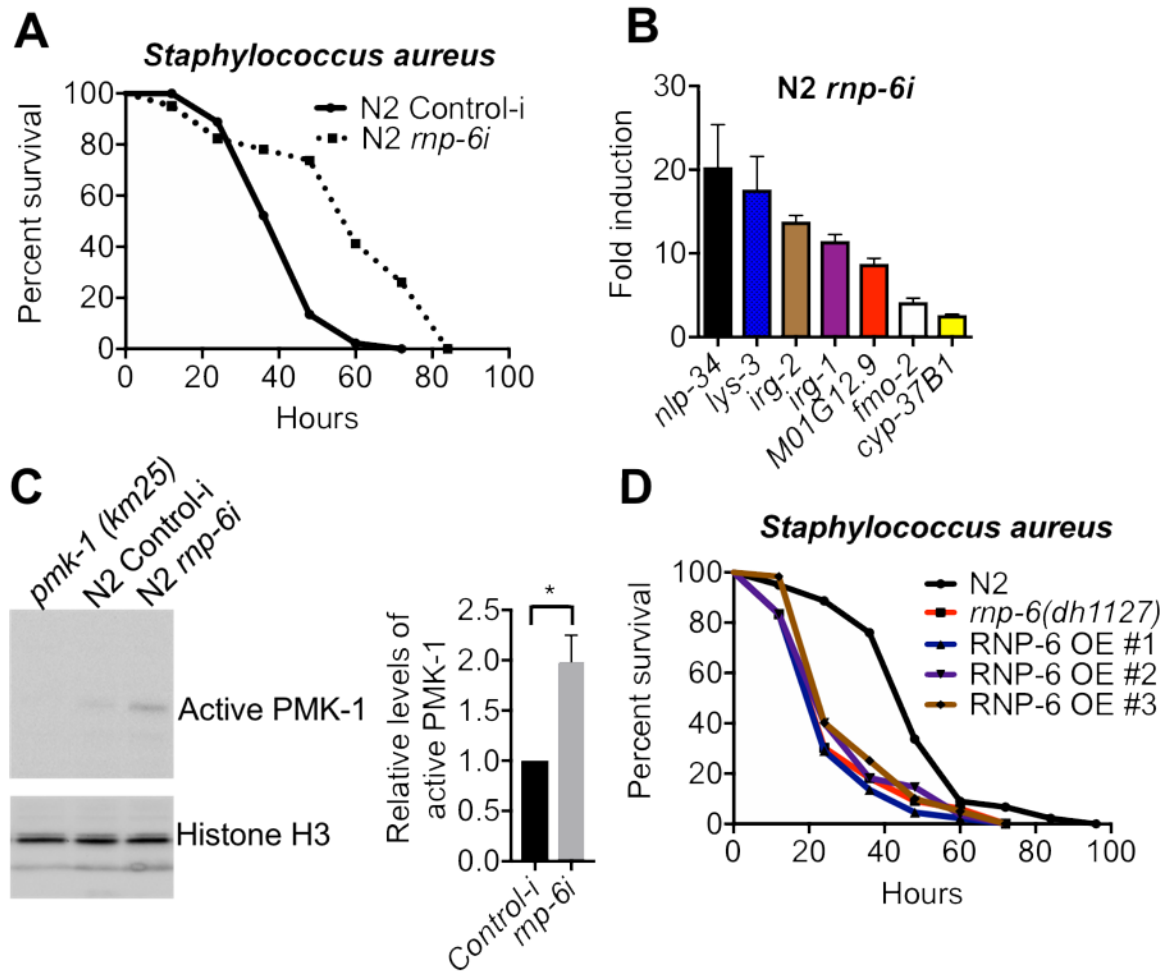


Figure 28. (A) RNAi against *rnp-6* confers resistance in wild-type N2 animals against *S. aureus* infection ($P < 0.0001$, log-rank test). (B) qRT-PCR results reveal infectious responsive genes are induced upon *rnp-6* RNAi (*nlp-34* $P = 0.0184$, *lys-3* $P = 0.0132$, *irg-2* $P < 0.0001$, *irg-1* $P = 0.0002$, *M01G12.9* $P = 0.0002$, *fmo-2* $P = 0.0021$, *cyp-37B1* $P < 0.0001$, unpaired t-test.) (C) Reduction of RNP-6 by RNAi induces activation of PMK-1 as indicated by an increase of phosphorylated PMK-1. * $P < 0.05$ unpaired t-test. Error bars represent mean \pm s.e.m. from three independent biological replicates. (D) RNP-6 overexpressing strains show enhanced sensitivity upon infection with *S. aureus* ($P = 0.0003$, log-rank test).

4.2.5 RNP-6 mediates immunity through PMK-1

We observed that reduction of RNP-6 triggers activation of PMK-1 (Fig. 28C). This immediately suggests PMK-1 may act downstream of RNP-6. To test this hypothesis, RNAi against *rnp-6* was performed in both wild-type N2 worms and also *pmk-1(km25)* mutants. Reduction of *rnp-6* expression improved survival of N2 but not the *pmk-1(km25)* mutants upon *S. aureus* infection (Fig. 29A), supporting the idea of PMK-1 acting downstream of RNP-6 to mediate resistance. Similar results were also obtained with *tir-1(tm3036)* (Fig. 29B), which encodes the worm's homolog of SARM. Notably, TIR-1 functions upstream of PMK-1 in a linear kinase signaling pathway that controls innate immunity in *C. elegans*.

Next, we tested how *rnp-6;pmk-1* double mutants behave in infection. While both *pmk-1* and *rnp-6* single mutants showed reduced survival when infected with *S. aureus*, *rnp-6;pmk-1* double mutants showed survival curves similar to *pmk-1* single mutant alone (Fig. 29C). This lack of additivity is consistent with the idea that *pmk-1* is epistatic and acts downstream of *rnp-6*. Similar observations were also made in *P. aeruginosa* infection. Both *pmk-1* and *rnp-6* mutants died faster compared to wild-type N2 animals during *P. aeruginosa* infection, though *rnp-6;pmk-1* double mutants showed a slightly higher resistance than *pmk-1* mutants (Fig. 29D).

Next, we tested how the gain of function mutation of *rnp-6* can affect PMK-1 activity. *P. aeruginosa* infection is known to stimulate PMK-1 activity (Kim et al., 2002, Liu, He et al., 2013). Interestingly, when wild-type N2 and *rnp-6(dh1127)* animals were infected with *P. aeruginosa*, an induction of phospho-PMK-1 was seen in N2 but not in *rnp-6(dh1127)* mutants (Fig. 29E). This result suggests that increased activity of RNP-6 hampers activity of PMK-1, which might potentially explain why the *rnp-6* mutants show compromised survival upon infection.

The potential involvement of other known regulators of innate immunity was also tested, namely *daf-16* and *hlh-30*. Unlike *pmk-1*, *rnp-6* RNAi was still able to confer resistance to the mutants of *daf-16* (Fig. 30A) and *hlh-30* (Fig. 30B), suggesting *daf-16* and *hlh-30* are unlikely to mediate the resistance phenotype of *rnp-6* knockdown.

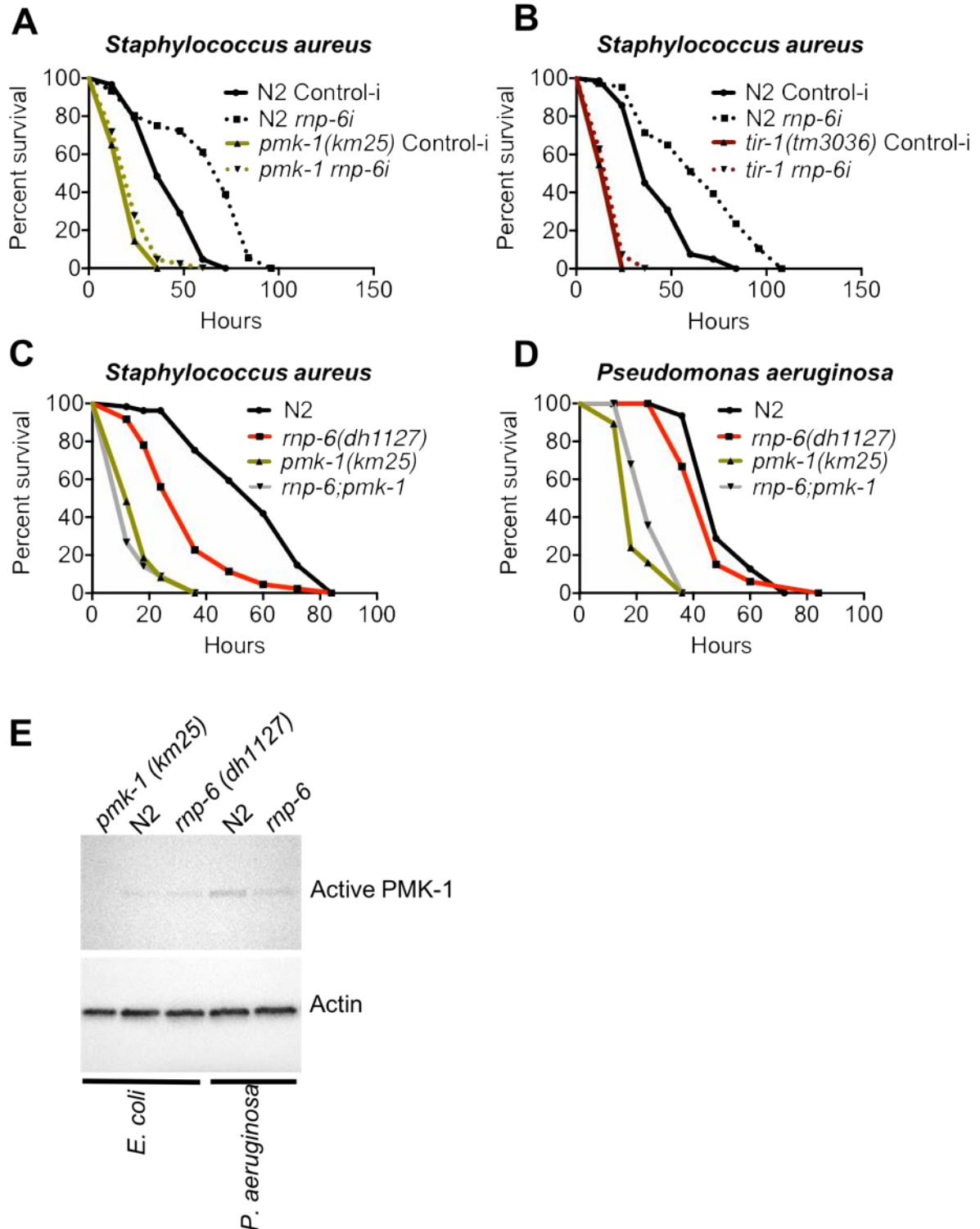


Figure 29. (A,B) RNAi against *rnp-6* confers resistance in wild-type N2 animals ($P<0.0001$, log-rank test), but not *pmk-1(km25)* ($P=0.1043$, log-rank test) and *tir-1(tm3036)* ($P=0.1074$, log-rank test) against *S. aureus* infection. (C,D) The effects of *rnp-6* and *pmk-1* are not fully additive. (C) Upon *S. aureus* infection, both *rnp-6(dh1127)* ($P<0.0001$, log-rank test) and *pmk-1(km25)* ($P<0.0001$, log-rank test) are sensitive, but the double mutant has sensitivity similar to *pmk-1(km25)* alone ($P=0.1847$, log-rank test). (D) Upon *P. aeruginosa* infection, both *rnp-6(dh1127)* ($P=0.0056$, log-rank test) and *pmk-1(km25)* ($P<0.0001$, log-rank test) are sensitive. The double mutant is slightly more resistant relative to *pmk-1(km25)* alone ($P<0.0001$, log-rank test). (E) *rnp-6(dh1127)* suppresses induction of phospho-PMK-1 upon *P. aeruginosa* infection. Animals were harvested for western blot 2 hours post-infection.

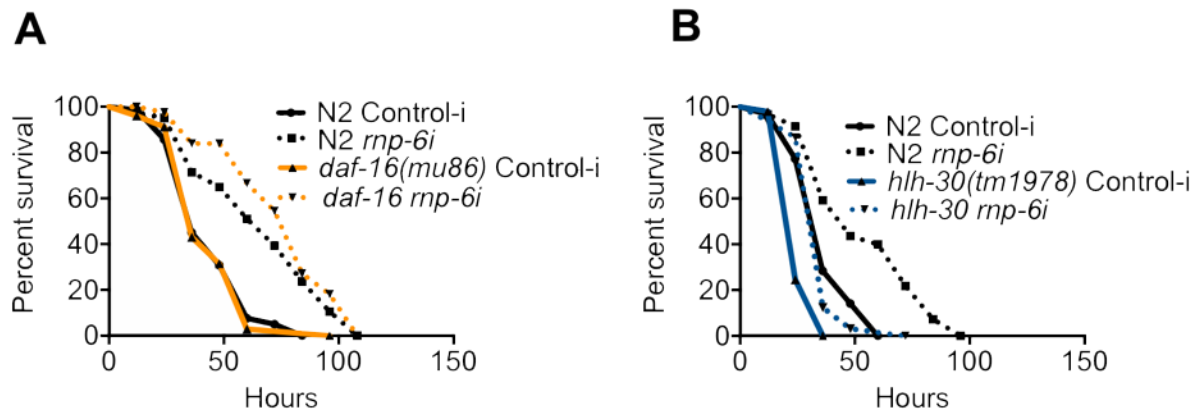


Figure 30. (A,B) *daf-16* and *hlh-30* are not required for resistance conferred by RNP-6 reduction. RNAi against *rnp-6* similarly confers resistance in wild-type N2 animals ($P<0.0001$, log-rank test), *daf-16(mu86)* ($P<0.0001$, log-rank test) and *hlh-30(tm1978)* ($P<0.0001$, log-rank test) against *S. aureus* infection.

4.2.6 Mutual regulation of splicing and host responses to infection

Given that RNP-6, a splicing factor, plays an important role in innate immunity, we next wondered whether other splicing factors also have similar effects on pathogen resistance and PMK-1 activation. RNAi against *prp-38* and *uaf-1* was performed in wild-type N2 animals. *prp-38* encodes a highly conserved splicing factor (mRNA-processing factor 38 in *Saccharomyces cerevisiae*), which functions as an interaction platform for protein assembly, activation, and catalysis of the spliceosome complex (Tan & Fraser, 2017). *uaf-1* encodes the large subunit of splicing factor U2AF, orthologous to mammalian and *Drosophila* U2AF65. U2AF recognizes a long polypyrimidine sequence located at the 3' end of the introns. PUF-60, the ortholog of RNP-6 in mammals, works cooperatively with U2AF for efficient splicing (Page-McCaw et al., 1999). Reducing expression of either splicing factor elicited improved survival upon *S. aureus* infection (Fig. 31A). Similar to *rnp-6*, RNAi against the splicing factors also triggered activation of PMK-1 as indicated by the increased phosphorylated PMK-1 levels (Fig. 31B). The results demonstrate that the splicing machinery may more generally control the immune response and suggest that perturbing splicing could induce immunity.

We next sought to further investigate the link between splicing and infection and how *rnp-6* affects the connection. Infection is able to perturb alternative splicing of *tos-1* (Fig. 17C,D). We therefore wondered whether alternative splicing would be similarly affected in the *rnp-6* mutant after infection. Interestingly, at the non-infected state, the *rnp-6(dh1127)* and *rnp-6(dh1125)* mutants already showed a drastically different splicing pattern of *tos-1* compared to wild-type N2 animals (Fig. 31C,D). The larger isoform became more abundant in the mutants. After infection, splicing of *tos-1* was altered as the abundance of the smaller isoform increased. Strikingly, the *rnp-6* mutants were refractory to the change induced by infection; i.e., the relative quantity between the larger and smaller isoforms remained the same (Fig 31C,D). Taken together, our results reveal a mutual regulation between splicing and host responses to infection in which RNP-6 plays a critical role.

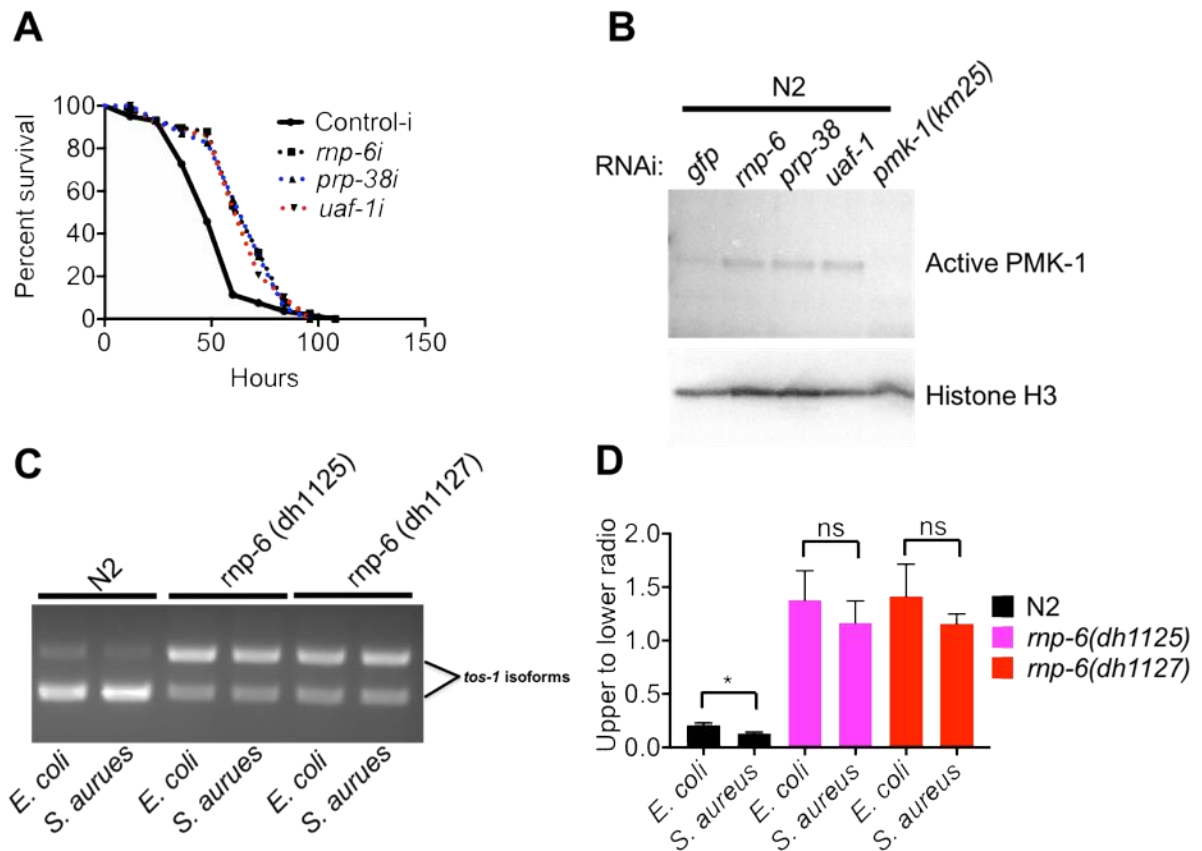


Fig 31. (A) *prp-38*, *uaf-1* and *rnp-6* RNAi all induce similar resistance phenotype upon *S. aureus* infection. ($P < 0.0001$, log-rank test) (B) PMK-1 phosphorylation is increased upon RNAi knockdown of *rnp-6*, *prp-38* and *uaf-1*, suggesting an activation of PMK-1. (C,D) RT-PCR shows that splicing of endogenous *tos-1* transcript in wild-type N2 animals is altered after 4 hours of infection with *S. aureus*. Intriguingly, splicing remains unchanged in *rnp-6(dh1125)* and *rnp-6(dh1127)* after *S. aureus* infection. * $P < 0.05$, ns non-significant, unpaired t-test.

4.3 Discussion

In the second part of the study, we identified *rnp-6* as a novel regulator of innate immunity. In *C. elegans*, bacterial infection alters alternative splicing of *ret-1* and *tos-1*, suggesting an interesting connection between infection and splicing. A novel missense mutation of *rnp-6* causes compromised survival during infection with *S. aureus*, *E. faecalis*, and *P. aeruginosa*. Further investigations revealed that the mutant of *rnp-6* shows dampened transcriptional responses to infection and also reduced activity of PMK-1, as indicated by the reduced levels of the phosphorylated form of the protein. Overexpression of RNP-6 phenocopies the sensitive phenotype of the missense mutant, while knocking down *rnp-6* results in enhanced resistance and activation of immune responses, suggesting that the mutation is a gain-of-function. Genetic epistasis is consistent with the idea of PMK-1 acting downstream of RNP-6, since RNA-6 RNAi induced infection resistance in a PMK-1 dependent manner, and PMK-1 phosphorylation was induced in an RNP-6 dependent manner. Finally, knocking down other splicing factors also induces similar resistance phenotype and PMK-1 activation, indicating that the splicing machinery may be a general control factor for induction of innate immune responses, and perturbing splicing is an inducer of immunity. An important question to be addressed in the future is whether infection regulates the protein or activity levels of RNP-6 and other splicing factors as part of an adaptive host response.

In mammals, splicing of pre-mRNAs yields key proteins in the adaptive immune system that regulate lymphocyte differentiation, apoptosis and activation (Yabas, Elliott et al., 2015). For example, antibody production is regulated by splicing. In B cells, IgM and IgD are co-expressed through alternative splicing of a long primary mRNA transcript from the *Igh* locus (Maki, Roeder et al., 1981). T cell activation also leads to an alteration of splicing in numerous target genes. The *Bcl2l1* gene, a pro-apoptotic protein, undergoes alternative splicing to yield three different isoforms that differ in their capacity to induce immune cell apoptosis (Yabas et al., 2015). However, our knowledge of the role of splicing in innate immunity is still limited. In this study, using *C. elegans*, we provide novel evidences of the involvement of splicing in innate host responses against bacterial infection.

The results of *rnp-6* can be considered as another example of effector-triggered immunity. Splicing is an essential cellular process. Other essential cellular processes are closely monitored, and perturbations of such processes have been shown to activate immune responses (Melo & Ruvkun, 2012). The results present here suggest RNP-6 activity specifically and splicing in general are also novel players in effector-triggered immunity. How perturbing splicing can lead to activation of PMK-1 and immune responses is not well-understood at this point. One possible way is that some important regulators of PMK-1 is controlled by splicing. For example, the active isoform is preferentially generated by splicing under splicing stress. Such downstream mediators remain to be seen.

Transcriptomic analysis suggests that *rnp-6(dh1127)* diminish expression of infection inducible immune defense genes. One interesting observation is that some infection downregulated genes are also dependent on *rnp-6*. GO analysis reveals the functions of these genes are enriched for metabolic process, especially for organic acid. The involvement of these metabolites in innate immunity is not well-understood. However, this suggests that *rnp-6* may affect immunity through metabolic control. The immunometabolism aspect of *rnp-6* or splicing in general merits further investigations.

In *C. elegans*, enhanced splicing activity has been shown to be sufficient to increase lifespan. Also, dietary restriction and inhibition of mechanistic target of rapamycin (mTOR) extend lifespan partially by maintaining high splicing capacity during ageing (Heintz et al., 2017). Results also indicate the gain of function mutation of *rnp-6* is long-lived at 20°C (unpublished data from Dr. Wenming Huang). Therefore, it seems that there is a tradeoff between longevity and immunity in the *rnp-6* mutant. This is interesting because long-lived mutants are usually resistant to pathogenic stress (Garsin et al., 2003, Wu et al., 2015), and the long-lived *rnp-6* mutant seems to be one exception. Also, it would be very interesting to see whether strains with enhanced splicing capacity, such as the SFA-1 overexpressing strains, which were shown to be long-lived (Heintz et al., 2017), are sensitive to pathogenic bacteria like the *rnp-6* mutant. Splicing fidelity deteriorates over age, and chronic inflammation is a common phenotype associated with ageing. Age-associated inflammation may be caused by decreased splicing capacity. Furthermore, it is well-known that dietary restriction has

a mixed effect on immunity rather than a beneficial one (Hale, Spencer et al., 2015). This could be due to improved splicing induced by dietary restriction, which inhibits activation of immunity.

How infection triggers changes in splicing is also an interesting question. Bacteria are known to produce small molecules to interfere cellular functions of the host. For example, exotoxins produced by *P. aeruginosa* inhibit translation of host cells (McEwan et al., 2012). It is possible that bacteria also produce small molecules to inhibit splicing. In fact, some antibiotics produced by bacteria are described as splicing inhibitors, namely tetracycline, streptomycin, and erythromycin. These molecules are known to inhibit translation by binding to specific RNA structures in the ribosome. The spliceosome is also an RNA-dependent enzyme, which could be inhibited by the antibiotics through a similar mechanism (Effenberger, Urabe et al., 2017). Another potential explanation is the kinetic competition for splicing machineries by nascent transcripts. Splicing is a co-transcriptional event, and the emerging RNA transcripts compete the limited splicing machineries (Coulon, Ferguson et al., 2014). Infection may trigger a surge of transcription, which overruns the splicing capacity of the cells. The results would be a change of splicing patterns. Alternatively, nucleic acid moieties from pathogens could affect splicing and trigger the innate immune response.

De novo variants in PUF60, the homolog of RNP-6 in mammals, can be found in human population. Loss of function mutations of PUF60 in heterozygous form cause Verheij syndrome, whose phenotypes include intellectual disability and developmental defects, such as delayed development and short stature (El Chehadeh, Kerstjens-Frederikse et al., 2016). As RNP-6 plays a crucial role in immunity in *C. elegans*, it would be very interesting to investigate whether the Verheij syndrome mutations also cause defects in immunity in the patients, or whether the pathology of Verheij syndrome is in fact driven by immune responses. Reduction of RNP-6 activity in *C. elegans* activates immune responses. It is predicted that the partial loss of function of PUF60 in human cells may also activate inflammatory responses which may exaggerate the pathology of Verheij syndrome.

Recently, discoveries from cancer research have raised the potential of the splicing machinery as a target for chemotherapeutics. Mutations in splicing factors can be

found in different cancer cells. For example, specific SF3B1 mutations are frequent in cancerous cells from patients with different kind of malignancy, such as chronic lymphocytic leukemia, breast cancer, and pancreatic cancer (Effenberger et al., 2017). SF3B1 is the subunit 1 of the splicing factor 3b protein complex, which is a key component of the U2 small nuclear ribonucleoproteins complex of the spliceosome. Changes in SF3B1 functions perturb normal gene expression and contribute to transformation and metastasis (Effenberger et al., 2017). For this reason, several splicing inhibitors targeting SF3B1 have been developed. Importantly, SF3B1 inhibitors arrest growth of most cancer cells at low nanomolar concentrations. Cells derived from normal tissues show higher resistance to SF3B1 inhibitors relative to cancer cells (Effenberger et al., 2017). Our results of the effects of splicing on immunity indicate a possibility of modulating immune responses by manipulating splicing. A recent study also suggests SF3A1 and SF3B1 can modulate immunity through alternative splicing of MyD88 (De Arras & Alper, 2013). If splicing is inhibited by splicing inhibitors, this may already be sufficient to activate immune responses. In cancer patients, this may lead to enhanced inflammation and contribute to cancer progression. Therefore, the use of splicing inhibitors as anti-cancer chemotherapeutics should be carefully tested before clinical applications. On the other hand, splicing inhibitors may function as a booster of immunity. For example, splicing inhibitors may function as a good adjuvant to vaccine to optimize the immune response. Also, splicing inhibitors may also be taken as anti-bacterial drugs to reduce the use of antibiotics.

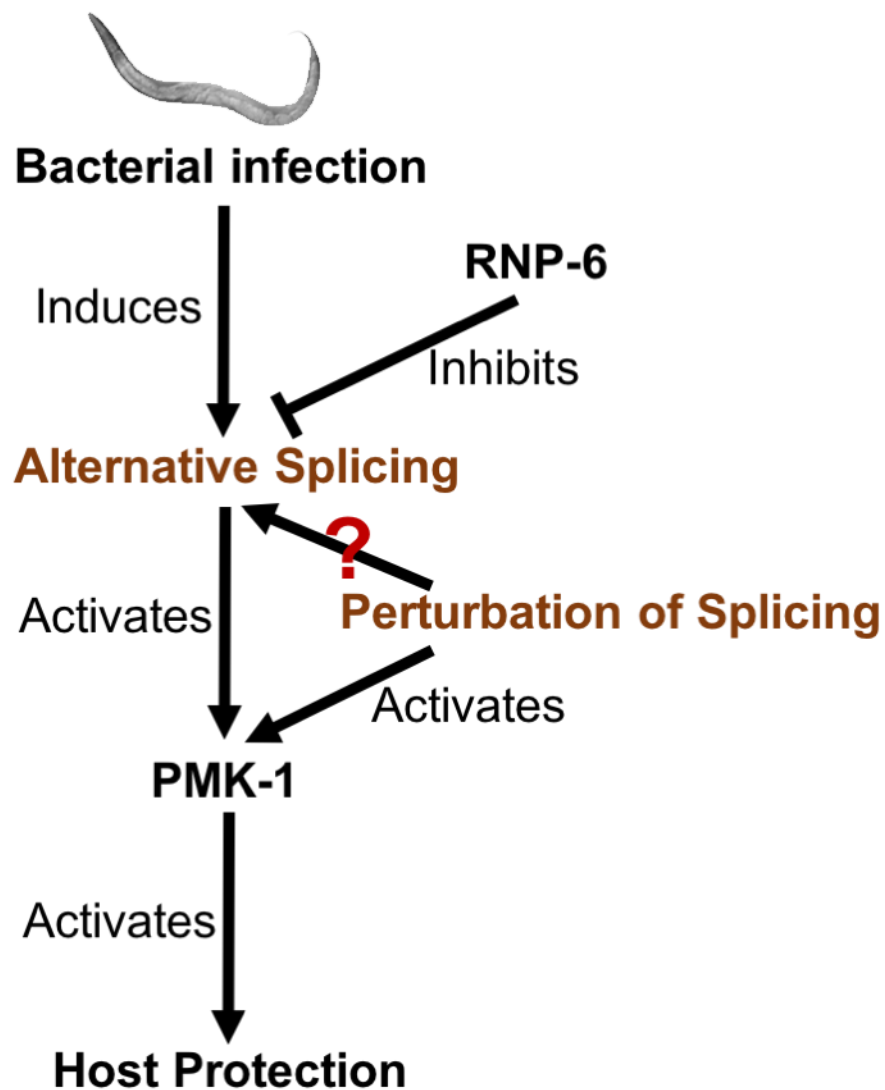


Fig 32. A summary of the study of *rnp-6*. In *C. elegans*, bacterial infection leads to alternative splicing, which is inhibited by the activity of RNP-6. Alternative splicing induced by infection or perturbing splicing activates PMK-1 and immune responses. Increased activity of RNP-6, on the other hand, inhibits activation of PMK-1 and immunity.

4.4 Work contribution

Except for RNA sequencing and bioinformatic analysis, all experiments included in this chapter were performed independently by me. Samples for RNA sequencing were prepared by me, and the sequencing reaction was performed by Cologne Center for Genomics (CCG), University of Cologne. Bioinformatic analysis was performed together by me and Dr. Rafael Cuadrat (MPI-AGE).

CHAPTER 5

FUTURE PERSPECTIVES

Future perspectives

5.1 Investigating the mechanism of nucleolar functions in innate immunity

Our findings point to the direction of mediation of immunity by nucleolar functions of rRNA biogenesis and translation. As nucleolar size reduces significantly after infection in both nematodes and mammalian cells, it is reasonable to presume other nucleolar functions also decrease. Whether other nucleolar functions also contribute to the phenotypes observed should be examined. Survival assays after knock-down of SRP subunits or tRNA modifying enzymes can be done.

We will also investigate the downstream mechanisms of the resistance conferred by fibrillarin reduction. As fibrillarin reduction leads to suppression of translation, it is predicted that a remodeling of proteome may occur. We propose an omics approach to tackle this question. Fibrillarin and control knockdown murine macrophages will be infection with *S. aureus* or mock infected. The samples will be harvested for both RNA and proteins. RNA sequencing and proteomics will be performed. By comparing the data from the two approaches, we can test how the proteome is changed upon fibrillarin knockdown and infection. It is possible to identify candidates, whose translation is preferentially affected by fibrillarin, which may be further pursued in the future studies.

5.2 Investigating the mechanism of fibrillarin reduction

Reduction of fibrillarin is an evolutionarily conserved host response to bacterial infection. How fibrillarin is reduced remains to be investigated. Possible mechanisms are proteasomal or autophagic degradation. To test these possibilities, proteasomal inhibitors, such as MG132, or autophagic inhibitors, such as bafilomycin, can be used to treat macrophages prior to infection. If the processes are involved in fibrillarin reduction, the fibrillarin levels should be unaltered in the respective treated cells. An unbiased approach can also be performed. We will perform RNAi screening in *C. elegans* to identify RNAi clones that can revert the infection induced reduction of FIB-1::GFP.

5.3 Probing nucleolar regulation of immunity in animal models

The functions of fibrillarin are well-conserved in both *C. elegans* and mammalian cells. The next step would be to test whether they are also conserved in mammalian animal models. A mouse model is ideal for this purpose. First, we will infect mouse with *S. aureus*, and cells will be isolated for nucleolar size measurement and fibrillarin western blot detection. Macrophages or peripheral blood mononuclear cells could be used. A decrease of nucleolar size and fibrillarin protein levels is predicted. Local in vivo administration of siRNAs can also be done in lung (Li, Tang et al., 2005). *S. aureus* pulmonary infection will be established in mice treated with fibrillarin or control siRNA. Pathology, survival and inflammation will be compared. An alternative to siRNA would be to generate a heterozygous fibrillarin knockout mouse strain.

5.4 Elucidating splicing control of innate immunity

Infection alters alternative splicing, and changes of splicing also impacts host responses to infection. How perturbing splicing can affect immune responses is unknown. Very likely, some important regulators of innate immunity are controlled by splicing. For examples, alternative splicing can yield different isoforms of the same gene that differ in their activity. We will perform a RNAi screening for such genes. Genes that undergo splicing changes upon infection in wild-type N2 animals but not in the *rnp-6* mutant (Table. 5) will be knock-down in the *rnp-6* mutant. Infection resistance against *S. aureus* will then be tested. RNAi clones that can reverse the sensitivity phenotype of the *rnp-6* mutant will be investigated further.

5.5 Studying control of innate immunity by splicing under other circumstances

Other than *rnp-6* gain-of-function and knocking-down *rnp-6*, splicing activity can be affected by other means. For example, partial loss of function alleles of *mfap-1* and *uaf-1* (Ma & Horvitz, 2009, Ma et al., 2011), which both are essential splicing factors, are viable. We will test whether these mutants exhibit the similar resistance phenotype. On the other hand, SFA-1 overexpressing animals were shown to have enhanced splicing capacity and extended lifespan (Heintz et al., 2017). Resistance of this strain

will also be tested in *S. aureus* infection experiments, and we predict it may have the similar sensitive phenotype as the RNP-6 overexpressing strains. Dietary restriction and inhibition of mTOR can also improve splicing capacity similarly to overexpression of SFA-1. How dietary restriction affects innate immunity is not very well-studied in *C. elegans*. We propose to perform survival studies and transcriptional profiling of dietary restricted animals under both control and infected condition.

5.6 Extending the findings of *rnp-6* to higher organisms

It is highly desirable to test whether the effects of *rnp-6* or splicing in general on immunity is conserved in higher organisms. We will knockdown and overexpress PUF60, the homolog of RNP-6, in murine macrophages and test whether activation of p38, the ortholog of PMK-1, secretion of cytokines and also cell survival are affected upon *S. aureus* pathogenic challenges. Also, effects of other splicing factors will also be tested. For example, the effects of knocking-down SF3B1 on immunity will be tested. Pharmacological inhibition of splicing is also feasible. Splicing inhibitors, such as spliceostatin A, will be used to treat murine macrophages. Signs of activation of immune responses, including phosphorylation of p38 and production of cytokines, will be examined.

The potential impact of Verheij syndrome mutations on immunity should also be carefully investigated. We propose to measure cytokine levels from serum of the patients to test whether the mutations of PUF60 cause any inflammation. The mutation can also be introduced in cell lines or *C. elegans* using CRISPR technology. The mutant strains can then be used for in depth studies of the effects of the mutations on immunity.

An in vivo mammalian model will also be very useful. Macrophages or peripheral blood mononuclear cells from infected mice will be isolated, and the RNA would be sequenced. Alternative splicing events induced by infection will be identified and characterized. Also, to manipulate splicing in vivo, administration of splicing inhibitors, such as spliceostatin A, can be done. Cytokine levels will then be measured and compared to the control. Effects of splicing inhibitors on survival and pathology upon *S. aureus* infection will also be observed.

5.7 Exploring possible links between the nucleolus, splicing and immunity

Lastly, we plan to explore the potential connection between fibrillarin and *rnp-6* in the regulation of innate immunity. To begin with, we propose to use a genetic approach. RNAi against *fib-1* will be done on *rnp-6(dh1127)* mutants to test for epistasis. Next, RNA sequencing will be used to profile alternative splicing in *C. elegans* subjected to *fib-1* RNAi and infection. The possible effects of *fib-1* RNAi with or without infection on splicing will be examined. On the other hand, nucleolar size, mature and pre-rRNA levels and translation rate will be measured in *rnp-6(dh1127)* mutants and also wild-type animals with *rnp-6* knockdown under both control and infection conditions.

CHAPTER 6

REFERENCES

References

Aballay A, Drenkard E, Hilbun LR, Ausubel FM (2003) *Caenorhabditis elegans* innate immune response triggered by *Salmonella enterica* requires intact LPS and is mediated by a MAPK signaling pathway. *Curr Biol* 13: 47-52

Aballay A, Yorgey P, Ausubel FM (2000) *Salmonella typhimurium* proliferates and establishes a persistent infection in the intestine of *Caenorhabditis elegans*. *Curr Biol* 10: 1539-42

Barberan-Soler S, Zahler AM (2008) Alternative splicing regulation during *C. elegans* development: splicing factors as regulated targets. *PLoS Genet* 4: e1000001

Berget SM, Moore C, Sharp PA (1977) Spliced segments at the 5' terminus of adenovirus 2 late mRNA. *Proc Natl Acad Sci U S A* 74: 3171-5

Boisvert FM, van Koningsbruggen S, Navascues J, Lamond AI (2007) The multifunctional nucleolus. *Nat Rev Mol Cell Biol* 8: 574-85

Boman HG, Nilsson I, Rasmuson B (1972) Inducible antibacterial defence system in *Drosophila*. *Nature* 237: 232-5

Brandt JP, Ringstad N (2015) Toll-like Receptor Signaling Promotes Development and Function of Sensory Neurons Required for a *C. elegans* Pathogen-Avoidance Behavior. *Curr Biol* 25: 2228-37

Brenner S (1974) The genetics of *Caenorhabditis elegans*. *Genetics* 77: 71-94

Bubulya PA, Prasanth KV, Deerinck TJ, Gerlich D, Beaudouin J, Ellisman MH, Ellenberg J, Spector DL (2004) Hypophosphorylated SR splicing factors transiently localize around active nucleolar organizing regions in telophase daughter nuclei. *J Cell Biol* 167: 51-63

Buchon N, Silverman N, Cherry S (2014) Immunity in *Drosophila melanogaster*--from microbial recognition to whole-organism physiology. *Nat Rev Immunol* 14: 796-810

Buchwalter A, Hetzer MW (2017) Nucleolar expansion and elevated protein translation in premature aging. *Nat Commun* 8: 328

Burgess DJ (2013) Gene expression: controls and roles for trans-splicing. *Nat Rev Genet* 14: 822

Cabreiro F, Au C, Leung KY, Vergara-Irigaray N, Cocheme HM, Noori T, Weinkove D, Schuster E, Greene ND, Gems D (2013) Metformin retards aging in *C. elegans* by altering microbial folate and methionine metabolism. *Cell* 153: 228-39

Chira S, Gulei D, Hajitou A, Berindan-Neagoe I (2018) Restoring the p53 'Guardian' Phenotype in p53-Deficient Tumor Cells with CRISPR/Cas9. *Trends Biotechnol*

Chousterman BG, Swirski FK, Weber GF (2017) Cytokine storm and sepsis disease pathogenesis. *Seminars in Immunopathology* 39: 517-528

Chow LT, Gelinas RE, Broker TR, Roberts RJ (1977) An amazing sequence arrangement at the 5' ends of adenovirus 2 messenger RNA. *Cell* 12: 1-8

Chuang CF, Bargmann CI (2005) A Toll-interleukin 1 repeat protein at the synapse specifies asymmetric odorant receptor expression via ASK1 MAPKKK signaling. *Genes Dev* 19: 270-81

Clark RI, Woodcock KJ, Geissmann F, Trouillet C, Dionne MS (2011) Multiple TGF-beta superfamily signals modulate the adult *Drosophila* immune response. *Curr Biol* 21: 1672-7

Cohen LB, Troemel ER (2015) Microbial pathogenesis and host defense in the nematode *C. elegans*. *Curr Opin Microbiol* 23: 94-101

Coulon A, Ferguson ML, de Turris V, Palangat M, Chow CC, Larson DR (2014) Kinetic competition during the transcription cycle results in stochastic RNA processing. *Elife* 3

Curt A, Zhang J, Minnerly J, Jia K (2014) Intestinal autophagy activity is essential for host defense against *Salmonella typhimurium* infection in *Caenorhabditis elegans*. *Dev Comp Immunol* 45: 214-8

Daelemans D, Costes SV, Cho EH, Erwin-Cohen RA, Lockett S, Pavlakis GN (2004) In vivo HIV-1 Rev multimerization in the nucleolus and cytoplasm identified by fluorescence resonance energy transfer. *J Biol Chem* 279: 50167-75

Dang CV (2012) MYC on the path to cancer. *Cell* 149: 22-35

De Arras L, Alper S (2013) Limiting of the innate immune response by SF3A-dependent control of MyD88 alternative mRNA splicing. *PLoS Genet* 9: e1003855

Demontis F, Patel VK, Swindell WR, Perrimon N (2014) Intertissue control of the nucleolus via a myokine-dependent longevity pathway. *Cell Rep* 7: 1481-1494

Deppe U, Schierenberg E, Cole T, Krieg C, Schmitt D, Yoder B, von Ehrenstein G (1978) Cell lineages of the embryo of the nematode *Caenorhabditis elegans*. *Proc Natl Acad Sci U S A* 75: 376-80

Dhanwani R, Takahashi M, Sharma S (2017) Cytosolic sensing of immuno-stimulatory DNA, the enemy within. *Curr Opin Immunol* 50: 82-87

Diard M, Baeriswyl S, Clermont O, Gouriou S, Picard B, Taddei F, Denamur E, Matic I (2007) *Caenorhabditis elegans* as a simple model to study phenotypic and genetic virulence determinants of extraintestinal pathogenic *Escherichia coli*. *Microbes Infect* 9: 214-23

Donato V, Ayala FR, Cogliati S, Bauman C, Costa JG, Lenini C, Grau R (2017) *Bacillus subtilis* biofilm extends *Caenorhabditis elegans* longevity through downregulation of the insulin-like signalling pathway. *Nat Commun* 8: 14332

Dunbar TL, Yan Z, Balla KM, Smelkinson MG, Troemel ER (2012) *C. elegans* detects pathogen-induced translational inhibition to activate immune signaling. *Cell Host Microbe* 11: 375-86

Duncan R, Bazar L, Michelotti G, Tomonaga T, Krutzsch H, Avigan M, Levens D (1994) A sequence-specific, single-strand binding protein activates the far upstream element of *c-myc* and defines a new DNA-binding motif. *Genes Dev* 8: 465-80

Effenberger KA, Urabe VK, Jurica MS (2017) Modulating splicing with small molecular inhibitors of the spliceosome. *Wiley Interdiscip Rev RNA* 8

El Chehadeh S, Kerstjens-Frederikse WS, Thevenon J, Kuentz P, Bruel AL, Thauvin-Robinet C, Bensignor C, Dollfus H, Laugel V, Riviere JB, Duffourd Y, Bonnet C, Robert MP, Isaiko R, Straub M, Creuzot-Garcher C, Calvas P, Chassaing N, Loeys B, Reyniers E et al. (2016) Dominant variants in the splicing factor PUF60 cause a recognizable syndrome with intellectual disability, heart defects and short stature. *Eur J Hum Genet* 25: 43-51

Estes KA, Dunbar TL, Powell JR, Ausubel FM, Troemel ER (2010) bZIP transcription factor zip-2 mediates an early response to *Pseudomonas aeruginosa* infection in *Caenorhabditis elegans*. *Proc Natl Acad Sci U S A* 107: 2153-8

Evans EA, Chen WC, Tan MW (2008) The DAF-2 insulin-like signaling pathway independently regulates aging and immunity in *C. elegans*. *Aging Cell* 7: 879-93

Evans EA, Kawli T, Tan MW (2008) *Pseudomonas aeruginosa* suppresses host immunity by activating the DAF-2 insulin-like signaling pathway in *Caenorhabditis elegans*. *PLoS Pathog* 4: e1000175

Ewbank JJ, Pujol N (2010) Cellular homeostasis: coping with ER overload during an immune response. *Curr Biol* 20: R452-5

Falaleeva M, Pages A, Matuszek Z, Hidmi S, Agranat-Tamir L, Korotkov K, Nevo Y, Eyras E, Sperling R, Stamm S (2016) Dual function of C/D box small nucleolar RNAs in rRNA modification and alternative pre-mRNA splicing. *Proc Natl Acad Sci U S A* 113: E1625-34

Felix MA, Ashe A, Piffaretti J, Wu G, Nuez I, Belicard T, Jiang Y, Zhao G, Franz CJ, Goldstein LD, Sanroman M, Miska EA, Wang D (2011) Natural and experimental infection of *Caenorhabditis* nematodes by novel viruses related to nodaviruses. *PLoS Biol* 9: e1000586

Felix MA, Duveau F (2012) Population dynamics and habitat sharing of natural populations of *Caenorhabditis elegans* and *C. briggsae*. *BMC Biol* 10: 59

Florentino DF, Presby M, Baer AN, Petri M, Rieger KE, Soloski M, Rosen A, Mammen AL, Christopher-Stine L, Casciola-Rosen L (2016) PUF60: a prominent new target of the autoimmune response in dermatomyositis and Sjogren's syndrome. *Ann Rheum Dis* 75: 1145-51

Fire A, Xu S, Montgomery MK, Kostas SA, Driver SE, Mello CC (1998) Potent and specific genetic interference by double-stranded RNA in *Caenorhabditis elegans*. *Nature* 391: 806-11

Friedland AE, Tzur YB, Esvelt KM, Colaiacovo MP, Church GM, Calarco JA (2013) Heritable genome editing in *C. elegans* via a CRISPR-Cas9 system. *Nat Methods* 10: 741-3

Friedman DB, Johnson TE (1988) A mutation in the *age-1* gene in *Caenorhabditis elegans* lengthens life and reduces hermaphrodite fertility. *Genetics* 118: 75-86

Fuhrman LE, Goel AK, Smith J, Shianna KV, Aballay A (2009) Nucleolar proteins suppress *Caenorhabditis elegans* innate immunity by inhibiting p53/CEP-1. *PLoS Genet* 5: e1000657

Fulginiti VA, Papier A, Lane JM, Neff JM, Henderson DA (2003) Smallpox vaccination: a review, part I. Background, vaccination technique, normal vaccination and revaccination, and expected normal reactions. *Clin Infect Dis* 37: 241-50

Garsin DA, Sifri CD, Mylonakis E, Qin X, Singh KV, Murray BE, Calderwood SB, Ausubel FM (2001) A simple model host for identifying Gram-positive virulence factors. *Proc Natl Acad Sci U S A* 98: 10892-7

Garsin DA, Villanueva JM, Begun J, Kim DH, Sifri CD, Calderwood SB, Ruvkun G, Ausubel FM (2003) Long-lived *C. elegans* daf-2 mutants are resistant to bacterial pathogens. *Science* 300: 1921

George-Raizen JB, Shockley KR, Trojanowski NF, Lamb AL, Raizen DM (2014) Dynamically-expressed prion-like proteins form a cuticle in the pharynx of *Caenorhabditis elegans*. *Biol Open* 3: 1139-49

Greco A, Arata L, Soler E, Gaume X, Coute Y, Hacot S, Calle A, Monier K, Epstein AL, Sanchez JC, Bouvet P, Diaz JJ (2012) Nucleolin interacts with US11 protein of herpes simplex virus 1 and is involved in its trafficking. *J Virol* 86: 1449-57

Grishok A (2013) Biology and Mechanisms of Short RNAs in *Caenorhabditis elegans*. *Adv Genet* 83: 1-69

Gupta A, Singh V (2017) GPCR Signaling in *C. elegans* and Its Implications in Immune Response. *Adv Immunol* 136: 203-226

Hale MW, Spencer SJ, Conti B, Jasoni CL, Kent S, Radler ME, Reyes TM, Sominsky L (2015) Diet, behavior and immunity across the lifespan. *Neurosci Biobehav Rev* 58: 46-62

Hammell CM, Hannon GJ (2012) Inducing RNAi in *C. elegans* by feeding with dsRNA-expressing *E. coli*. *Cold Spring Harb Protoc* 2012

Hanlon CD, Andrew DJ (2015) Outside-in signaling--a brief review of GPCR signaling with a focus on the *Drosophila* GPCR family. *J Cell Sci* 128: 3533-42

Haskins KA, Russell JF, Gaddis N, Dressman HK, Aballay A (2008) Unfolded protein response genes regulated by CED-1 are required for *Caenorhabditis elegans* innate immunity. *Dev Cell* 15: 87-97

Head B, Aballay A (2014) Recovery from an acute infection in *C. elegans* requires the GATA transcription factor ELT-2. *PLoS Genet* 10: e1004609

Hedgecock EM, Herman RK (1995) The *ncl-1* gene and genetic mosaics of *Caenorhabditis elegans*. *Genetics* 141: 989-1006

Heintz C, Doktor TK, Lanjuin A, Escoubas C, Zhang Y, Weir HJ, Dutta S, Silva-Garcia CG, Bruun GH, Morante I, Hoxhaj G, Manning BD, Andresen BS, Mair WB (2017) Splicing factor 1 modulates dietary restriction and TORC1 pathway longevity in *C. elegans*. *Nature* 541: 102-106

Hernandez-Verdun D, Roussel P, Thiry M, Sirri V, Lafontaine DL (2010) The nucleolus: structure/function relationship in RNA metabolism. *Wiley Interdiscip Rev RNA* 1: 415-31

Hibbett DS, Binder M, Bischoff JF, Blackwell M, Cannon PF, Eriksson OE, Huhndorf S, James T, Kirk PM, Lucking R, Thorsten Lumbsch H, Lutzoni F, Matheny PB, McLaughlin DJ, Powell MJ, Redhead S, Schoch CL, Spatafora JW, Stalpers JA, Vilgalys R et al. (2007) A higher-level phylogenetic classification of the Fungi. *Mycol Res* 111: 509-47

Hirano M, Das S, Guo P, Cooper MD (2011) The evolution of adaptive immunity in vertebrates. *Adv Immunol* 109: 125-57

Hollins C, Zorio DA, MacMorris M, Blumenthal T (2005) U2AF binding selects for the high conservation of the *C. elegans* 3' splice site. *RNA* 11: 248-53

Iglewski BH, Liu PV, Kabat D (1977) Mechanism of action of *Pseudomonas aeruginosa* exotoxin A: adenosine diphosphate-ribosylation of mammalian elongation factor 2 in vitro and in vivo. *Infect Immun* 15: 138-44

Irazoqui JE, Ng A, Xavier RJ, Ausubel FM (2008) Role for beta-catenin and HOX transcription factors in *Caenorhabditis elegans* and mammalian host epithelial-pathogen interactions. *Proc Natl Acad Sci U S A* 105: 17469-74

Jansson HB (1994) Adhesion of Conidia of *Drechmeria coniospora* to *Caenorhabditis elegans* Wild Type and Mutants. *J Nematol* 26: 430-5

Jiang H, Wang D (2018) The Microbial Zoo in the *C. elegans* Intestine: Bacteria, Fungi and Viruses. *Viruses* 10

Jones JD, Dangl JL (2006) The plant immune system. *Nature* 444: 323-9

Joshua GW, Karlyshev AV, Smith MP, Isherwood KE, Titball RW, Wren BW (2003) A *Caenorhabditis elegans* model of *Yersinia* infection: biofilm formation on a biotic surface. *Microbiology* 149: 3221-9

Kamath RS, Ahringer J (2003) Genome-wide RNAi screening in *Caenorhabditis elegans*. *Methods* 30: 313-21

Kang C, You YJ, Avery L (2007) Dual roles of autophagy in the survival of *Caenorhabditis elegans* during starvation. *Genes Dev* 21: 2161-71

Kawli T, Wu C, Tan MW (2010) Systemic and cell intrinsic roles of Gqalpha signaling in the regulation of innate immunity, oxidative stress, and longevity in *Caenorhabditis elegans*. *Proc Natl Acad Sci U S A* 107: 13788-93

Kenyon C (2011) The first long-lived mutants: discovery of the insulin/IGF-1 pathway for ageing. *Philos Trans R Soc Lond B Biol Sci* 366: 9-16

Kenyon C, Chang J, Gensch E, Rudner A, Tabtiang R (1993) A *C. elegans* mutant that lives twice as long as wild type. *Nature* 366: 461-4

Kim DH, Ewbank JJ (2015) Signaling in the innate immune response. *WormBook*: 1-51

Kim DH, Feinbaum R, Alloing G, Emerson FE, Garsin DA, Inoue H, Tanaka-Hino M, Hisamoto N, Matsumoto K, Tan MW, Ausubel FM (2002) A conserved p38 MAP kinase pathway in *Caenorhabditis elegans* innate immunity. *Science* 297: 623-6

Kim SH, Macfarlane S, Kalinina NO, Rakitina DV, Ryabov EV, Gillespie T, Haupt S, Brown JW, Taliansky M (2007) Interaction of a plant virus-encoded protein with the major nucleolar protein fibrillarin is required for systemic virus infection. *Proc Natl Acad Sci U S A* 104: 11115-20

Kirienko NV, Ausubel FM, Ruvkun G (2015) Mitophagy confers resistance to siderophore-mediated killing by *Pseudomonas aeruginosa*. *Proc Natl Acad Sci U S A* 112: 1821-6

Klass MR (1983) A method for the isolation of longevity mutants in the nematode *Caenorhabditis elegans* and initial results. *Mech Ageing Dev* 22: 279-86

Lapierre LR, De Magalhaes Filho CD, McQuary PR, Chu CC, Visvikis O, Chang JT, Gelino S, Ong B, Davis AE, Irazoqui JE, Dillin A, Hansen M (2013) The TFEB orthologue HLH-30 regulates autophagy and modulates longevity in *Caenorhabditis elegans*. *Nat Commun* 4: 2267

Lee LW, Lee CC, Huang CR, Lo SJ (2012) The nucleolus of *Caenorhabditis elegans*. *J Biomed Biotechnol* 2012: 601274

Lee LW, Lo HW, Lo SJ (2010) Vectors for co-expression of two genes in *Caenorhabditis elegans*. *Gene* 455: 16-21

Lee RC, Feinbaum RL, Ambros V (1993) The *C. elegans* heterochronic gene *lin-4* encodes small RNAs with antisense complementarity to *lin-14*. *Cell* 75: 843-54

Lemaitre B, Nicolas E, Michaut L, Reichhart JM, Hoffmann JA (1996) The dorsoventral regulatory gene cassette *spatzle/Toll/cactus* controls the potent antifungal response in *Drosophila* adults. *Cell* 86: 973-83

Li BJ, Tang Q, Cheng D, Qin C, Xie FY, Wei Q, Xu J, Liu Y, Zheng BJ, Woodle MC, Zhong N, Lu PY (2005) Using siRNA in prophylactic and therapeutic regimens against SARS coronavirus in Rhesus macaque. *Nat Med* 11: 944-51

Li MM, MacDonald MR, Rice CM (2015) To translate, or not to translate: viral and host mRNA regulation by interferon-stimulated genes. *Trends Cell Biol* 25: 320-9

Lin YM, Chu PH, Li YZ, Ouyang P (2017) Ribosomal protein pNO40 mediates nucleolar sequestration of SR family splicing factors and its overexpression impairs mRNA metabolism. *Cell Signal* 32: 12-23

Liu F, He CX, Luo LJ, Zou QL, Zhao YX, Saini R, Han SF, Knolker HJ, Wang LS, Ge BX (2013) Nuclear hormone receptor regulation of microRNAs controls innate immune responses in *C. elegans*. *PLoS Pathog* 9: e1003545

Liu Y, Olnagier D, Lin R (2016a) Host and Viral Modulation of RIG-I-Mediated Antiviral Immunity. *Front Immunol* 7: 662

Liu Y, Sellegounder D, Sun J (2016b) Neuronal GPCR OCTR-1 regulates innate immunity by controlling protein synthesis in *Caenorhabditis elegans*. *Sci Rep* 6: 36832

Low KJ, Ansari M, Abou Jamra R, Clarke A, El Chehadeh S, FitzPatrick DR, Greenslade M, Henderson A, Hurst J, Keller K, Kuentz P, Prescott T, Roessler F, Selmer KK, Schneider MC, Stewart F, Tatton-Brown K, Thevenon J, Vigeland MD, Vogt J et al. (2017) PUF60 variants cause a syndrome of ID, short stature, microcephaly, coloboma, craniofacial, cardiac, renal and spinal features. *Eur J Hum Genet* 25: 552-559

Ma L, Gao X, Luo J, Huang L, Teng Y, Horvitz HR (2012) The *Caenorhabditis elegans* gene *mfap-1* encodes a nuclear protein that affects alternative splicing. *PLoS Genet* 8: e1002827

Ma L, Horvitz HR (2009) Mutations in the *Caenorhabditis elegans* U2AF large subunit UAF-1 alter the choice of a 3' splice site in vivo. *PLoS Genet* 5: e1000708

Ma L, Tan Z, Teng Y, Hoersch S, Horvitz HR (2011) In vivo effects on intron retention and exon skipping by the U2AF large subunit and SF1/BBP in the nematode *Caenorhabditis elegans*. *RNA* 17: 2201-11

Macneil LT, Walhout AJ (2013) Food, pathogen, signal: The multifaceted nature of a bacterial diet. *Worm* 2: e26454

Maki R, Roeder W, Traunecker A, Sidman C, Wabl M, Raschke W, Tonegawa S (1981) The role of DNA rearrangement and alternative RNA processing in the expression of immunoglobulin delta genes. *Cell* 24: 353-65

Mallo GV, Kurz CL, Couillault C, Pujol N, Granjeaud S, Kohara Y, Ewbank JJ (2002) Inducible antibacterial defense system in *C. elegans*. *Curr Biol* 12: 1209-14

Maniatis T, Tasic B (2002) Alternative pre-mRNA splicing and proteome expansion in metazoans. *Nature* 418: 236-43

Martin A, Rex EA, Ishidate T, Lin R, Gammon DB (2017) Infection of *Caenorhabditis elegans* with Vesicular Stomatitis Virus via Microinjection. *Bio Protoc* 7

Matsushita K, Kitamura K, Rahmutulla B, Tanaka N, Ishige T, Satoh M, Hoshino T, Miyagi S, Mori T, Itoga S, Shimada H, Tomonaga T, Kito M, Nakajima-Takagi Y, Kubo S, Nakaseko C, Hatano M, Miki T, Matsuo M, Fukuyo M et al. (2015) Haploinsufficiency of the c-myc transcriptional repressor FIR, as a dominant negative-alternative splicing model, promoted p53-dependent T-cell acute lymphoblastic leukemia progression by activating Notch1. *Oncotarget* 6: 5102-17

McEwan DL, Kirienko NV, Ausubel FM (2012) Host translational inhibition by *Pseudomonas aeruginosa* Exotoxin A Triggers an immune response in *Caenorhabditis elegans*. *Cell Host Microbe* 11: 364-74

Melen K, Tynell J, Fagerlund R, Roussel P, Hernandez-Verdun D, Julkunen I (2012) Influenza A H3N2 subtype virus NS1 protein targets into the nucleus and binds primarily via its C-terminal NLS2/NoLS to nucleolin and fibrillarin. *Virology* 9: 167

Melo JA, Ruvkun G (2012) Inactivation of conserved *C. elegans* genes engages pathogen- and xenobiotic-associated defenses. *Cell* 149: 452-66

Mochii M, Yoshida S, Morita K, Kohara Y, Ueno N (1999) Identification of transforming growth factor-beta-regulated genes in *Caenorhabditis elegans* by differential hybridization of arrayed cDNAs. *Proc Natl Acad Sci U S A* 96: 15020-5

Mogensen TH (2009) Pathogen recognition and inflammatory signaling in innate immune defenses. *Clin Microbiol Rev* 22: 240-73, Table of Contents

Najibi M, Labeled SA, Visvikis O, Irazoqui JE (2016) An Evolutionarily Conserved PLC-PKD-TFEB Pathway for Host Defense. *Cell Rep* 15: 1728-42

Nargund AM, Pellegrino MW, Fiorese CJ, Baker BM, Haynes CM (2012) Mitochondrial import efficiency of ATFS-1 regulates mitochondrial UPR activation. *Science* 337: 587-90

Neumuller RA, Gross T, Samsonova AA, Vinayagam A, Buckner M, Founk K, Hu Y, Sharifpoor S, Rosebrock AP, Andrews B, Winston F, Perrimon N (2013) Conserved regulators of nucleolar size revealed by global phenotypic analyses. *Sci Signal* 6: ra70

Osman GA, Fasseas MK, Koneru SL, Essmann CL, Kyrou K, Srinivasan MA, Zhang G, Sarkies P, Felix MA, Barkoulas M (2018) Natural Infection of *C. elegans* by an Oomycete Reveals a New Pathogen-Specific Immune Response. *Curr Biol* 28: 640-648 e5

Osorio F, Lambrecht BN, Janssens S (2018) Antigen presentation unfolded: identifying convergence points between the UPR and antigen presentation pathways. *Curr Opin Immunol* 52: 100-107

Pacheco AR, Sperandio V (2012) Shiga toxin in enterohemorrhagic *E. coli*: regulation and novel anti-virulence strategies. *Front Cell Infect Microbiol* 2: 81

Page-McCaw PS, Amonlirdviman K, Sharp PA (1999) PUF60: a novel U2AF65-related splicing activity. *RNA* 5: 1548-60

Pellegrino MW, Nargund AM, Kirienko NV, Gillis R, Fiorese CJ, Haynes CM (2014) Mitochondrial UPR-regulated innate immunity provides resistance to pathogen infection. *Nature* 516: 414-7

Ponti D, Troiano M, Bellenchi GC, Battaglia PA, Gigliani F (2008) The HIV Tat protein affects processing of ribosomal RNA precursor. *BMC Cell Biol* 9: 32

Powell JR, Ausubel FM (2008) Models of *Caenorhabditis elegans* infection by bacterial and fungal pathogens. *Methods Mol Biol* 415: 403-27

Pujol N, Link EM, Liu LX, Kurz CL, Alloing G, Tan MW, Ray KP, Solari R, Johnson CD, Ewbank JJ (2001) A reverse genetic analysis of components of the Toll signaling pathway in *Caenorhabditis elegans*. *Curr Biol* 11: 809-21

Pujol N, Zugasti O, Wong D, Couillault C, Kurz CL, Schulenburg H, Ewbank JJ (2008) Anti-fungal innate immunity in *C. elegans* is enhanced by evolutionary diversification of antimicrobial peptides. *PLoS Pathog* 4: e1000105

Quinn LM, Dickins RA, Coombe M, Hime GR, Bowtell DD, Richardson H (2004) *Drosophila* Hfp negatively regulates dmyc and stg to inhibit cell proliferation. *Development* 131: 1411-23

Ragland SA, Criss AK (2017) From bacterial killing to immune modulation: Recent insights into the functions of lysozyme. *PLoS Pathog* 13: e1006512

Rahmutulla B, Matsushita K, Satoh M, Seimiya M, Tsuchida S, Kubo S, Shimada H, Ohtsuka M, Miyazaki M, Nomura F (2014) Alternative splicing of FBP-interacting repressor coordinates c-Myc, P27Kip1/cyclinE and Ku86/XRCC5 expression as a molecular sensor for bleomycin-induced DNA damage pathway. *Oncotarget* 5: 2404-17

Rajamuthiah R, Mylonakis E (2014) Effector triggered immunity. *Virulence* 5: 697-702

Reddy KC, Andersen EC, Kruglyak L, Kim DH (2009) A polymorphism in npr-1 is a behavioral determinant of pathogen susceptibility in *C. elegans*. *Science* 323: 382-4

Reed R (2000) Mechanisms of fidelity in pre-mRNA splicing. *Curr Opin Cell Biol* 12: 340-5

Reinhold-Hurek B, Shub DA (1992) Self-splicing introns in tRNA genes of widely divergent bacteria. *Nature* 357: 173-6

Richardson CE, Kooistra T, Kim DH (2010) An essential role for XBP-1 in host protection against immune activation in *C. elegans*. *Nature* 463: 1092-5

Rio DC, Ares M, Jr., Hannon GJ, Nilsen TW (2010) Purification of RNA using TRIzol (TRI reagent). *Cold Spring Harb Protoc* 2010: pdb prot5439

Rodriguez-Corona U, Sobol M, Rodriguez-Zapata LC, Hozak P, Castano E (2015) Fibrillarin from Archaea to human. *Biol Cell* 107: 159-74

Rohlfing AK, Miteva Y, Hannenhalli S, Lamitina T (2010) Genetic and physiological activation of osmosensitive gene expression mimics transcriptional signatures of pathogen infection in *C. elegans*. *PLoS One* 5: e9010

Rosen SA, Getz AE, Kingdom T, Youssef AS, Ramakrishnan VR (2016) Systematic review of the effectiveness of perioperative prophylactic antibiotics for skull base surgeries. *Am J Rhinol Allergy* 30: e10-6

Rual JF, Ceron J, Koreth J, Hao T, Nicot AS, Hirozane-Kishikawa T, Vandenhoute J, Orkin SH, Hill DE, van den Heuvel S, Vidal M (2004) Toward improving *Caenorhabditis elegans* phenome mapping with an ORFeome-based RNAi library. *Genome Res* 14: 2162-2168

Ryu JH, Nam KB, Oh CT, Nam HJ, Kim SH, Yoon JH, Seong JK, Yoo MA, Jang IH, Brey PT, Lee WJ (2004) The homeobox gene Caudal regulates constitutive local expression of antimicrobial peptide genes in Drosophila epithelia. *Mol Cell Biol* 24: 172-85

Samuel BS, Rowedder H, Braendle C, Felix MA, Ruvkun G (2016) Caenorhabditis elegans responses to bacteria from its natural habitats. *Proc Natl Acad Sci U S A* 113: E3941-9

Schaefer L (2014) Complexity of danger: the diverse nature of damage-associated molecular patterns. *J Biol Chem* 289: 35237-45

Schmittgen TD, Livak KJ (2008) Analyzing real-time PCR data by the comparative C(T) method. *Nat Protoc* 3: 1101-8

Senger K, Harris K, Levine M (2006) GATA factors participate in tissue-specific immune responses in Drosophila larvae. *Proc Natl Acad Sci U S A* 103: 15957-62

Shapira M, Hamlin BJ, Rong J, Chen K, Ronen M, Tan MW (2006) A conserved role for a GATA transcription factor in regulating epithelial innate immune responses. *Proc Natl Acad Sci U S A* 103: 14086-91

Sheaffer KL, Updike DL, Mango SE (2008) The Target of Rapamycin pathway antagonizes pha-4/FoxA to control development and aging. *Curr Biol* 18: 1355-64

Sifri CD, Begun J, Ausubel FM, Calderwood SB (2003) Caenorhabditis elegans as a model host for Staphylococcus aureus pathogenesis. *Infect Immun* 71: 2208-17

Singh V, Aballay A (2012) Endoplasmic reticulum stress pathway required for immune homeostasis is neurally controlled by arrestin-1. *J Biol Chem* 287: 33191-7

Siqueira MDS, Ribeiro RM, Travassos LH (2018) Autophagy and Its Interaction With Intracellular Bacterial Pathogens. *Front Immunol* 9: 935

Styer KL, Singh V, Macosko E, Steele SE, Bargmann CI, Aballay A (2008) Innate immunity in Caenorhabditis elegans is regulated by neurons expressing NPR-1/GPCR. *Science* 322: 460-4

Sulston JE, Horvitz HR (1977) Post-embryonic cell lineages of the nematode, Caenorhabditis elegans. *Dev Biol* 56: 110-56

Sun J, Singh V, Kajino-Sakamoto R, Aballay A (2011) Neuronal GPCR controls innate immunity by regulating noncanonical unfolded protein response genes. *Science* 332: 729-32

Sun S, Nakashima K, Ito M, Li Y, Chida T, Takahashi H, Watashi K, Sawasaki T, Wakita T, Suzuki T (2017) Involvement of PUF60 in Transcriptional and Post-transcriptional Regulation of Hepatitis B Virus Pregenomic RNA Expression. *Sci Rep* 7: 12874

Tan JH, Fraser AG (2017) The combinatorial control of alternative splicing in *C. elegans*. *PLoS Genet* 13: e1007033

Tan MW, Mahajan-Miklos S, Ausubel FM (1999a) Killing of *Caenorhabditis elegans* by *Pseudomonas aeruginosa* used to model mammalian bacterial pathogenesis. *Proc Natl Acad Sci U S A* 96: 715-20

Tan MW, Rahme LG, Sternberg JA, Tompkins RG, Ausubel FM (1999b) *Pseudomonas aeruginosa* killing of *Caenorhabditis elegans* used to identify *P. aeruginosa* virulence factors. *Proc Natl Acad Sci U S A* 96: 2408-13

Tenor JL, Aballay A (2008) A conserved Toll-like receptor is required for *Caenorhabditis elegans* innate immunity. *EMBO Rep* 9: 103-9

Tiku V, Jain C, Raz Y, Nakamura S, Heestand B, Liu W, Spath M, Suchiman HED, Muller RU, Slagboom PE, Partridge L, Antebi A (2016) Small nucleoli are a cellular hallmark of longevity. *Nat Commun* 8: 16083

Tomlin H, Piccinini AM (2018) A complex interplay between the extracellular matrix and the innate immune response to microbial pathogens. *Immunology*

Travis MA, Sheppard D (2014) TGF-beta activation and function in immunity. *Annu Rev Immunol* 32: 51-82

Troemel ER, Felix MA, Whiteman NK, Barriere A, Ausubel FM (2008) Microsporidia are natural intracellular parasites of the nematode *Caenorhabditis elegans*. *PLoS Biol* 6: 2736-52

Urano F, Calfon M, Yoneda T, Yun C, Kiraly M, Clark SG, Ron D (2002) A survival pathway for *Caenorhabditis elegans* with a blocked unfolded protein response. *J Cell Biol* 158: 639-46

Van Buskirk C, Schupbach T (2002) Half pint regulates alternative splice site selection in *Drosophila*. *Dev Cell* 2: 343-53

Vijay K (2018) Toll-like receptors in immunity and inflammatory diseases: Past, present, and future. *Int Immunopharmacol* 59: 391-412

- Visvikis O, Ihuegbu N, Labed SA, Luhachack LG, Alves AF, Wollenberg AC, Stuart LM, Stormo GD, Irazoqui JE (2014) Innate host defense requires TFEB-mediated transcription of cytoprotective and antimicrobial genes. *Immunity* 40: 896-909
- Wani S, Kuroyanagi H (2017) An emerging model organism *Caenorhabditis elegans* for alternative pre-mRNA processing in vivo. *Wiley Interdiscip Rev RNA* 8
- Wei JZ, Hale K, Carta L, Platzer E, Wong C, Fang SC, Aroian RV (2003) *Bacillus thuringiensis* crystal proteins that target nematodes. *Proc Natl Acad Sci U S A* 100: 2760-5
- Wightman B, Ha I, Ruvkun G (1993) Posttranscriptional regulation of the heterochronic gene *lin-14* by *lin-4* mediates temporal pattern formation in *C. elegans*. *Cell* 75: 855-62
- Wilkins C, Dishongh R, Moore SC, Whitt MA, Chow M, Machaca K (2005) RNA interference is an antiviral defence mechanism in *Caenorhabditis elegans*. *Nature* 436: 1044-7
- Wu Q, Cao X, Yan D, Wang D, Aballay A (2015) Genetic Screen Reveals Link between the Maternal Effect Sterile Gene *mes-1* and *Pseudomonas aeruginosa*-induced Neurodegeneration in *Caenorhabditis elegans*. *J Biol Chem* 290: 29231-9
- Yabas M, Elliott H, Hoyne GF (2015) The Role of Alternative Splicing in the Control of Immune Homeostasis and Cellular Differentiation. *Int J Mol Sci* 17
- Yi YH, Ma TH, Lee LW, Chiou PT, Chen PH, Lee CM, Chu YD, Yu H, Hsiung KC, Tsai YT, Lee CC, Chang YS, Chan SP, Tan BC, Lo SJ (2015) A Genetic Cascade of *let-7-ncl-1-fib-1* Modulates Nucleolar Size and rRNA Pool in *Caenorhabditis elegans*. *PLoS Genet* 11: e1005580
- Zhou X, Feng X, Mao H, Li M, Xu F, Hu K, Guang S (2017) RdRP-synthesized antisense ribosomal siRNAs silence pre-rRNA via the nuclear RNAi pathway. *Nat Struct Mol Biol* 24: 258-269
- Zorio DA, Blumenthal T (1999) Both subunits of U2AF recognize the 3' splice site in *Caenorhabditis elegans*. *Nature* 402: 835-8
- Zugasti O, Bose N, Squiban B, Belougne J, Kurz CL, Schroeder FC, Pujol N, Ewbank JJ (2014) Activation of a G protein-coupled receptor by its endogenous ligand triggers the innate immune response of *Caenorhabditis elegans*. *Nat Immunol* 15: 833-8
- Zugasti O, Ewbank JJ (2009) Neuroimmune regulation of antimicrobial peptide expression by a noncanonical TGF-beta signaling pathway in *Caenorhabditis elegans* epidermis. *Nat Immunol* 10: 249-56

Zugasti O, Thakur N, Belougne J, Squiban B, Kurz CL, Soule J, Omi S, Tichit L, Pujol N, Ewbank JJ (2016) A quantitative genome-wide RNAi screen in *C. elegans* for antifungal innate immunity genes. *BMC Biol* 14: 35

SUPPLEMENTARY

INFORMATION

Erklärung zur Dissertation

Ich versichere, dass ich die von mir vorgelegte Dissertation selbstständig angefertigt, die benutzten Quellen und Hilfsmittel vollständig angegeben und die Stellen der Arbeit - einschließlich Tabellen, Karten und Abbildungen -, die anderen Werken im Wortlaut oder dem Sinn nach entnommen sind, in jedem Einzelfall als Entlehnung kenntlich gemacht habe; dass diese Dissertation noch keiner anderen Fakultät oder Universität zur Prüfung vorgelegen hat; dass sie - abgesehen von unten angegebenen Teilpublikationen - noch nicht veröffentlicht worden ist sowie, dass ich eine solche Veröffentlichung vor Abschluss des Promotionsverfahrens nicht vornehmen werde. Die Bestimmungen dieser Promotionsordnung sind mir bekannt. Die von mir vorgelegte Dissertation ist von Prof. Dr. Adam Antebi betreut worden.

Chun Kew
Köln, Juli 2018